SMALL-SIGNAL PERFORMANCE AND NOISE PROPERTIES OF MICROWAVE TRIODES

PROEFSCHRIFT

TER VERKRIJGING VAN DE GRAAD VAN DOCTOR IN DE TECHNISCHE WETENSCHAP AAN DE TECHNISCHE HOGESCHOOL TE EINDHOVEN, OP GEZAG VAN DE RECTOR MAGNIFICUS Dr H. B. DORGELO, HOOGLERAAR IN DE AFDELING DER ALGEMENE WETENSCHAPPEN, VOOR EEN COMMISSIE UIT DE SENAAT TE VERDEDIGEN OP DINSDAG 15 DECEMBER, DES NAMIDDAGS TE 4 UUR

DOOR

MARINUS TEUNIS VLAARDINGERBROEK
NATUURKUNDIG INGENIEUR

GEBOREN TE 's-GRAVENHAGE

DIT PROEFSCHRIFT IS GOEDGEKEURD DOOR DE PROMOTOR

PROF. DR K. S. KNOL

aan mijn ouders
aan Annie

CONTENTS

SMALL-SIGNAL PERFORMANCE AND NOISE PROPERTIES OF MICROWAVE TRIODES

1. GENERAL SURVEY OF THE PROBLEMS

1.1. Introduction

With the introduction of a third electrode into the diode, which had at the time been known for some years, Lee De Forest constructed in 1907 the first triode, which he called the "audion" [1]). Triodes have always been designed with telecommunication requirements in mind; the first one of all was intended to be a detector for wireless signals. As telecommunications have ever since been one of the most important fields of application of the triode — and of the multigrid tubes derived from it — they have always had a decisive influence on the development of electron tubes. This influence manifests itself mainly in ever increasing demands with respect to frequency, power and bandwidth of the transmitters and receivers embodying triodes.

The demand for higher frequencies is closely connected with the rapidly increasing number of telecommunication systems. Moreover high transmitting power is required in systems which are intended to carry signals over long distances. The requirement of a greater bandwidth in many systems is due to the large amount of information to be conveyed by any of the systems involved.

The influence of telecommunications, as outlined above, has stimulated the whole trend of development from the first audion to the modern microwave triode, which is capable of amplifying signals with a carrier frequency well above 1000 Mc/s. The small-signal performance and the noise properties of these microwave triodes are the subject of this study. The factors governing the behaviour of microwave triodes are much the same as those entering the theory of triodes at lower frequencies. Accordingly we shall first outline the theory of triodes operating at intermediate and low frequencies.

At low frequencies the behaviour of triodes can be adequately explained with reference to the convection current caused by the electron flow from cathode to anode. At higher frequencies, for instance at 100 kc/s, displacement currents also play an important role.

These displacement currents act as capacitive currents in the inter-electrode spaces. The importance of these capacitances becomes evident when we realize that the tetrode was designed in the first place as a tube having a lower capacitance between the anode and the control grid. This results in lower capacitive coupling between the input and output circuits. Up to frequencies of some tens

of Mc/s it has proved possible to describe the performance of triodes by considering only the convection and capacitive currents.

A phenomenon which becomes increasingly important at frequencies higher than some tens of Mc/s, is the inductance of the leads connecting the electrode system of the triode with the external circuits. Together with the interelectrode capacitances, mentioned above, these inductances seem to impose an upper limit on the frequency range within which triodes can be employed; this limit lies below 1000 Mc/s. However, it has been found possible for this limit to be lifted to much higher frequencies by making the connections between the electrode system and the external circuits through the vacuum envelope in the form of disks. These disks can be integral parts of the walls of the waveguide circuits which form, together with the triode, a microwave amplifier or oscillator. The microwave triode, which on account of its appearance is also known by the name of "disc-seal triode", can at present be used as an amplifier for frequencies up to about 7000 Mc/s and as an oscillator for frequencies up to about 10 000 Mc/s.

For two reasons the distance between the electrodes should be very small. The first reason is that a microwave amplifier intended for use in a telecommunication system, should be able to amplify throughout a wide frequency band, for the reasons given at the beginning of this section. Theoretical investigation reveals that this requirement can be fulfilled with triodes having a very high transconductance and a low anode-grid capacity; in other words, having short interelectrode distances and a high current density [3]).

The second reason for narrow electrode spacings is found in the effects caused by the finite transit time of the electrons (in the case of noise these effects start manifesting themselves at much lower frequencies). At low frequencies, where the transit time of the electrons is small in comparison with the period of the signal to be amplified, the convection current is the same in any plane perpendicular to the electron stream *). However, when the transit time becomes comparable with the period of the alternating electric field, the convection current will become dependent on the position of such a plane. Therefore, the current induced in the external circuit by the motion of the electrons cannot be equal to the convection current, as is the case at low frequencies. At high frequencies the instantaneous value of the induced current is equal to the average value of the convection current between the electrodes. It will be clear that in this case the amplitude of the alternating part of the induced current decreases with increasing frequency. If, however, by making the electrode distances short the transit time of the electrons can be restricted to about half the period of the signal to be amplified, the influence of the transit-time effects on the small-signal

*) Most microwave triodes have plane-parallel electrode systems, and therefore our discussion is restricted to systems with 1 parameter.

performance of microwave triodes will be of virtually no import as far as gain and bandwidth are concerned [3]).

Naturally, at increasing operating frequencies the electrode spacings must decrease. Therefore, the construction of triodes which continue to amplify over an acceptable bandwidth at frequencies above 7000 Mc/s, or which oscillate at frequencies of over 10 000 Mc/s, becomes rather difficult. However, also the dimensions of the anode cavity, which is loaded with the anode-grid capacity of the triode, decrease at increasing frequencies. This forms the main obstacle to the design of triodes for higher frequencies, although it does not impose a definite limit on the frequency range in which triodes can be used **).

1.2. Microwave tubes

In addition to the "classic" triode, many new types of electron tubes have been constructed in the last few decades. In contrast to the triode, their operation is based upon the transit-time effects of the electrons. In many types a long cylindrical electron beam interacts with an electromagnetic circuit consisting, for example, of two or more cavities (as in klystrons) or of a slow-wave circuit in the form of a helix (as in traveling-wave tubes). From the constructional and electrical point of view these tubes are more complicated than the classic triodes. Their performance, too, deviates from the performance of the old triode. Although we shall not enter into a discussion of the properties of electron-beam tubes, which have been studied extensively, we should like to mention the noise figure which can be obtained with these tubes. This noise figure, which is a measure of the noise contributed by the amplifying device to the noise in the amplified signal, is between about 2 and 6. This will be discussed later in connection with the noise theory of microwave triodes.

Many different types of microwave triodes operating at frequencies below 1000 Mc/s have been built. In our study we shall restrict ourselves to the small-signal and noise performance of microwave triode amplifiers for about 4000 Mc/s. The first triode constructed for this frequency band, type 416 A, was developed at the Bell Laboratories in about 1946 [4]). Later a series of microwave triodes was developed by Philips. Three of these triodes will be mentioned. The first one is the triode type EC 57, a triode for 4000 Mc/s with an approximately 20-fold power gain and a half-power bandwidth, measured with one single resonant anode circuit, of 100 Mc/s [5])[6]). The maximum output power is 1·5 W. Since for some transmitting systems a higher output was required, the triode type EC 59, having a maximum output of about 15 W was constructed. This tube has an approximately 10-fold power gain at a bandwidth of 100 Mc/s [7])[8]). The third triode, occurring in this discussion, is an experimental triode for 6000 Mc/s, having an approximately 12-fold power gain at 100 Mc/s bandwidth

**) It is possible to use a higher electromagnetic mode in the anode cavity. This has, however, serious disadvantages.

and an output of 1·5 W [9]). For the description of these triodes and their circuits we would refer the reader to the original papers, [5]) to [9]). In this treatise we shall restrict ourselves to a sketch of the EC 57 and the associated amplifier (fig. 1).

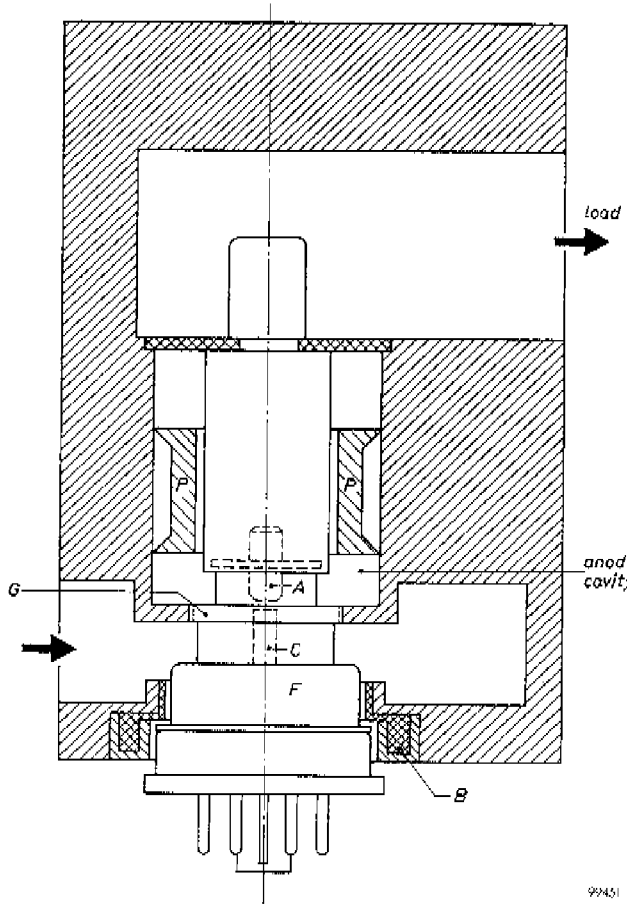

Fig. 1. Sketch of a triode amplifier for 4000 Mc/s. A and C are the anode and cathode of the triode, F. G is the grid disc. The anode cavity, which is of the reentrant type, is coupled through a slot with the load and is tunable by means of the plunger *P*.

Microwave triodes are always used in grounded-grid circuits. This has the advantage of a small feedback capacity between the input and output circuits. Besides, up to now it has proved impossible to realise a microwave amplifier with a triode in a grounded-cathode circuit.

The noise factor of a triode-amplifier at 4000 Mc/s is about 40 to 50, which is about 10 times as high as that of a low-noise electron-beam amplifier. Although the triode noise factor appeared to be no hindrance for the employment of triodes in microwave television and telephony links *), the large difference between the noise factors of the different electron devices is very intriguing.

1.3. Outline of the problems to be discussed

As was stated in the preceding section, far more experimental and theoretical work has been carried out on electron-beam amplifiers than on microwave triodes. It is the aim of this paper to arrive at a better understanding of the small-signal performance and the noise properties of microwave triodes.

(a) Small-signal performance

The first question to be answered concerns the degree of agreement between electronic admittances measured in microwave triodes and the values calculated from transit-time theories. We use the transit-time theory in the form given by Llewellyn and Peterson [10]). Our notation, however, will be the same as that used by Van der Ziel, ref. [11]) pp. 120-126. Robertson [12]) has shown that the correspondence between the measured and the calculated values of electronic admittances of the 416A triode is only slight. It is useful, however, to repeat his measurements for the EC 57, since the current density used in this triode is much higher. The high current density is available from the L-cathode [13]), used in the EC 57. The distance between the cathode and the potential minimum can be made small in comparison with the distance between the cathode and the grid, without a too large transit time of the electrons at high current densities. The importance of this in connection with the Llewellyn-Peterson theory will become clear, when we realise that this transit-time theory is essentially a single-velocity theory. This means that all electrons crossing a plane perpendicular to the electron stream have the same velocity in that plane. This requirement is certainly not fulfilled in the region between the cathode and the potential minimum, where the bulk of the electrons emitted return to the cathode. Therefore, it may be expected that at high current densities, where the electron motion between the cathode and the potential minimum exercises relatively less influence than at low current densities, the single-velocity transit-time theory is a good approximation [14]).

Another problem is whether the internal feedback in microwave triodes [15]) has any appreciable influence on the product of power gain and bandwidth, which is a measure for the quality of a triode. By means of measurements carried out on the triode type EC 57, the triode type EC 59 and the triode for 6000 Mc/s, we shall study the effect of the electron transit time and of the internal feedback on the microwave behaviour of a triode.

*) The receivers used in these links mostly have a crystal mixer as their input stage.

(b) Noise in microwave triodes

Much work has been done concerning the noise behaviour in electron beam devices. Haus and Robinson [16]) have shown that there exists a minimum noise figure of electron-beam tubes that depends directly on the random fluctuations present in the electron beam, provided that the velocity spread in the beam is small in comparison with the average velocity *). The propagation of the fluctuations in the multi-velocity part of the beam (near the cathode) is very difficult to trace. However, one can make an estimate of the influence of the space-charge action in the potential minimum and of the multi-velocity character of the beam just beyond the potential minimum. Combination of this with the theory of Haus and Robinson shows that a minimum noise figure between 2 and 6 is practicable. These low noise figures have, indeed, been realised [17])[18]).

In this connection it may seem strange that the noise figure of triodes, in which the cathode is the chief source of noise — as it is in electron-beam tubes — is 10 times as high as the noise figure of a low-noise electron-beam tube.

Each electron leaving the cathode is emitted individually, without reference to any of the other electrons, and the consequent fluctuations in the electron stream induce noise currents in the external circuits of the triode-amplifier. The current induced in the external circuit between the cathode and the grid can be supposed to be generated by a noise current source i_1 connected in parallel to the circuit. In the external circuit between the anode and the grid the noise current can in the same way be supposed to be generated in a noise current source i_2. It will be clear that when the external circuits are short-circuited, currents i_1 and i_2 flow through the short-circuit leads.

At low frequencies, say below 100 Mc/s, the noise currents are almost entirely due to the fluctuation in the instantaneous value of the average velocity of the electrons just beyond the potential minimum, as has been shown by Rack [19]). The fluctuation in the instantaneous value of the convection current proved to be almost completely suppressed by the space-charge action of the potential minimum. As only one noise source is present, it can be assumed that the short-circuit noise-currents i_1 and i_2 are completely correlated, which means that there exists a fixed relationship between the amplitudes and the phases of i_1 and i_2. The current induced in the grid lead of a triode $(i_1 - i_2)$, which is small in comparison with the short-circuit noise-currents, must of course be correlated with i_1 and i_2. Experimentally, the correlation between i_1 and i_2 has been found to be almost complete. However a certain lack of correlation was found between the induced grid noise current $(i_1 - i_2)$ and i_2 in the frequency range considered. Therefore, it cannot but be assumed that there is at least one more source of noise in a triode. As such might be mentioned

*) It is assumed here that the energy necessary for the power gain of an electron-beam tube is delivered by the d.c. power supply. Therefore modern tubes, using high-frequency "pump signals" are excluded from this discussion.

(1) shot-noise caused by the reflection of electrons at the anode surface;
(2) noise caused by the spread in the transit-times of the electrons travelling to the anode along different paths;
(3) total-emission noise caused by the electrons rejected to the cathode in front of the potential minimum;
(4) noise caused by incomplete suppression of the convection-current fluctuation referred to above by the space-charge action in the potential minimum.

In view of experiments carried out by Talpey and MacNee [20]) it is commonly assumed that the uncorrelated induced grid-noise is mainly caused by the electrons reflected at the anode. Experimental work by Van der Boorn [21]) and by Van der Ziel and Versnel [22]) suggested that the sources of noise mentioned under (2) and (3), respectively, may be unimportant, if the current density is high. The noise source mentioned under (4) has not been discussed in the literature although it might be that the convection-current fluctuation, which is not completely suppressed, has a considerable influence on the small induced grid-noise current. The effects mentioned under (2) to (4) will be discussed in more detail in chapter 5.

At 4000 Mc/s the fluctuation of the average velocity as well as the four sources of noise mentioned under (1) to (4) will be present. We shall try to find out experimentally which sources must be considered to be of consequence. Besides, it should be emphasized that an estimate of the magnitude of the fluctuation of the average velocity and of the average convection current in a plane just beyond the potential minimum, is of importance when the noise behaviour of a microwave triode is compared with that of an electron-beam tube. Because in both tubes the random fluctuations produced by the cathode are equal and the only difference affecting the noise propagation between the cathode and the potential minimum is a focussing magnetic field in electron-beam tubes, the noise fluctuations beyond the potential minimum should be of the same order of magnitude.

Finally, the influence of internal feedback on the noise figure of a microwave triode will be studied in the light of the theory of the noise measure developed recently by Haus and Adler [23]).

The problems propounded above will be studied on the basis of measurements carried out mainly on the EC 57 at 4000 Mc/s.

(c) *Outline of the paper*

In dealing with the theory and discussing our experiments, we shall proceed along the following lines.

First the most important properties of a microwave triode will be expressed in terms of the alternating currents induced in the external circuit as a result of the modulation of the electron stream, of the interelectrode capacities and of the electric and magnetic coupling between the input and output circuits of the

triode amplifier. These properties include: the product of power gain and bandwidth, the input admittance of the triode and the noise factor. The noise power which originates in the triode will be assumed to be generated in a noise-current source and a noise-voltage source connected directly to the input of the triode [24]). The magnitude and the phase of the induced currents and, as far as noise currents are concerned, the cross correlation, are not taken into consideration here. This theory results in an equivalent circuit which describes a triode at microwave frequencies. As a second step using the transit-time theory the induced currents will be expressed in more fundamental quantities such as the geometry of the triode, the transit-time of the electrons and the noise fluctuations in the potential minimum.

The theoretical picture resulting from this "phenomenological" theory complemented by the transit-time theory, will have to be checked against experimental results. The measuring methods are discussed separately. They are rather complicated owing to the fact that the electrical distance between the triode to be measured and the measuring devices is of the same order of magnitude as the wavelength of the electromagnetic signal.

Finally, the results of the experiments will be used in order to find out, according to the theory developed, which physical processes mainly determine the properties of a microwave triode and which processes have only little effect.

2. EQUIVALENT CIRCUIT OF MICROWAVE TRIODES

2.1. Introduction

The derivation of an equivalent lumped circuit describing the behaviour of a microwave triode is possible in virtue of the small dimensions of the active part of such a triode compared with the wavelength of the amplified signal. It is therefore possible to define the potential of one of the electrodes, which potential is nearly constant over the whole surface, as is the case at low frequencies. Hence an equivalent network consisting of lumped elements can be deduced in a manner analogous to the derivation of the equivalent circuit of triodes at low frequencies. This equivalent circuit will be regarded as a fourpole, called the triode fourpole.

Our object will be to express the coefficients of the linear equations describing the triode fourpole in the electronic admittances of the triode. These admittances give the relations between the alternating currents induced in the external circuits as a result of the modulation of the electron stream, and the alternating voltages applied to the electrodes. The coefficients of the triode fourpole equations are also dependent on displacement currents flowing through the interelectrode capacities, and the coupling between the electromagnetic fields on both sides of the grid plane.

In order to describe the noise properties of the microwave triode the triode

fourpole is assumed to be noise free but preceded by a noise-voltage source and a noise-current source [24]). The magnitudes of these noise sources will be expressed in the currents that are induced in the external circuits as a result of the random fluctuations present in the electron stream.

The derivation of the equivalent triode fourpole is divided in two parts. To begin with the triode fourpole of an ideal triode being a triode without any internal feedback is discussed. Secondly, the elements of this fourpole will be extended to include terms describing the internal feedback. Using the triode fourpole the magnitude of the product of the power gain and the bandwidth can be calculated.

The noise sources will be calculated in the same way. First the noise sources of an ideal triode will be obtained; secondly the influence of feedback on the noise sources will be calculated. The noise-factor will then be worked out from these findings.

2.2. Equivalent network of an ideal triode

For our present purposes, an ideal triode is defined as a triode without electric or magnetic coupling between the input and output circuits when it is used in a grounded-grid circuit. An alternating voltage between the anode and the grid will have no influence on the currents between the cathode and the grid. The voltages, currents and admittances occurring in the fourpole equations of ideal triodes will be written as v', i' and Y'; for triodes with feedback the primes will be omitted. The signs are taken in such a way that the anode and cathode currents flow into the triode (see fig. 2).

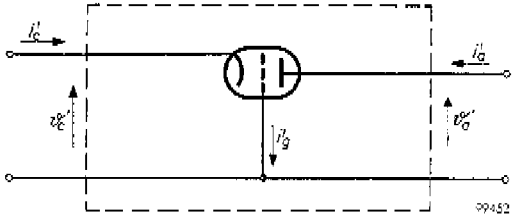

Fig. 2. Direction of the currents in an ideal triode.

When an alternating voltage v_c' is applied between the grid and the cathode of an ideal triode, a current $S_1 v_c'$ will be induced in the cathode-grid circuit as a result of the modulation of the electron stream by v_c'. Besides this induced current a displacement current will flow in the capacity between the cathode and the grid, C_c. The total alternating current flowing between the cathode and the grid, i_c', is then

$$i_c' = v_c' (S_1 + j\omega C_c) = v_c' S_1', \tag{1}$$

The same voltage v_c' will cause a current in the anode-grid circuit which is equal to

$$i_a' = - v_c' S_2. \tag{2}$$

S_1 and S_2 are called the electronic admittances.

An alternating voltage v_a' between the anode and the grid only causes a displacement current to flow through the capacity between the anode and the grid, C_a, hence

$$i_a' = j\omega C_a v_a'. \tag{3}$$

When both v_c' and v_a' are present, the currents in an ideal triode can be written as the input and output currents of a fourpole in the following way:

$$\left.\begin{aligned} i_c' &= S_1' v_c' - Y_c' v_c' + Y_{ac}' v_a', \\ i_a' &= -S_2 v_c' + j\omega C_a v_a' - Y_{ca}' v_c' + Y_a' v_a'. \end{aligned}\right\} \tag{4}$$

These equations are the fourpole equations describing an ideal triode. Since there is no internal feedback the admittance Y_{ac}' is zero.

2.3. Internal feedback

In order to describe the behaviour of a microwave triode we must extend the fourpole equations of an ideal triode with terms describing the electric and magnetic feedback. The two types of feedback will be treated separately. This is possible because the electric fields in the anode cavity and in the input (cathode) cavity are concentrated mainly in the space between the electrodes. Therefore the coupling of the electric fields on both sides of the grid plane is concentrated mainly in this space, which is called the "active" space. However, the magnetic fields in the input and output circuits are negligible in the active space and are mainly present outside this space. Therefore magnetic coupling through the grid occurs mainly in the part of the grid extending outside the active space (fig. 3).

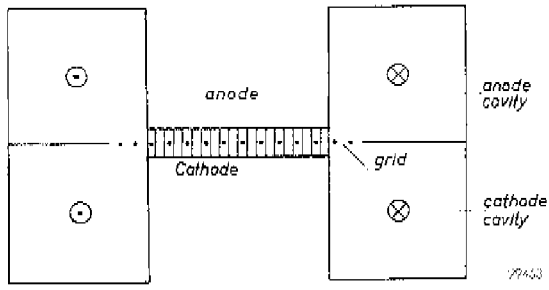

Fig. 3. The electric field of the anode cavity is concentrated mainly in the anode-grid space of the triode. The magnetic flux is there negligible and is found mainly outside this space.

(*a*) *Electric feedback*

The electric feedback is caused by the penetration of the electric field between the grid and the anode through the grid into the cathode-grid space. This penetration is expressed by the amplification factor μ. This is the ratio between the effect of a grid-voltage variation and of an anode-voltage variation on the fieldstrength at the cathode surface of a cut-off triode in grounded-cathode circuit. Therefore an alternating voltage between the anode and the grid causes a current in the cathode-grid circuit which is about $1/\mu$ times the current in this circuit caused by the same voltage but now applied between the cathode and the grid. The triode fourpole of a triode with electric feedback can be deduced from this [25]).

We shall adopt a somewhat different approach, which will simplify the theory when we come to combine the electric and magnetic feedback. Accordingly we shall start with the potential theory in a space-charge free triode. However in the triodes considered we have complete space charge but in a small region on both sides of the grid plane the space charge can be neglected if the distance between the grid and the potential minimum is sufficiently large. By applying this theory to this small region Tellegen [26]) has deduced an equation for the difference in electrical field strength on both sides of the grid. We shall only use the time dependent part of this equation and assume that the time dependence has the form $\exp(j\omega t)$. We then find that

$$(e_c - e_a)e^{j\omega t} = \frac{\mu}{d_{ag}}(v_g - v_e)e^{j\omega t}, \tag{5}$$

where e_c and e_a are the amplitudes of the alternating electric fields in the cathode-grid space and in the grid-anode space, respectively, d_{ag} is the anode-grid distance, v_g is the alternating voltage applied between the cathode and the grid and v_e is the equivalent potential difference between the cathode and the grid plane.

The total current i_c in the cathode-grid space is equal to the sum of the convection current q_c and the displacement current $\epsilon_0 \partial e_c/\partial t$. Omitting the factors $e^{j\omega t}$, we find that

$$i_c = q_c + j\omega\epsilon_0\sigma e_c, \tag{6}$$

where σ is the cathode area which is the same as the cross-section of the electron beam, since only plane-parallel electrode systems are considered. In the anode-grid space we have, analogously

$$i_a = q_a - j\omega\epsilon_0\sigma e_a, \tag{7}$$

where i_a and q_a are the anode current and the convection current between the anode and the grid, respectively; the minus sign is caused by the fact that i_a and q_a are directed towards the grid and the field strength e_a away from the grid.

Since the d.c. potential of the grid wires is negative in comparison with the cathode potential no electrons can reach the grid wires. Therefore $q_a = -q_c$ (the minus sign is again due to the fact that the currents i_a and i_c are taken to flow into the triode, fig. 2). The current induced in the grid i_g is equal to the sum of i_a and i_c. Taking the sum of eqs (6) and (7) and combining with eq. (5) we find that:

$$i_g = i_c + i_a = \frac{j\omega\varepsilon_0\mu\sigma}{d_{ag}}(v_g - v_c) = j\omega\mu\, C_a(v_g - v_c), \tag{8}$$

since $C_a = \varepsilon_0\sigma d_{ag}^{-1}$.

Therefore the difference between the applied grid voltage and the equivalent grid voltage, which is caused by the penetration of the electric field through the grid, can be assumed to be caused by a capacity μC_a between the grid connection and the equivalent grid plane.

This reasoning is only exactly valid for infinitesimally fine grids. The relatively large diameter of the grid wires (7 μ) compared with the pitch (50 μ) or the cathode-grid distance (40 μ) of an EC 57 makes the real situation much more complicated. From the results of the measurements, however, it appears that the approximate description of electric feedback in a microwave triode with the aid of a capacity μC_a in the grid lead is very useful.

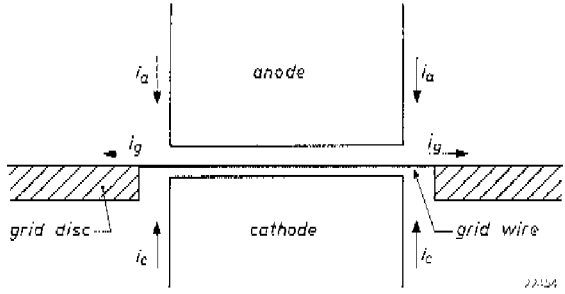

Fig. 4. The currents approach the active space along the surfaces of anode, cathode and grid wires.

(*b*) *Magnetic feedback*

Because of the complicated form of the electrode system outside the active space, we cannot do more than demonstrate that the magnetic feedback can be described with an inductance in the grid lead [27]). In fig. 4 it is shown that the anode and cathode currents flow to the active spaces of the triode, in which the electron current is present, over the surfaces of the anode, the grid disc and the cathode. In the part of the grid extending outside the active space there may be magnetic coupling of the input and output circuits. Inside the

active space this magnetic coupling is unimportant since the magnetic flux is, due to the small dimensions, very small.

The part of the grid outside the active space, together with the surfaces of the anode and the cathode may be regarded as two transmission lines which are mutually coupled (fig. 5). Since these lines are short in comparison with the wavelength, the voltage drop over the upper transmission line is

$$v_2 = -j\omega L_2 i_a - j\omega M i_c, \tag{9}$$

where L_2 is the total inductance of the transmission line and M the total mutual

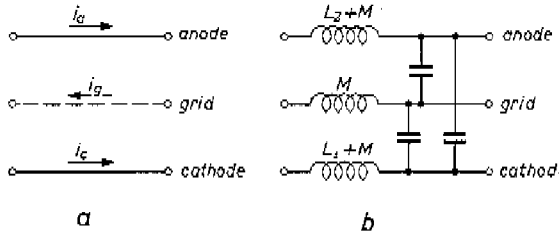

Fig. 5. The currents approach the active space along short lengths of mutually coupled transmission lines. The equivalent lumped network is given in 5b.

inductance with the transmission line on the cathode side (fig. 5). The capacity of this line is negligible in comparison with the capacities between the electrodes which are in parallel with it.

For the lower line we have analogously

$$v_1 = -j\omega L_1 i_c - j\omega M i_a. \tag{10}$$

The equivalent circuit for the two transmission lines obeying eqs (9) and (10) is given in fig. 5b. The inductances $L_1 + M$ and $L_2 + M$ are in series with the input and the output admittance of the triode. They may therefore be neglected. However, the inductance M in series with the grid accounts for the magnetic feedback, since both i_a and i_c flow through this inductance.

(c) Combination of both types of feedback

The electric and magnetic feedback have been shown to be expressible by a capacitance and an inductance, respectively, in series with the grid. Ohmic losses in the grid wires may be described with a resistance r. Hence the internal feedback of a triode can be described by a series-resonant circuit between the grid connection and the equivalent grid plane. The impedance of the circuit is given by

$$Z_i = r + j\left(\omega M - \frac{1}{\omega \mu C_a}\right). \tag{11}$$

From this equation it follows that the passive feedback has a minimum at the frequency

$$\omega_0 = (\mu M C_a)^{-\frac{1}{2}}. \tag{12}$$

Experimentally this compensation frequency has been determined by two different methods that will be discussed later (sec. 2.5). Measurement of ω_0 allows the value of M to be calculated.

2.4. Triode fourpole

Combination of the equivalent fourpole of an ideal triode, deduced in sec. 2.2, and the series-resonant circuit in the grid lead, describing the internal feedback, gives a fourpole describing the properties of an actual microwave triode (fig. 6).

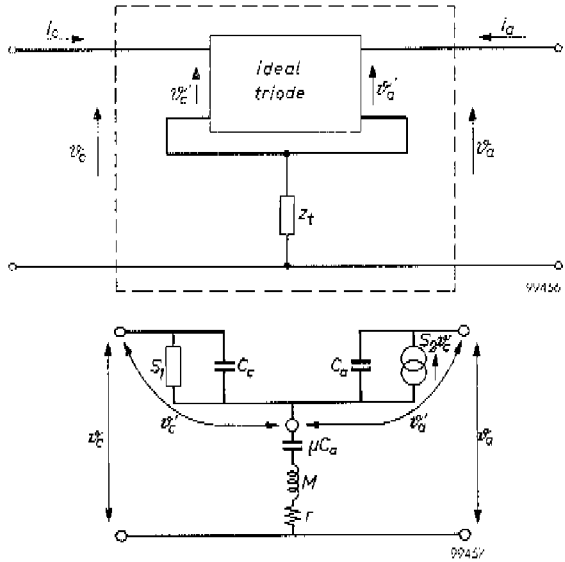

Fig. 6. The triode fourpole of a microwave triode consists of the triode fourpole of an ideal triode which has a series-resonant circuit in the grid lead.

Let the triode fourpole be given by

$$\left.\begin{aligned} i_c &= Y_c\, v_c + Y_{ac} v_a, \\ i_a &= Y_{ca} v_c + Y_a\, v_a. \end{aligned}\right\} \tag{13}$$

The four admittances occurring in this fourpole, expressed in terms of the four admittances of an ideal triode eq. (4) and in the feedback admittance, eq. (11), are calculated to be (fig. 6):

$$Y_c = Y_c' - \frac{(Y_c' + Y_{ac}')(Y_c' + Y_{ca}')}{Y_t + Y_c' + Y_{ca}' + Y_{ac}' + Y_a'}, \tag{14}$$

$$Y_{ac} = Y_{ac}' - \frac{(Y_{ac}' + Y_c')(Y_{ac}' + Y_a')}{Y_t + Y_c' + Y_{ca}' + Y_{ac}' + Y_a'}, \tag{15}$$

$$Y_{ca} = Y_{ca}' - \frac{(Y_{ca}' + Y_a')(Y_{ca}' + Y_c')}{Y_t + Y_c' + Y_{ca}' + Y_{ac}' + Y_a'}, \tag{16}$$

$$Y_a = Y_a' - \frac{(Y_a' + Y_{ca}')(Y_a' + Y_{ac}')}{Y_t + Y_c' + Y_{ca}' + Y_{ac}' + Y_a'}, \tag{17}$$

where $Y_t = Z_t^{-1}$.

Introducing the values of Y_c', Y_{ac}', Y_{ca}', Y_a' and Y_t results in very complicated equations. Therefore we shall introduce some approximations expressed by the inequalities

$$|Y_t| \gg |S_1|;\ |Y_t| \gg |S_2|;\ |Y_t| \gg \omega C_c \text{ and } |Y_t| \gg \omega C_a,$$

which mean, physically, that the passive feedback of energy in the triode is much smaller than the active energy transfer by the electron stream. Of course these inequalities are satisfied in all usable triodes.

Using these inequalities and substituting eq. (4) in eqs (14) to (17) we obtain approximate values for the triode-fourpole admittancies

$$Y_c = S_1 + j\omega C_c, \tag{18}$$

$$Y_{ac} = -\frac{S_1 + j\omega C_c}{\mu}\left(1 - \frac{\omega^2}{\omega_0^2} + j\omega r_\mu C_a\right), \tag{19}$$

$$Y_{ca} = -S_2, \tag{20}$$

$$Y_a = \frac{S_2 - j\omega C_a}{\mu}\left(1 - \frac{\omega^2}{\omega_0^2} + j\omega r_\mu C_a\right) + j\omega C_a, \tag{21}$$

with $\omega_0^2 = (\mu M C_a)^{-1}$.

Despite the approximations which had to be introduced for the purpose of deducing the triode fourpole, these fourpole admittances give a good insight into the behaviour of microwave triodes.

2.5. Input admittance and feedback

In this section the magnitude and the phase of the input admittance will be studied. This will allow information on the feedback properties to be obtained since feedback determines the effect of variations in the anode circuit on the input impedance. The anode circuit consists of a cavity coupled to the amplifier load through the slit between the tuning plunger and the central conductor of the coaxial line at the anode side of the amplifier (see fig. 1) [6].

The behaviour of a triode in a microwave amplifier is described theoretically by loading the triode fourpole with the admittance of the anode cavity Y_0 and the load admittance Y_L, both reflected to the active space of the triode:

$$Y_L + Y_0 = g_L + g_0 + j(b_L + b_0).$$

The input admittance of the triode fourpole loaded with these two admittances is given by:

$$Y_{in} = Y_e - \frac{Y_{ac}\, Y_{ca}}{g_L + g_0 + j(b_L + b_0) + Y_a}. \tag{22}$$

We shall now discuss the dependence of the input admittance on the tuning of the anode cavity. In this case $b_L + b_0$ are varied between $-\infty$ and $+\infty$. The locus of the input admittance in the complex admittance plane for different values of $b_L + b_0$ appears to be a circle [28]). The diameter connecting the two points on this circle for which $b_L + b_0 + \mathrm{Re}(Y_a)$ is zero or infinity, respectively, called $2P$, is given by the complex number (cf. fig. 7)

$$2P = -\frac{Y_{ac}\, Y_{ca}}{\mathrm{Re}(Y_a) + g_0 + g_L}. \tag{23}$$

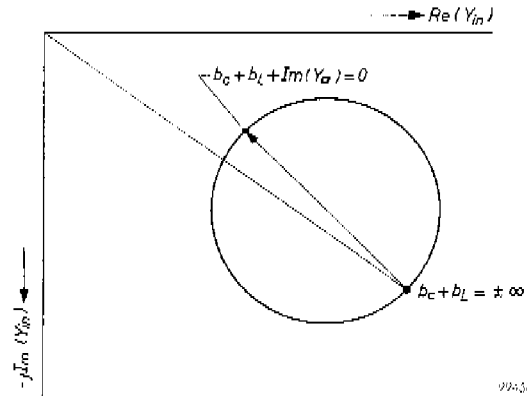

Fig. 7. The locus of the input admittance by varying susceptance of the anode resonant circuit is a circle. Its diameter depends strongly on the bandwidth and on the feedback properties.

The argument of P is therefore equal to the sum of the arguments of the two triode-fourpole admittances Y_{ac} and Y_{ca}. If the denominator of eq. (23) is known, the product of Y_{ac} and Y_{ca} can be calculated from the magnitude and phase of $2P$. If Y_{ca} has also been measured it is possible to calculate the feedback admittance Y_{ac} and hence the values of ω_0, M and r, if it is assumed that the feedback capacity in series with the grid is equal to μC_a. This is one method by which the feedback properties can be measured.

A second method, referred to in the last paragraph of sec. 2.3, is obtained by measuring the passive feedback of a "cut-off" triode directly. In a "cut-off" triode the grid potential is so negative that no electron current can flow, and hence S_1 and S_2 are zero. In this case the triode-fourpole feedback-admittance Y_{ac} is given by

$$Y_{ac} = -\frac{j\omega C_c}{\mu}\left(1 - \frac{\omega^2}{\omega_0^2} + j\omega r \mu C_a\right). \tag{24}$$

When ω is equal to ω_0 the feedback admittance Y_{ac} is at a minimum. This compensation frequency ω_0 is found experimentally by measuring the power transfer through a cut-off triode as a function of the frequency. Minimum power transfer is obtained when $\omega = \omega_0$ and the bandwidth of this minimum is given by

$$B = \frac{r}{M}. \tag{25}$$

The last two equations agree with the equations for passive feedback that have been given by Diemer [15])*).

2.6. Product of power gain and bandwidth

As was noticed in Chapter 1, the product of power gain and bandwidth between the half-power points, called the gain-band product, can be taken as a measure of the usefulness of a microwave triode amplifier. A general formula for the gain-band product of an active fourpole with internal feedback has been given by van der Ziel and Knol [29]) (see eq. (35) in their paper). In deducing this formula they assumed that the bandwidth of the cathode circuit is large in comparison with the bandwidth of the anode circuit. For microwave triodes used in a grounded-grid circuit, this assumption is usually correct, since the input admittance is large.

When the general formula for the gain-band product is applied to the triode fourpole given by eqs (14) to (17), loaded with $Y_L + Y_0$ (eq. (22)) we find, using also eq. (23):

$$GB = \frac{|S_2|^2}{2\pi C_a \operatorname{Re}(S_1)} \frac{C_a}{C_{at}} \frac{g_L}{g_L + g_0 + \operatorname{Re}(Y_a)} \frac{1}{1 + \dfrac{\operatorname{Re}(P)}{\operatorname{Re}(S)}}, \tag{26}$$

where C_{at} is the total capacity of the anode circuit.

We shall discuss the successive factors of eq. (26). The first factor is sometimes called the intrinsic gain-band product, as it is determined by the triode only.

*) When the complete eqs (15) and (16) are used Y_{ac} and Y_{ca} are found to be equal, as might be expected in a passive fourpole, of a cut-off triode.

For low frequencies this factor approaches the value

$$GB = \frac{g_m}{2\pi C_a}, \tag{27}$$

since S_1 and S_2 both become equal to the transconductance g_m. The intrinsic gain-band product is high when g_m is high and when C_a is low. This means that the current density should be as high as possible [3]). At high frequencies g_m is replaced by $|S_2|^2/\mathrm{Re}(S_1)$. When the electron transit times in the cathode grid space and in the anode-grid space are not longer than the half period of the high-frequency signal considered, this quotient remains nearly equal to g_m [3]). This transit-time requirement, however, means that the cathode-grid distance has to be small.

The total capacity C_{at} of the anode-cavity is larger than the anode-grid capacity C_a. Therefore the value of the gain-band product decreases, as is expressed by the second factor of eq. (26). The value of C_a/C_{at}, which can be of the order of 0·2 to 0·4, is discussed by van Wijngaarden [30]).

The third factor $g_L\{g_L + g_0 + \mathrm{Re}(Y_a)\}^{-1}$ gives that part of the total output power delivered by the triode, which is dissipated as usefull output power in the load conductance g_L.

The last factor, $[1 + \mathrm{Re}(P)/\mathrm{Re}(S_1)]^{-1}$, requires more discussion. From eq. (23) it follows that $\mathrm{Re}(P)$ is proportional to the reciprocal of $g_L + g_0 + \mathrm{Re}(Y_a)$. However, the sum of this factor also determines the bandwidth of the anode circuit, which is proportional to it. Therefore P is proportional to the reciprocal value of the bandwidth of the anode cavity. Now there are two possibilities: either $\mathrm{Re}(P) > 0$ or $\mathrm{Re}(P) < 0$. When the frequency at which the tube is studied lies far below the compensation frequency then $\mathrm{Re}(P) < 0$ (compare eqs (19), (20) and (23)). *In this case an increase of bandwidth results in a decrease of the gain-band product. At frequencies which are higher than the compensation frequency an increasing bandwidth results in an increase of the gain-band product.* At the compensation frequency ω_0 the value of $\mathrm{Re}(P)$ is unequal to zero, due to the presence of ohmic losses in the grid lead.

2.7. Equivalent noise sources of an ideal triode

Becking, Groendijk and Knol [24]) have shown that any linear noisy fourpole can be described theoretically by an identical but noise-free fourpole preceded by a noise-voltage source and a noise-current source (fig. 8). If the bandwidth considered is sufficiently small, these sources can be regarded as generators producing a nearly sinusoidal voltage and current, respectively. The mean squares of the voltage and of the current are closely related to the product of the bandwidth considered and the power density spectrum of the noise fluctuations at the mean frequency [31]).

Correlation between the voltage and current fluctuations is expressed by the cross-power density spectrum of these random fluctuations. This power density spectrum has also a definite value if the bandwidth considered is sufficiently small [31]).

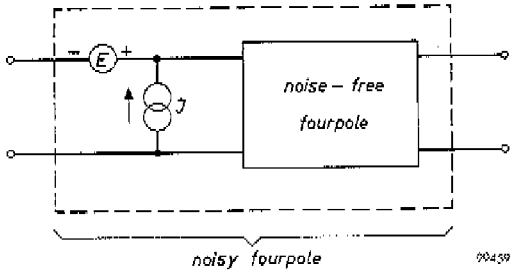

Fig. 8. Noisy fourpole characterized by a noise free fourpole preceded by a noise-current and a noise-voltage source.

We shall apply this convention to a microwave triode in order to express the noise-voltage source and the noise-current source in terms of the currents which are induced in the external circuits as a result of the random fluctuations in the electron stream.

The current induced in the cathode-grid circuit by the random fluctuations in the electron stream can be assumed to be generated in a noise-current source i_1 circuited parallel to the cathode-grid circuit. In the same manner the induced current in the anode-grid circuit can be imagined to originate in a noise-current source i_2.i_1 and i_2 are called the short-circuit noise currents since these currents flow through the external circuits when they have zero impedance (fig. 9).

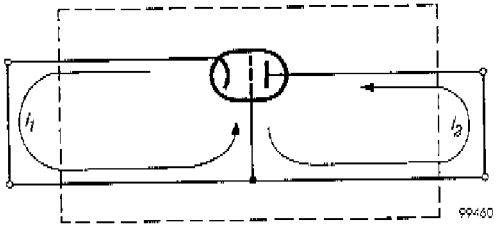

Fig. 9. Induced noise currents in a short-circuited triode.

We now assume the ideal triode to be noise-free but preceded by a noise-voltage source and a noise-current source. In this case the noise sources should be such that the short-circuit noise currents are also equal to i_1 and i_2 (fig. 10).

This requirement is satisfied when

$$E' = \frac{i_2}{S_2} \; ; \; J' = \frac{i_2 S_1' - i_1 S_2}{S_2}, \tag{28}$$

in which S_1' is defined in eq. (1). Therefore the noise sources describing the noise behaviour of an ideal triode are given in eq. (28), expressed in the short-circuit noise currents i_1 and i_2. For the calculation of the characteristic noise quantities the minus signs in front of the quotients in eq. (28) can be omitted (cf. eq. (32)).

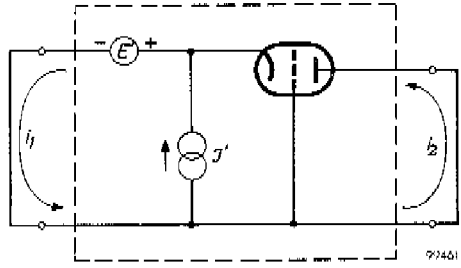

Fig. 10. Noise-free triode with external noise sources.

2.8. Noise sources and noise factor of a microwave triode

In order to find the complete triode fourpole of a microwave triode a series resonant circuit had to be inserted in the grid lead of an ideal triode. In this section we shall calculate the influence of this feedback admittance on the noise sources of an ideal triode.

In order to do this we shall use an artifice, proposed by Beeking, Groendijk and Knol [32]), and explained in fig. 11. The triode fourpole, the feedback impedance and the noise sources of the ideal triode are combined, together with two

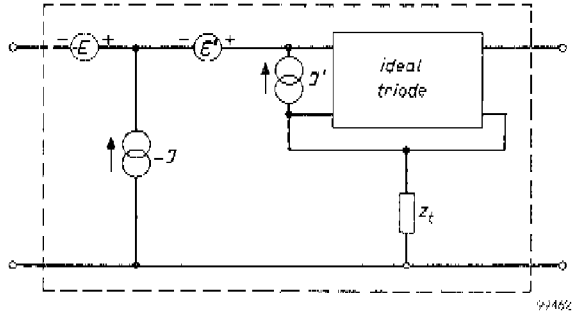

Fig. 11. Artifice used in order to calculate the noise sources of a microwave triode; the whole fourpole is assumed to be noise free.

artificial noise sources, a voltage source $-E$ and a current source $-J$, in a new fourpole. In order to make this new fourpole noise free the two artificial noise sources must be equal to

$$E = E' + J'Z_t \frac{Y_a' + Y_{ca}'}{Y_{ca}' - D'Z_t}, \tag{29}$$

$$J = J' \frac{Y_{ca}'}{Y_{ca}' - D'Z_t}, \tag{30}$$

where D' is the fourpole determinant of the ideal triode *). Therefore the noise sources of the triode, including feedback are given by $+E$ and $+J$.

The noise sources of a microwave triode are thus expressed in terms of the short-circuit noise currents i_1 and i_2, the electronic admittances S_1 and S_2 and the circuit elements determining the internal feedback of a microwave triode.

The noise figure of a fourpole is defined as the ratio of the total available noise power at the output of the fourpole when a noise generator is connected across its input terminals to the available output power if this noise generator were the only noise-producing element. Therefore the noise figure is given by [24]:

$$F = \frac{\overline{|E_s + E + JZ_g|^2}}{\overline{|E_s|^2}} = 1 + \frac{\overline{|E + JZ_g|^2}}{4kT\,\mathrm{Re}(Z_g)\,\delta f}, \tag{31}$$

where Z_g is the internal impedance of the generator and E_s is the noise voltage produced by this generator which is given by Nyquists' equation: $\overline{|E_s|^2} = 4\,kT\,\mathrm{Re}(Z_g)\,\delta f$. The noise voltage E_s of the generator is uncorrelated with the noise sources E and J of the fourpole, and therefore the second form of eq. (31) is indentical to the first one.

In order to express the noise figure in measurable quantities we introduce the four characteristic noise quantities. These quantities are defined by [24]:

$$\begin{aligned} 4kTR_n\,\delta f &= \overline{EE^*}, \\ 4kTG_r\,\delta f &= \overline{JJ^*}, \\ 4kT\zeta\,\delta f &= \overline{EJ^* + E^*J}, \\ 4kTj\kappa\,\delta f &= \overline{EJ^* - E^*J}. \end{aligned} \tag{32}$$

With the aid of these definitions eq. (31) can be rewritten in the form

$$F - 1 = \frac{R_n + G_r\,|Z_g|^2 + \zeta\,\mathrm{Re}\,(Z_g) + \kappa\,\mathrm{Im}\,(Z_g)}{\mathrm{Re}\,(Z_g)}. \tag{33}$$

*) Since in an ideal triode the feedback admittance Y_{ac}' is equal to zero this determinant is equal to the product of Y_a' and Y_c'.

The minimum value of the noise figure, which depends on Z_g, can be found by equating to zero the derivatives of $F-1$ with respect to $\mathrm{Re}(Z_g)$ and $\mathrm{Im}(Z_g)$. This results in a minimum value equal to

$$(F-1)_{\min} = \zeta + \sqrt{4R_nG_r - \kappa^2}\,, \tag{34}$$

when:

$$\mathrm{Re}(Z_g) = \frac{1}{2G_r}\sqrt{4R_nG_r - \kappa^2} \text{ and } \mathrm{Im}(Z_g) = -\frac{\kappa}{2G_r}. \tag{35}$$

Using these equations together with eqs (28), (29) and (30) the noise figure, the minimum noise figure and the optimal value of the generator impedance are expressed in the short-circuit noise currents, the electronic admittances and the feedback impedance.

3. EFFECT OF THE ELECTRON TRANSIT TIME ON THE PROPERTIES OF A TRIODE AT MICROWAVE FREQUENCIES

3.1. Introduction

In the preceding chapter an equivalent circuit for a microwave triode has been deduced, see fig. 6. Using this equivalent circuit the externally measurable properties of a microwave triode, such as the gain-band product and the noise figure, can be expressed in terms of the electronic admittances S_1 and S_2 and in terms of the four characteristic noise quantites R_n, G_r, ζ and κ. However, during the derivation of this circuit we did not go into the physical factors determining the amplitudes and the phases of S_1 and S_2 and of the short-circuit noise currents i_1 and i_2 on which the characteristic noise quantities are based. These factors are the geometry of the triode, the voltage applied to the electrodes and the fluctuations present in the electron stream emitted by the cathode. The relation between these basic properties and S_1, S_2, i_1 and i_2 can be found with the aid of the transit-time theory. In this chapter we shall apply this theory, as given by Llewellyn and Peterson [10]), to a microwave triode. The notation used will be similar to that used by van der Ziel [11]).

The transit-time theory mentioned above can only be applied when two basic requirements are satisfied. The first is that all a.c. quantities are small compared with the corresponding d.c. quantities. That means that on the basis of this theory only the small-signal behaviour of triodes can be studied. This requirement is satisfied for all cases considered in this study.

The second requirement is that the velocities of all electrons in a plane perpendicular to the direction of the electron stream are equal. For microwave triodes having plane parallel electrode systems, this means that in a plane parallel to the cathode all electrons have the same velocity.

In the space between the cathode and the potential minimum this requirement is certainly not satisfied since most of the emitted electrons reverse their direc-

tion of motion in front of the potential minimum and return to the cathode. These returning electrons will absorb energy from the high-frequency electric field ("total emission damping" [14]). This energy absorption increases the input admittance. The returning electrons also give rise to a noise current ("total emission noise" [33]).

When the cathode current density in the triode is increased, the distance between the cathode and the potential minimum decreases [34]. When the current density is sufficiently high, this distance becomes much smaller than the cathode-grid distance. In this case the interaction of the high-frequency electric field in the cathode-grid space with the returning electrons decreases since they only cross a small part of this field. Therefore the total-emission damping and the total-emission noise become negligible at high current densities. This will be shown in chapter 5 when dealing with the results of the measurements. In connection herewith *we shall ignore the effects caused by the returning electrons. Also the fact that in the vicinity of the cathode the velocity spread is of the same order of magnitude as the average velocity of the electrons is ignored.* Due to these two approximations the single-velocity transit-time theory can be applied to the cathode-grid space of a triode.

The approximations made by Child for his deduction of the 3/2-power law for the static characteristic of a diode too include the neglection of the returning electrons [35]. This law appears to be a good approximation at high current densities when the distance between the cathode and the potential minimum is much smaller than the cathode-grid distance.

The application of the single-velocity transit-time theory, particularly to noise problems, requires a more detailed discussion which will be given later in this chapter.

3.2. Outline of the single-velocity transit-time theory

The single-velocity transit-time theory has been treated extensively in the original papers of Benham [36], Müller [37], Bakker and de Vries and Ferris and North [38], Llewellyn and Peterson [10] and in several handbooks [11][39]. However, in order to trace the limits within which this theory can be applied it will be profitable to outline its basic principles.

We shall therefore consider the electron motion between two plane parallel electrodes with area σ. The problem is assumed to be one-dimensional. The total current $I(t)$ between both planes is given by the sum of the convection current and the displacement current in a cross section of the electron stream between both electrodes. Suppose the electron velocity u in this cross section to be equal for all electrons and the space-charge density in this cross section to be equal to $-\rho$. Then

$$I(t) = \sigma\left(-\rho u + \epsilon_0 \frac{\partial E_s}{\partial t}\right), \tag{36}$$

where E_s is the fieldstrength in the cross section considered.

If we combine eq. (36) with Poissons' equation

$$\frac{\partial E_s}{\partial t} = \frac{\rho}{\epsilon_0}, \tag{37}$$

we find that

$$I(t) = \sigma\epsilon_0 \left(\frac{\partial E_s}{\partial t} \cdot \frac{\mathrm{d}x}{\mathrm{d}t} + \frac{\partial E_s}{\partial t} \right) = \sigma\epsilon_0 \frac{\mathrm{d}E_s}{\mathrm{d}t}, \tag{38}$$

in which equation u is replaced by $\mathrm{d}x/\mathrm{d}t$.

The equation of motion of a single electron is expressed by

$$E_s = -\frac{m}{e} \frac{\mathrm{d}^2x}{\mathrm{d}t^2}, \tag{39}$$

where e is a positive number.

Differentiating this equation with respect to time and substituting the result in eq. (38) yields:

$$I(t) = -\frac{m}{e} \epsilon_0\sigma \frac{\mathrm{d}^3x}{\mathrm{d}t^3}. \tag{40}$$

This equation is the basic equation of the single-velocity transit-time theory of Llewellyn and Peterson [10]). We shall apply this equation first to two special cases. The first one is the static electron flow in a diode in which both the electron velocity and the field strength at the cathode surface are zero. The second is the electron flow in a diode without space-charge. These examples have been chosen in view of the application of the theory to microwave triodes which can be considered theoretically to be divided into two diodes, one with full space charge, the other with negligible space charge.

In the first case, if the electrons considered enter the diode at time $t = t_a$ integration of eq. (40) yields [11])

$$\begin{aligned} \frac{\mathrm{d}^2x}{\mathrm{d}t^2} &= -\frac{e}{m} \frac{I_a}{\sigma\epsilon_0} (t - t_a), \\ \frac{\mathrm{d}x}{\mathrm{d}t} &= -\frac{eI_a}{2m\sigma\epsilon_0} (t - t_a)^2, \\ x &= -\frac{eI_a}{6m\sigma\epsilon_0} (t - t_a)^3, \end{aligned} \tag{41}$$

where I_a is the static anode current. Putting x equal to the electrode distance d and the transit time of the electrons $t_a - t_a$ equal to τ we find

$$\tau = \left(\frac{6m\epsilon_0\sigma d}{eI_a} \right)^{1/3}. \tag{42}$$

Substitution of eq. (42) into eq. (41) yields

$$\frac{I_a}{\sigma} = \frac{4}{9}\,\epsilon_0 \left(\frac{2e}{m}\right)^{1/2} V_a^{3/2}\, d^{-2} = 2{\cdot}3.10^{-6}\; V_a^{3/2}\, d^{-2}, \tag{43}$$

where V_a is the anode voltage, which is related to the velocity u_a of the electrons at the anode by

$$^1/_2\; m u_a^2 = e V_a.$$

Equation (43) is the $^3/_2$-power law which has been deduced by Child [35]. This equation appears to be a good approximation of the static characteristic of a space-charge limited diode with high anode current density.

Apparently the electrons returning between the cathode and the potential minimum have only a small effect on this characteristic. Therefore we may expect that the transit-time theory, which is developed from the same basic equation (40), describes the high-frequency properties of a microwave triode with a high anode current-density fairly accurate. This expectation is also based on the fact that the high-frequency currents induced in the external circuits by the returning electrons decrease with increasing current density, as was discussed in the introduction of this chapter.

Equation (40) will now be applied to the second case of a discharge space with negligible space charge. Then the term $\partial E_s/\partial x$ becomes zero, so that E_s is constant, eq. (37). When the electrons enter the space between the electrodes with a velocity u_1 and leave this space with the velocity u_2, the difference in velocity being caused by the linear electric field, their transit time is given by

$$\tau = \frac{2d}{u_1 + u_2}. \tag{44}$$

The integration of eq. (40) for the general case including a.c. effects will not be performed here. The reader is referred to the papers quoted at the beginning of this section. Since the integration can only be performed analytically for the case when the a.c. disturbances are small in comparison with the corresponding d.c. quantities, the results of the integration are restricted to the small-signal case. These results are given in the form of linear relations between the alternating voltage $v(t)$ applied between the two electrodes considered, the total alternating current $i(t)$, the modulations of the convection currents $q_1(t)$ and $q_2(t)$ and the modulations of the velocity of the electrons $u_1(t)$ and $u_2(t)$ at the input and output planes, respectively.

The linear relations are:

$$i(t) = b_{11}v(t) + b_{12}q_1(t) + b_{13}u_1(t), \tag{45a}$$
$$q_2(t) = b_{21}v(t) + b_{22}q_1(t) + b_{23}u_1(t), \tag{45b}$$
$$u_2(t) = b_{31}v(t) + b_{32}q_1(t) + b_{33}u_1(t). \tag{45c}$$

The coefficients b_{mn} are called the transit-time coefficients.

Up to now eq. (40) has been applied to the electron stream between two arbitrary electrodes. In order to apply the theory to a triode we divide this triode into two diodes separated by the grid plane. The diode between the cathode and the grid is a diode with full space charge. Its plate potential is equal to the equivalent potential in the grid plane. The diode between the grid plane and the anode has negligible space charge. The transit time coefficients for a triode are for our purposes given in table I. They appear to be functions of the transit-time angle which is defined as the product of the electron transit time and the angular frequency:

$$\alpha = \omega\tau$$

However, we use the variable $\beta = j\alpha$ where j is the imaginary unit.

TABLE I

TRANSIT-TIME COEFFICIENTS OF A TRIODE *)

cathode-grid space (full space charge) u_c = average electron velocity at the cathode u_g = average electron velocity in the grid plane d_{cg} = cathode-grid distance	anode-grid space (negligible space-charge) u_a = average electron velocity at the anode normally $u_g \ll u_a$ d_{ag} = anode-grid distance
$b_{11} = \dfrac{3\eta I_a}{(u_c+u_g)^2}\dfrac{1}{\Phi_6(\beta_1)}$	$b_{11}' = j\omega C_a + \dfrac{2\eta I_a}{(u_a+u_g)^2}\dfrac{\beta_2}{3}\Phi_4(\beta_2)$
$b_{12} = \dfrac{u_c}{u_c+u_g}\dfrac{\Phi_4(\beta_1)}{\Phi_6(\beta_1)}$	$b_{12}' = \dfrac{u_g}{u_a+u_g}\Phi_2(\beta_2) + \dfrac{u_a}{u_a+u_g}\Phi_3(\beta_2)$
$b_{13} = \dfrac{3I_a}{u_c+u_g}\dfrac{\Phi_3(\beta_1)}{\Phi_6(\beta_1)}$	$b_{13}' = \dfrac{I_a}{u_a+u_g}\beta_2\Phi_3(\beta_2)$
$b_{21} = \dfrac{3I_a\eta}{u_g(u_c+u_g)}\dfrac{\Phi_3(\beta_1)}{\Phi_6(\beta_1)}$	$b_{21}' = \dfrac{\eta I_a}{u_a(u_a+u_g)}\beta_2\Phi_3(\beta_2)$
$b_{22} = \dfrac{u_c}{u_g}\Xi(\beta_1)$	$b_{22}' = e^{-\beta_2}$
$b_{23} = \dfrac{3I_a}{u_g}\Theta(\beta_1)$	$b_{23}' = \dfrac{I_a}{u_a}\beta_2 e^{-\beta_2}$
$\beta_1 = j\alpha_1;\ \beta_1 = j\dfrac{3\omega d_{cg}}{u_c+u_g}$	$\beta_2 = j\alpha_2;\ \beta_2 = j\dfrac{2\omega d_{ag}}{u_a+u_g}$
$g_0 = \dfrac{3\eta I_a}{(u_c+u_g)^2}$	$j\omega C_a = j\omega\dfrac{\varepsilon_0 a}{d_{ag}}$

$$\Phi_3(\beta) = \frac{2}{\beta^2}(1 - e^{-\beta} - \beta e^{-\beta})$$

$$\Phi_4(\beta) = \frac{6}{\beta^3}(-2 + \beta + 2e^{-\beta} + \beta e^{-\beta})$$

$$\Phi_6(\beta) = \frac{12}{\beta^4}\left(\frac{\beta^3}{6} + 2 - \beta - 2e^{-\beta} - \beta e^{-\beta}\right)$$

$$\Theta(\beta) = \frac{1}{3}\beta e^{-\beta} + \frac{\Phi_3^2(\beta)}{\Phi_6(\beta)}$$

$$\Xi(\beta) = e^{-\beta} + \frac{\Phi_3(\beta)\Phi_4(\beta)}{\Phi_6(\beta)}$$

$$\eta = \frac{e}{m}$$

The functions $\Phi_3(\beta)$, $\Phi_4(\beta)$, $\Phi_6(\beta)$, $\Theta(\beta)$ and $\Xi(\beta)$ have been plotted in the figs 12-16.

*) Contrary to the example given in sec. (3-2) it has been assumed here that the electron velocity at the cathode is not equal to zero.

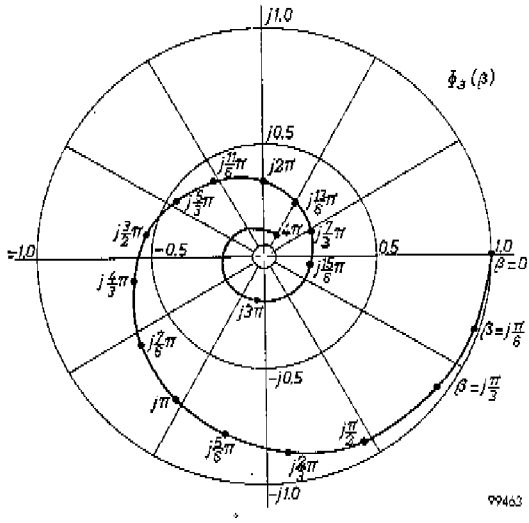

Fig. 12

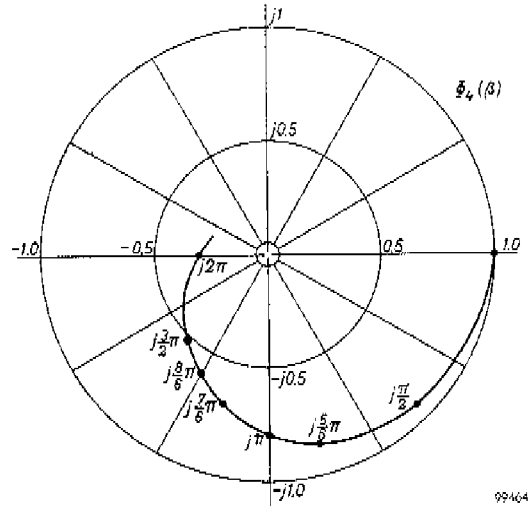

Fig. 13

Figs 12, 13, 14, 15, 16. Polar diagrams of transit time functions; the corresponding values of β have been plotted along the curves.

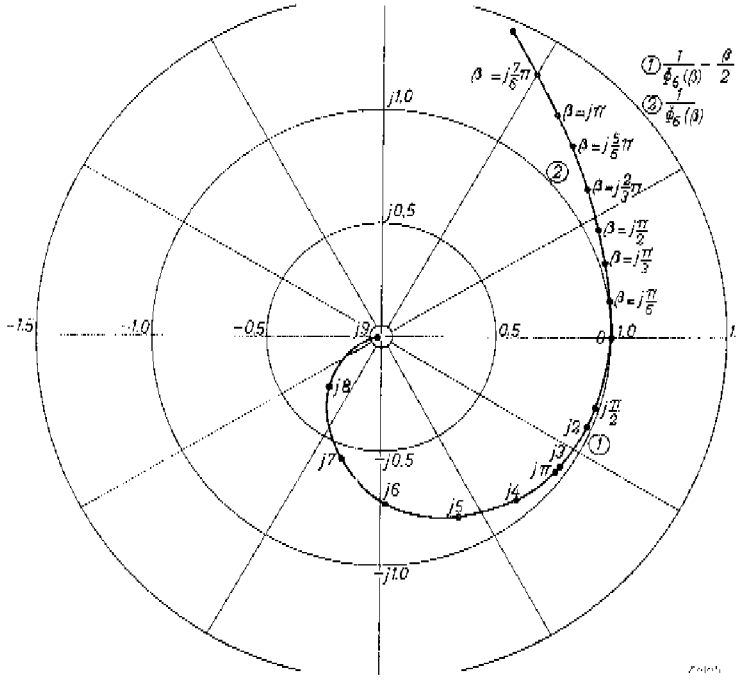

Fig. 14

For the cathode-grid space of a diode this transit time angle is given by (see eq. (42)):

$$\beta = j\,4{\cdot}19\,f_0\left(\frac{\sigma d}{I_a}\right)^{1/3}, \tag{46}$$

where f_0 is given in Gc/s, I_a in A/cm², σ in cm² and d in cm.

3.3. Calculation of the electronic admittances S_1 and S_2

The values of S_1 and S_2 will be expressed in the transconductance g_0 and the transit-time angles β_1 and β_2 for a triode without feedback (amplification factor $\mu = \infty$).

If a signal voltage $v_c'(t)$ is applied between the equivalent grid plane and the cathode, which voltage must be small in comparison with the d.c. voltages applied between the cathode and the grid, a current $i_c'(t)$ is caused to flow in the cathode-grid circuit. This current $i_c'(t)$ is given by:

$$i_c'(t) = h_{11}v_c'(t) = (S_1 + j\omega C_c)v_c'(t), \tag{47}$$

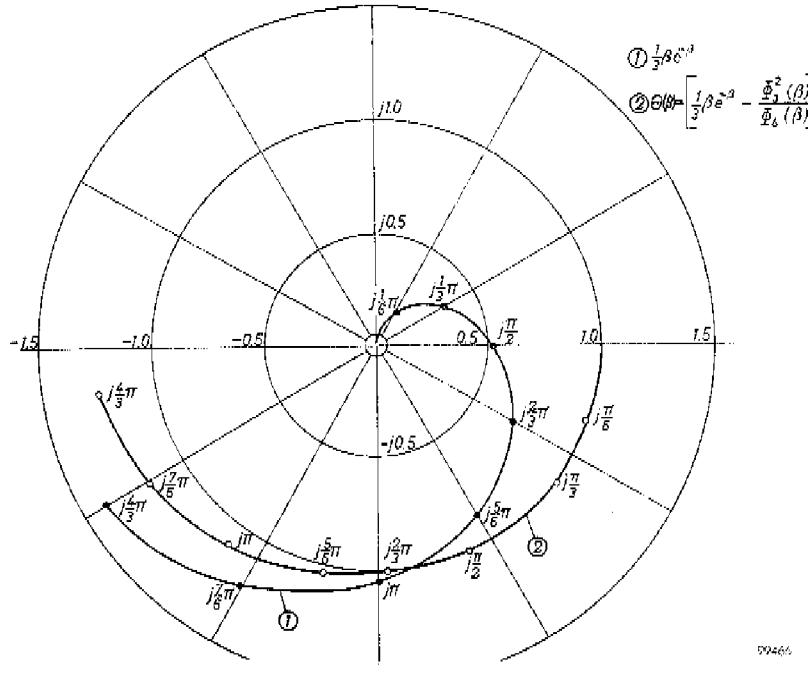

Fig. 15

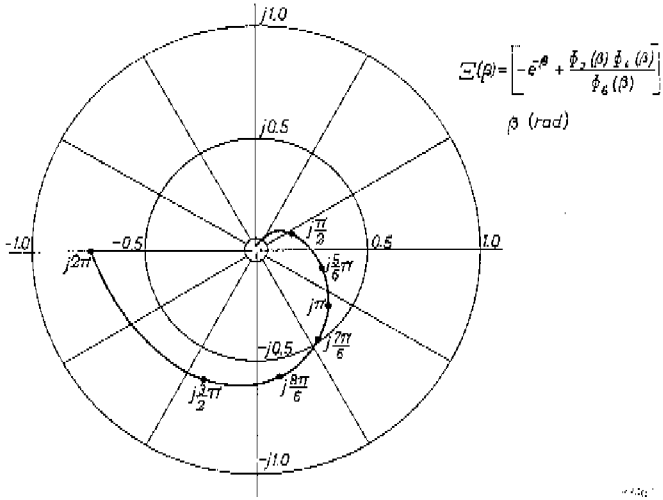

Fig. 16

Figs 12, 13, 14, 15, 16. Polar diagrams of transit time functions; the corresponding values of β have been plotted along the curves.

(cf. eqs (45a) and (4)). The value of b_{11} for complete space charge is given in table I.

The alternating convection current in the grid $q_g(t)$ is found from eq. (45b) to be equal to:

$$q_g(t) = b_{21} v_c'(t).$$

The current in the anode-grid circuit, due to this convection-current modulation is found from eqs (45a) and (4) to be equal to:

$$i_a'(t) = -b_{21} b_{12}' v_c'(t) = -S_2 v_c'(t), \tag{48}$$

where the prime of b_{12}' denotes that this transit-time coefficient corresponds to the case of negligible space charge in the anode-grid space. Of course $v_c'(t)$ also causes a velocity modulation in the grid plane and this velocity modulation causes another current to flow in the anode circuit. If, however, the d.c. anode voltage is much larger than the equivalent d.c. grid voltage this current can be neglected as is confirmed by the value of the transit-time coefficients for this case.

Substituting the values found for the transit-time coefficients from table I in eqs (47) and (48) gives

$$S_1 + j\omega C_e = \frac{g_0}{\Phi_6(\beta_1)} \text{ and } S_2 = \frac{g_0 \Phi_3(\beta_1)\Phi_3(\beta_2)}{\Phi_6(\beta_1)}, \tag{49}$$

where g_0 is the low frequency transconductance. For decreasing frequencies both $\Phi_3(\beta)$ and $\Phi_6(\beta)$ approach unity so that S_1 and S_2 approach g_0, the low frequency value of the transconductance.

3.4. Noise fluctuations at the cathode and the potential minimum

After having expressed the values of S_1 and S_2 in terms of the transit-time coefficients b_{nm} we now come to the calculation of the short-circuit noise currents i_1 and i_2. The assumptions made in order to be able to perform this calculation, viz. the application of the single-velocity transit-time theory, make a more detailed discussion of the present state of knowledge concerning the noise behaviour of an electron stream in the vicinity of the cathode necessary.

The electrons emitted by a thermionic cathode have an almost Maxwellian velocity distribution. The random fluctuations occurring in the emitted electron stream are due to the fact that the emission of each single electron is completely independent of the emission of any other electron. Therefore the shot noise occurring in any one velocity interval of the Maxwellian velocity distribution is uncorrelated with the shot-noise in any other interval.

From the facts summarised above it can be concluded that the random fluctuations of an electron stream at the cathode surface can be divided into two types of fluctuations (sec. 14.3 of ref. [11]).

The first one is the fluctuation in the instantaneous value of the average convection current. Its mean square value is given by the well known shot-noise equation

$$\overline{q_1^2(t)} = 2eI_e\delta f, \tag{50}$$

where I_e is the emitted current and δf is the bandwidth. Equation (50) is known as Schottky's theorem [40]).

The second type is the fluctuation in the instantaneous value of the average electron velocity. Its mean square value has been shown by Rack to be equal to [19])

$$\overline{u_1^2(t)} = \frac{4kT_c e}{mI_e}\left(1 - \frac{\pi}{4}\right)\delta f, \tag{51}$$

where T_c is the cathode temperature.

The r.m.s. value of the electron velocity is found by averaging the Maxwellian velocity distribution of the emitted electrons over all velocity classes. The result is

$$\sqrt{\overline{u_e^2}} = \sqrt{\frac{\overline{2kT_c}}{m}}, \tag{52}$$

where u_e is the velocity of an emitted electron.

The fluctuations $q_1(t)$ and $u_1(t)$ at the cathode surface can be proved to be uncorrelated, (cf. ref [11]) page 370).

The fluctuations present in the electron stream at the cathode surface give rise to fluctuations at the potential minimum. The relation between the noise near the cathode and the noise near the potential minimum has been the subject of intensive study. At low frequencies the influence of the space charge in the vicinity of the potential minimum on the fluctuations results in an almost complete suppression of the convection-current fluctuation in the stream of electrons which passes the potential minimum [41]). Based on the presence of only the velocity fluctuation Rack [19]) calculated the noise currents in a triode at low frequencies. His results are in good agreement with the experiments.

At high frequencies, no exact analytical description of the propagation of the fluctuations between the cathode and the potential minimum can be given. However, a numerical calculation, performed by Tien and Moshman [42]) showed that the convection-current fluctuation in the electron stream beyond the potential minimum is not suppressed at high frequencies and can even be amplified when the frequency considered becomes comparable with the plasma frequency of the space charge near the potential minimum. The velocity fluctuations in the electron stream beyond the potential minimum appeared to be unaffected by the space-charge action and uncorrelated with the convection current fluctuations. Studies by Whinnery [43]) and by Watkins, Bloom and

Siegman [44]) showed the same results and seem to indicate that the amount of amplification of the convection-current fluctuation depends on the ratio of the saturation current of the cathode and the anode current.

The studies referred to above are restricted to the one-dimensional case, which means that the electron emission is at every moment constant over the whole cathode surface and that the direction in which the electrons are emitted is always perpendicular to the cathode surface.

For several reasons the problem is essentially three dimensional in an actual triode. In the first place the emission of the electrons from one point of the cathode is independent of the emission from any other point on the cathode surface. In the second place the grains from which the porous tungsten cap of the L-cathode has been sintered, have dimensions comparable with the distance between the cathode and the potential minimum. Therefore the work function and the saturation current vary considerably over similar distances since they depend, for example, on the lattice plane of the tungsten crystals in the surface of the cathode. In the third place, transverse velocities will be unsuppressed since in a microwave triode there is no focussing magnetic field. Therefore electrons coming from different points of the cathode surface will intermingle. Finally the geometrical roughness of the cathode surface and the cathode diameter being much larger than the cathode-grid distance emphasise the complicated nature of the processes occuring between the cathode and the potential minimum.

We therefore start with a simplified model for the electron motion in the vicinity of the cathode, in order to calculate the short-circuit noise currents i_1 and i_2 in a microwave triode.

3.5. Simplified model for the calculation of the noise currents

In order to obtain a simplified model, the complicated electron motion between the cathode and the potential minimum is assumed to be replaced by a much simpler one to which the single-velocity transit-time theory can be applied. This means that all electrons are assumed to be emitted with the same velocity u_e and that there are no returning electrons. The same assumption has also been made in secs 3.2 and 3.3 for the calculation of Child's law and the electronic admittances S_1 and S_2. At a sufficiently high current density this model provides a good approximation for the triode admittances as will be shown by the experiments discussed in chapter 5.

However, when using this model it is impossible to account for the effect of the space charge between the cathode and the potential minimum on the random fluctuations which are present in the electron stream crossing the potential minimum. It is also impossible to account for multi-velocity effects which are caused by the electron velocity spread being of the same order of magnitude as the average velocity [45]). Therefore the results of these effects

are assumed to be already present in the electron stream at the cathode surface of the model.

Based on the assumptions discussed above we arrive at the following set of properties of the electron stream at the cathode surface:

(1) The average electron velocity at the cathode surface, u_c, is given by

$$u_c = \sqrt{\frac{2kT_c}{m}}, \tag{52a}$$

which is the r.m.s. value of the emission velocities of a cathode with a temperature T_c, see eq. (52).

(2) If the bandwidth considered is sufficiently small the fluctuation of the convection current can be described as an almost sinusoidal modulation [46]). The amplitude is given by the well-known shot-noise equation multiplied by *a factor L, which translates the effect of the space charge between the cathode and the potential minimum in an actual triode into a modified convection current fluctuation at the cathode surface of the simplified model.* Therefore at the cathode surface of the simplified model the convection-current modulation is given by

$$q_1(t) = L\sqrt{2eI_a\delta f}\ \mathbf{q}, \tag{53}$$

where $\mathbf{q}$ is a unit vector having the same argument as $q_1(t)$ and I_a is the cathode current. At low frequencies the factor L is equal to Spenke's space-charge suppression factor Γ [41]). At high frequencies it must also account for the space charge influence on the convection-current fluctuation such as the amplification of this fluctuation for frequencies near the plasma frequency of the space charge at the potential minimum [42]).

(3) In a similar manner the velocity fluctuation can be considered as an almost sinusoidal modulation [46]) superposed on the average velocity with its amplitude and phase given by

$$u_1(t) = K\sqrt{\frac{4kT_c}{mI_a}\frac{e}{\left(1-\frac{\pi}{4}\right)}\delta f}\ \mathbf{u}, \tag{54}$$

where $\mathbf{u}$ has the same argument as $u_1(t)$. This equation for $u_1(t)$ is the Rack velocity fluctuation at the cathode surface multiplied by a factor K. *This factor K accounts for the space-charge action near the potential minimum of a triode, which action is not described in the simplified model.* The value of K equals unity for low frequencies as has been found from the measurement of the equivalent noise-resistance. At high frequencies its value too equals unity for the one-dimensional case [42]) [44]). For the complicated three dimensional case its value may depart from unity.

(4) Although the velocity and the convection-current fluctuations are uncorrelated at the cathode surface of a triode, correlation can result from space-charge

action in the vicinity of the potential minimum and the multi-velocity effect in the accelerating region immediately beyond the potential minimum. The latter effect has been discussed by Siegman, Watkins and Hsieh [45]). Since these effects cannot be expressed by the single-velocity theory of the simplified model it will be assumed that both modulations $q_1(t)$ and $u_1(t)$ are partly correlated. The complex correlation constant $pe^{j\phi}$ is defined by

$$pe^{j\phi} = \frac{q_1(t)u_1^*(t)}{\{q_1(t)q_1^*(t)\ u_1(t)u_1^*(t)\}^{1/2}} = \mathbf{qu}^*, \tag{55}$$

where the averaging process is extended over a time which is much longer than the period of the frequency considered.

Measurements of the four characteristic noise quantites R_n, G_r, ζ and κ, cf. eq. (32), can be used to find the values of K, L, p and ϕ characterising the space charge action and the influence of the multi-velocity effect on the fluctuations in the stream of electrons crossing the potential minimum.

Noise measurements performed on electron-beam amplifiers can be used to find a similar set of quantities K, L, p and ϕ based on the same model of the electron motion in the vicinity of the cathode. Although the noise figure of a microwave triode is higher by a factor of 10 than that of an electron-beam amplifier, the noise quantities K, L, p and ϕ must be of the same order of magnitude, since in both types of amplifiers the cathode is the main source of noise. The agreement between these noise quantities K, L, p and ϕ with the corresponding noise quantities in electron-beam tubes has been found from the experiments discussed in chapter 5.

3.6. Calculation of the short-circuit noise currents i_1 and i_2

In sec. 2.7 we have shown that the short-circuit noise-currents in an ideal triode (no feedback; $\mu = \infty$) can be related to the noise sources E' and J'. Therefore we start from the initial fluctuations given by eqs (53) and (54) and calculate the short-circuit noise currents using eq. (52a), the Llewellyn-Peterson equations given by eq. (45) and table I. The total noise-current in the cathode-grid space is (see fig. 9, sec. 2.7):

$$i_1(t) = b_{12}q_1(t) + b_{13}u_1(t), \tag{56}$$

since the voltage $v(t)$ between the cathode and the grid is zero. The convection current $q_g(t)$ in the grid plane is

$$q_g(t) = b_{22}q_1(t) + b_{23}u_1(t).$$

The total current in the anode-grid space is given by

$$i_2(t) = b_{12}'q_g(t) + b_{13}'u_g(t),$$

where $u_g(t)$ is the velocity fluctuation in the grid and the primes denote that the transit-time coefficients b_{mn} must be taken for the anode-grid space. As

has been done in sec. (3.3) the term $u_g(t)b_{13}'$ will be neglected since the anode voltage is much larger than the grid voltage. Therefore

$$i_2(t) = b_{12}'\{b_{22}q_1(t) + b_{23}u_1(t)\}. \tag{57}$$

When we now combine eqs (28), (47), (48), (56) and (57) we find for the noise sources E' and J'

$$E' = \frac{b_{22}}{b_{21}}\, q_1(t) + \frac{b_{23}}{b_{21}}\, u_1(t) \tag{58}$$

and

$$J' = \left(\frac{b_{22}b_{11}}{b_{21}} - b_{12}\right) q_1(t) + \left(\frac{b_{23}b_{11}}{b_{21}} - b_{13}\right) u_1(t). \tag{59}$$

The equations for E' and J' permit the calculation of the characteristic noise quantities R_n, G_r, ζ and κ (defined in eq. (32)). In order to do this we first substitute the values of the coefficients b_{nm}.

3.7. Substitution of the transit-time coefficients

The transit-time coefficients as found in table I will be substituted in the eqs (58) and (59). These equations relate the noise-voltage source and the noise-current source of an ideal triode, having an infinitely high amplification factor and without any feedback, to the transit-time angle β_1 of the electrons in the cathode-grid space and the transconductance. The latter is given by

$$g_0 = \frac{3eI_a}{m(u_c + u_g)^2} \tag{60}$$

where u_c and u_g are the d.c. velocities of the electrons at the cathode surface and in the grid plane, respectively.

From eqs (58) and (60) together with eqs (52a), (53), (54) and table I we find for the noise-voltage source *)

$$E' = \sqrt{\frac{4kT_c}{g_0}\, 3\left(1 - \frac{\pi}{4}\right)\delta f}\, \frac{\Phi_6}{\Phi_3}\left(K\Theta\mathfrak{u} + \frac{L}{3\sqrt{1 - \frac{\pi}{4}}}\,\Xi\mathfrak{q}\right), \tag{61}$$

where Φ_3, Φ_6, Θ and Ξ are transit time functions of β_1 which are drawn in the figs 12, 14, 15 and 16.

In an analogous manner we find for the noise-current source:

$$J' = \sqrt{4kT_c g_0\, 3\left(1 - \frac{\pi}{4}\right)\delta f}\left(\frac{\beta_1 e^{-\beta_1}}{3\Phi_3}\right)\left(K\mathfrak{u} - \frac{L}{\beta_1\sqrt{1 - \frac{\pi}{4}}}\,\mathfrak{q}\right). \tag{62}$$

*) Since in eqs (58) and (59) only the transit time coefficients of the cathode-grid space occur, which have the argument β_1 only, we shall not repeat this transit time angle β_1 in the following equations.

Eqs (61) and (62) give the noise-voltage source E' and the noise-current source J' of an "ideal" triode without feedback ($\mu = \infty$) on the basis of the simplified model of sec. 3.5.

3.8. Application of the theory at very low frequencies

At very low frequencies the noise-convection current can be supposed to be suppressed by space-charge action. Therefore we neglect $q_1(t)$ [41][42].

If in eq. (61) the coefficient K is equal to unity we find for the noise voltage source

$$E' = \sqrt{\frac{4kT_e}{g_0} 3\left(1 - \frac{\pi}{4}\right)\delta f}\ \frac{\Phi_6}{\Phi_3}\Theta\mathbf{u}. \tag{63}$$

Therefore, for the equivalent noise resistance R_n, defined in eq. (32) we find:

$$R_n = \frac{1}{g_0}\frac{T_e}{T} 3\left(1 - \frac{\pi}{4}\right)\left|\frac{\Phi_6\Theta}{\Phi_3}\right|^2, \tag{64}$$

where T is room temperature.

The last factor of this equation, expressing the effect of the electron transit time on the noise resistance, approaches unity at low frequencies.

Equation (64) is, strictly speaking, only correct for a triode with an infinitively high amplification factor μ in which the applied grid voltage is equal to the effective grid voltage. However, we want to express the high-frequency characteristic noise quantities, which will be calculated later, in terms of the equivalent-noise resistance and the transconductance which are measured at low frequencies in a triode with a finite amplification factor μ. Therefore it is useful to discuss here the difference between values calculated for R_n and g_0 when $\mu = \infty$ and those measured, which will be called R_{eq} and g_m respectively.

The relation between the applied d.c. grid voltage V_g and the equivalent d.c. grid voltage V_e is given by *)

$$V_e = \frac{V_g + \frac{1}{\mu}V_a}{1 + \frac{1}{\mu}\left(1 + \frac{4\,d_{ag}}{3\,d_{cg}}\right)} \quad \text{or} \quad \frac{\partial V_e}{\partial V_g} = \xi = \left\{1 + \frac{1}{\mu}\left(1 + \frac{4\,d_{ag}}{3\,d_{cg}}\right)\right\}^{-1}, \tag{65}$$

where d_{cg} and d_{ag} are the cathode-grid distance and the anode-grid distance, respectively. The relation between g_m and g_0 is then

$$g_m = g_0 \frac{\partial V_e}{\partial V_g} = g_0\,\xi. \tag{66}$$

*) Equation (65) is found easily from the equivalent circuit, discussed in the preceding chapter consisting of the capacity μC_a in the grid lead and the capacities C_a and C_c. The total charge of the three capacities is constant and when space charge is present C_c must be increased to $4/3 C_c$. Furthermore $C_a d_{cg} = C_a d_{ac}$.

It will be clear that the anode noise current in a triode and that in a diode are equal if the cathodes are identical, if the anode currents are the same and if the anode voltage of the diode is equal to the equivalent grid voltage of the triode. Using this it can be proved that [11])

$$R_{eq}\, g_m{}^2 = R_n\, g_0{}^2. \tag{67}$$

Combining eqs (64), (66) and (67) we find:

$$R_{eq}\, g_m = \frac{1}{\xi}\frac{T_e}{T} 3\left(1 - \frac{\pi}{4}\right). \tag{68}$$

This equation has been tested experimentally. It gives a good approximation for the equivalent noise resistance of a triode. The product of R_{eq} and g_m theoretically turns out to be 3·85 for an EC 57; the measured value is generally $\approx$4, for reasons which will be discussed later.

3.9. Characteristic noise quantities of a microwave triode

The four characteristic noise quantities are defined in eq. (32). We repeat these definitions in a somewhat different form:

$$R_n = \frac{\overline{E'E'^*}}{4kT\delta f};\; G_r = \frac{\overline{J'J'^*}}{4kT\delta f} \text{ and } \zeta + j\kappa = \frac{\overline{2E'J'^*}}{4kT\delta f}.$$

The primes in these equations denote that the internal feedback will not yet be taken into account. The characteristic noise quantities are now calculated by substituting eqs (61) and (62) in the equations defining R_n, G_r, ζ and κ. The product $\overline{qu}^*$ occurring in the equations is replaced by $pe^{j\phi}$, in accordance with eq. (55). Equations (66) and (67) can be used in order to relate the noise quantities calculated for high frequencies to the equivalent noise resistance and the transconductance measured at low frequencies. Working through the straight forward algebra and using the first three properties of the transit time functions listed in appendix 1 we find for the four characteristic noise quantities at high frequencies:

$$R_n(\omega) = R_n \left|\frac{\Phi_6}{\Phi_3}\right|^2 \left(K^2|\Theta|^2 - \frac{2KLp\sin\phi}{3\sqrt{1-\frac{\pi}{4}}}|\Theta\Xi| + \frac{L^2|\Xi|^2}{9\left(1-\frac{\pi}{4}\right)}\right), \tag{69}$$

$$G_r(\omega) = R_n\, g_0{}^2 \left|\frac{\beta_1}{3\Phi_3}\right|^2 \left(K^2 - \frac{2KLp\sin\phi}{|\beta_1|\sqrt{1-\frac{\pi}{4}}} + \frac{L^2}{|\beta_1|^2\left(1-\frac{\pi}{4}\right)}\right), \tag{70}$$

$$\zeta(\omega) = -2R_n\, g_0 \frac{KLp\cos\phi}{|\Phi_3|^2\sqrt{1-\frac{\pi}{4}}}\left|\frac{\beta_1\Phi_6}{3}\right|\left(\left|\frac{\Theta}{\beta_1}\right| - \left|\frac{\Xi}{3}\right|\right), \tag{71}$$

$$\kappa(\omega) = -2R_n g_o \frac{1}{|\Phi_3|^2} \left\{ \left| \frac{\beta_1 \Phi_6}{3} \left(K^2 \Theta + \frac{L^2 \Xi}{3\beta_1 \left(1 - \frac{\pi}{4}\right)} \right) \right|^2 - \left| \frac{\beta_1 \Phi_6}{3} \right| \frac{KL\rho \sin \phi}{\sqrt{1 - \frac{\pi}{4}}} \left(\left| \frac{\Theta}{\beta_1} \right| + \left| \frac{\Xi}{3} \right| \right) \right\}. \quad (72)$$

Using these equations, the measured noise quantities at high frequencies can be related to the four quantities K, L, p and ϕ, which characterise the noise in the vicinity of the cathode. At low frequencies, where p can be assumed to be zero since the transit time of the electrons between the cathode and the potential minimum is much smaller than the period of the frequency considered, ζ is always zero [48]). This is in agreement with measurements. In order to be able to compare the four quantities with the corresponding quantities of electron beam amplifiers, some results of the theory of noise in electron-beam amplifiers will be summarised.

3.10. Noise in electron-beam amplifiers

The noise properties of electron-beam amplifiers have been the subject of intensive study. As has already been noted earlier their noise figure is much lower than the noise figure of triodes, although in both types of amplifiers the cathode is the most important source of noise. In this section we shall give an outline of the results of the theory on the noise in electron-beam amplifiers.

Haus [46]) has shown that if the bandwidth considered is sufficiently small the noise behaviour of electron-beam amplifiers can be described in terms of the power-density spectra of the convection-current fluctuation and the velocity fluctuation and of the cross-power density spectrum of both fluctuations. In order to exclude multi-velocity effects, these fluctuations must be considered in a cross section of the beam where the electron velocity spread is much smaller than the average electron velocity. The power density spectra Φ_b, Ψ_b, Λ_b and Π_b for the considered frequency band and in such a cross section of the beam are given by [46])*)

$$|U_b(t)|^2 = \left\{ -\frac{u_0 u_b(t)}{\eta} \right\}^2 = 4\pi \Phi_b \delta f,$$

$$|q_b(t)|^2 = 4\pi \Psi_b \delta f,$$

$$U_b(t) q_b^*(t) = 4\pi (\Pi_b - j\Lambda_b) \delta f, \quad (73)$$

*) Note the analogy between these definitions and the definitions of the characteristic noise quantities, eq. (32). The consequences of this have been discussed elsewhere by the author [47]).

where u_0 is the mean electron velocity and u_b is the fluctuation of its instantaneous value.

The quantity $U_b(t)$ is referred to as the kinetic voltage, the suffix b indicates that the power-density spectra must be taken in a cross section that is sufficiently far from the cathode to exclude multi-velocity effects. It can be proved that Π_b, which is a measure of the noise power on the beam is constant along the beam. Furthermore a quantity S_b, which is a measure for the noise standing wave pattern on the beam and which is defined by $S_b^2 = \Phi_b \Psi_b - \Lambda_b^2$, is too invariant along the beam. S_b and Π_b are only invariant if there is no power exchange between the beam and its surroundings. Haus and Robinson [16]) have shown that the minimum obtainable noise figure of every electron-beam amplifier operating under this condition is given by

$$(F_{\min} - 1) = \frac{2\pi}{kT}(S_b - \Pi_b)\left(1 - \frac{1}{g}\right), \tag{74}$$

where g is the gain of the amplifier.

In order to compare the random fluctuations of electron-beam amplifiers and of microwave triodes we apply the simplified model of the electron motion in the vicinity of the cathode, as has been discussed in sec. 3.5, also to electron beam amplifiers. Then the quantities Φ, Ψ, Π and Λ can also be defined at the cathode surface which is symbolised by the index a. They can also be related to the four quantities K, L, p and ϕ. Substituting eqs (52a), (53) and (54) into the definitions (73) we find:

$$S_a = \sqrt{\Phi_a \Psi_a - \Lambda_a^2} = \frac{kT_c KL}{2\pi}\sqrt{(4-\pi)(1-p^2\sin^2\phi)} \tag{75}$$

and

$$\frac{\Pi_a}{S_a} = \frac{p\cos\phi}{\sqrt{1-p^2\sin^2\phi}}. \tag{76}$$

Using this we find for the minimum noise figure

$$F_{\min} - 1 = KL\,\frac{T_c}{T}\,(4-\pi)^{1/2}\{(1-p^2\sin^2\phi)^{1/2} + p\cos\phi\}. \tag{77}$$

Now we have the possibility to estimate the minimum noise figure for an electron-beam amplifier using the values of K, L, p and ϕ which have been calculated from measurements performed on a microwave triode provided that the electron-beam amplifier is equipped with an identical cathode.

In a later chapter it will be shown that experimental values of K, L, p and ϕ indeed give a noise figure of electron-beam amplifiers which is much lower than the triode noise figure and which is of the correct order of magnitude. This agreement supports the simplified model of sec. 3.5 which is essentially an extension of the low-frequency theories of the triode noise behaviour.

3.11. Other noise sources in a triode

Up to now only the noise caused by the random fluctuations in the cathode emission and the effect of the space charge in the potential minimum on these fluctuations has been taken into account. In sec. 1.3(*b*) several other effects which possibly result in additional noise currents have already been discussed. They are:

(1) electron reflection at the anode surface,
(2) spread in the transit times of the electrons,
(3) fluctuations in the electron stream which returns to the cathode in front of the potential minimum,
(4) feedback.

The noise from these effects must be estimated separately since otherwise it is hidden in the factors K, L, p and ϕ. The discussion of the points (2), (3) and (4) will be postponed to chapter 5 where it will be shown that they have little effect on the noise behaviour of microwave triodes. The noise source mentioned in (1), as has been shown by Talpey and MacNee [20]), has a major effect on the induced grid noise $i_1(t) - i_2(t)$, at intermediate frequencies (say 30 Mc/s). At microwave frequencies this effect is relatively smaller. In order to obtain some insight into this matter we first give a discussion on the induced-grid noise at intermediate frequencies and then estimate the influence of the reflection on the characteristic noise quantities.

(*a*) *Noise currents at intermediate frequencies*

The induced grid noise current $i_1(t) - i_2(t)$ can be found from eqs (56) and (57) to be given by

$$i_1(t) - i_2(t) = (b_{12} - b_{12}'b_{22})q_1(t) + (b_{13} - b_{12}'b_{23})u_1(t). \tag{78}$$

If we substitute the transit-time coefficients b_{nm} from table I and approximate the transit-time functions by the first terms of their series expansion, we find, assuming that $u_c \ll u_g$:

$$\overline{i_1(t) - i_2(t)} = \sqrt{12kT_c g_m \left(1 - \frac{\pi}{4}\right) \delta f} \left\{ \left(\frac{\beta_1}{3} + \frac{2\beta_2}{3} \right) \mathbf{u} + \sqrt{\frac{L^2}{9\left(1 - \frac{\pi}{4}\right)}} \mathbf{q} \right\}, \tag{79}$$

where K is put equal to unity as is known to be the case at low frequencies. L is for low and intermediate frequencies equal to the noise suppression factor of Shottky and Spenke [41]). If we take $\mathbf{u}$ and $\mathbf{q}$ to be uncorrelated the mean square value of the induced grid noise current is equal to:

$$\overline{|i_1(t) - i_2(t)|^2} = 4kTR_{eq}\, g_m^2\, \delta f \left\{ \frac{1}{9} |\beta_1 + 2\beta_2|^2 + \frac{\Gamma^2}{9\left(1 - \frac{\pi}{4}\right)} \right\}, \tag{80}$$

which equation becomes equal to Bakkers' equation when Γ^2 is put equal to zero [49]). However, if we substitute the values for an EC 57 with an anode current density of 0·45 A/cm^2 and a saturation current density of 3 A/cm^2 then Γ^2 appears to be equal to 0·078*). Substituting now the values of the transit time angles for 100 Mc/s ($\beta_1 \approx j\pi/40$ and $\beta_2 \approx j\pi/80$) in eq. (80) it appears that the contribution of the convection current fluctuation to the induced grid noise is of the same order of magnitude as that of the velocity fluctuation:

$$\overline{|i_1(t) - i_2(t)|^2} = 4kTR_{eq}\, g_m^2\, \{27 + 31\}10^{-4}\delta f. \qquad (80a)$$

The relatively large contribution of the convection-current fluctuation to the induced grid current at intermediate frequencies is explained by the fact that $i_1(t)$ and $i_2(t)$, which are caused almost completely by the velocity fluctuation (Rack [19]), have only a small difference in phase and amplitude. Therfore $i_1(t) - i_2(t)$ is small in comparison with $i_1(t)$ or $i_2(t)$. Small effects such as the convection current fluctuation or the noise caused by reflected electrons, having nearly no influence on the short-circuit noise currents $i_1(t)$ and $i_2(t)$ themselves, enlarge the induced grid noise $i_1(t) - i_2(t)$ considerably. Indeed the reflected electrons appear experimentally to have an important effect on the induced grid noise [20]) [39]).

(b) Influence of reflected electrons at high frequencies

Since the value of $i_1(t) - i_2(t)$ is at microwave frequencies not small in comparison with $i_1(t)$ or $i_2(t)$ one might expect that the influence of the reflected electrons on the induced grid noise current is rather small at 4000 Mc/s. However, there is another effect at high frequencies. The transit time angle of the reflected electrons is increased. This results in the fact that the current pulses induced have large fourier components at 4000 Mc/s. It is therefore necessary to make an estimate of the effect of the reflection of electrons on the four characteristic noise quantities of a microwave triode.

There are two mechanisms which result in a noise contribution of the reflected electrons to the noise currents in a triode [39]). First, since a fraction of the primary electron stream is reflected, the same fraction of the fluctuations present in this primary stream again crosses the anode-grid space inducing additional noise current pulses. Because only 2 or 3% of the electrons are reflected the noise currents $i_1(t)$ and $i_2(t)$ and their difference change somewhat, but not enough to change the characteristic noise quantities essentially.

The second mechanism is due to the fact that also the chance that some electron is reflected or not obeys the laws of statistics so that a new shot noise occurs in the stream of reflected electrons, which is uncorrelated with the pri-

*) The value of Γ^2 can be found in fig. 15 of ref. [41]); the geometry of the triode is given in sec. 5.3.

mary random fluctuations due to the random emission of electrons. Therefore we may assume that a noise convection current

$$q_r(t) = \sqrt{2e\, I_a r\, \delta f}\, \mathbf{q}_r, \tag{81}$$

r being the reflection coefficient and $\mathbf{q}_r$ the unit vector with the same argument as $q_r(t)$, has its origin at the anode.

Theoretically the reflected electrons can return as far as the potential minimum since the velocity of the reflected electrons is about the same as the velocity of the primary electrons. However, the velocity component in the direction perpendicular to the anode surface is nearly always smaller. The reasons are that the direction of the reflected electrons is distributed according to a $\cos^2\theta$-law, as Jonker [50]) has shown, and that the heterogeneity of the electric field in the vicinity of the grid wires scatters the reflected electrons. Therefore it may be assumed that the reflected electrons reach the grid and then return to the anode. This assumption is justified at low frequencies by the experience that the space-charge suppression action of the potential minimum is not influenced by reflected electrons as is the case in plane-parallel diodes.

The transit-time angle is taken to be β_r, which is, of course, twice the transit time angle of the primary electrons flowing from the grid to the anode.

From eq. (45) it follows, that the reflected electrons going from anode to grid induce a current

$$i_{2r}'(t) = b_{12}' q_r(t) \tag{82}$$

in the anode grid circuit. Since the electrons are injected at the electrode with the highest potential (the anode) b_{12}' is found in table I to be about $\Phi_2(\beta_r/2)$. The convection current fluctuation near the grid plane is

$$q_{gr}(t) = b_{22}' q_r(t) - e^{-1/2\beta_r}\, q_r(t).$$

The current induced in the anode grid circuit by the reflected electrons returning to the anode $i_{2r}''(t)$ which is given by $q_{gr}(t) b_{12}'$ must be added to $i_{2r}'(t)$, bearing in mind that these electrons travel from a low potential to a high potential. Therefore, using the properties of the transit time functions given in the appendix:

$$i_{2r}(t) = q_r(t) \left\{ \Phi_2\left(\frac{\beta_r}{2}\right) - e^{-1/2\beta_r}\, \Phi_3\left(\frac{\beta_r}{2}\right) \right\} = \frac{2}{3}\, q_r(t)\, \beta_r \Phi_4(\beta_r), \tag{83}$$

in which $q_r(t)$ is uncorrelated with $u_1(t)$ and $q_1(t)$. The characteristic noise quantities calculated from $i_{2r}(t)$ are uncorrelated with those calculated from the primary short circuit noise current $i_1(t)$ and $i_2(t)$ and can therefore simply be added to the noise quantities due to the primary electron stream.

Since $i_{1r}(t)$ is zero the noise sources due to the reflections are (see eq. (28) with $i_1 = 0$):

$$E_r' = -\frac{i_{2r}(t)}{S_2} \text{ and } J_r' = -\frac{S_1}{S_2} i_{2r}(t). \tag{84}$$

Using the definitions in eq. (32) and the eqs (45), (49) and (83) we calculate from eq. (84):

$$R_{nr} = \frac{80 r I_a}{9 g_m^2} \left| \frac{\beta_r \Phi_4(\beta_r)}{\Phi_3(\beta_1)\Phi_3(\beta_2)} \right|^2 |\Phi_6(\beta_1)|^2, \tag{85}$$

$$G_{rr} = \frac{80 r I_a}{9} \left| \frac{\beta_r \Phi_4(\beta_r)}{\Phi_3(\beta_1)\Phi_3(\beta_2)} \right|^2, \tag{86}$$

$$\zeta_r = \frac{160 r I_a}{9 g_m} \left| \frac{\beta_r \Phi_4(\beta_r)}{\Phi_3(\beta_1)\Phi_3(\beta_2)} \right|^2 \operatorname{Re}\{\Phi_6(\beta_1)\}, \tag{87}$$

$$\kappa_r = \frac{160 r I_a}{9 g_m} \left| \frac{\beta_r \Phi_4(\beta_r)}{\Phi_3(\beta_1)\Phi_3(\beta_2)} \right|^2 \operatorname{Im}\{\Phi_6(\beta_1)\}. \tag{88}$$

It will appear later that these noise quantities can be important but that they are not large enough to explain the large difference between the characteristic noise quantities at intermediate and those at microwave frequencies. A calculation performed by Benham and Harries [39]), including both mechanisms by which reflections contribute to the noise performance of a triode together with the Rack velocity fluctuation at the cathode only, led to a minimum noise figure of 6·6, or, when the anode is covered with BaO so that the reflection coefficient increases, of 13 both at 4000 Mc/s. The measured value, however, is about 50. Therefore we may expect that the convection current fluctuation must be included in the calculation.

The calculation of the reflection noise sources makes it possible to separate the effect of the reflected electrons on the triode noise from the effect of the cathode noise so that a comparison with the cathode noise in an electron beam tube, in which reflections can be avoided, is more realistic.

4. METHODS OF MEASUREMENT

4.1. Introduction

In this chapter the methods developed in order to measure the quantities describing the triode fourpole and its noise sources will be discussed. As has already been said earlier this triode fourpole can be imagined to consist of lumped circuit elements (sec. 2.1). However, it is impossible to connect the measuring devices, available at microwave frequencies, directly to the triode fourpole, i.e. the active space of the triode. Therefore the conventional methods for the measurement of fourpole characteristics cannot be applied.

The method developed for microwave frequencies is essentially the following. In both the input waveguide and the output waveguide of the triode amplifier

we define a reference plane. The coefficients of the fourpole equations and the characteristic noise quantities of the microwave circuit between both reference planes can be measured [61]).

The microwave circuit between the two reference planes can be split up into three fourpoles: the input fourpole, the triode fourpole and the output fourpole. The input fourpole is the passive circuit extending between the input reference plane and the cathode-grid space of the triode and therefore consists of a part of the input waveguide and of the cathode-grid structure of the triode. The output fourpole is the passive circuit between the output reference plane and the anode-grid space. Between both passive fourpoles lies the triode fourpole. All electromagnetic phenomena occurring in the input and output waveguides of the triode amplifier, such as the losses in the glass of the triode and the existence of cut-off modes in the vicinity of the triode, are described by the coefficients of the passive input and output fourpoles.

In order to calculate the quantities characterizing this triode fourpole from the quantities measured for the total microwave fourpole between the two reference planes, the properties of both the input fourpole and the output fourpole must be known separately. Therefore the first problem to be solved is the measuring of the coefficients of the fourpole equations of the in- and output fourpoles.

4.2. Input and output fourpoles

In fig. 17 a microwave triode amplifier has been sketched. The circuit between a reference plane AA′ and the cathode-grid space of the triode can be

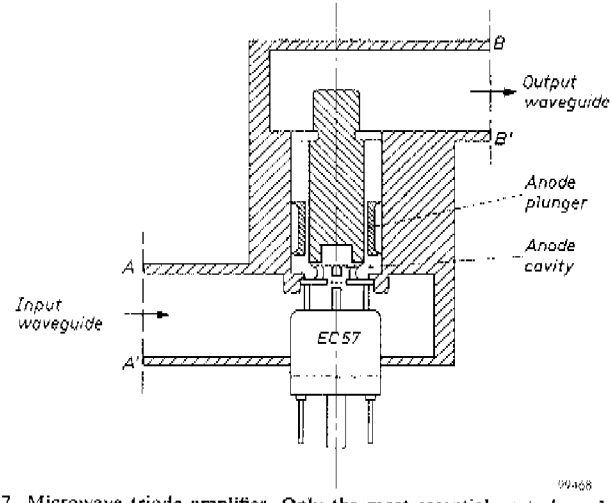

Fig. 17. Microwave triode amplifier. Only the most essential parts have been drawn. The planes AA′ and BB′ are the reference planes in the in- and output waveguides respectively.

described as a passive network (input fourpole). All discontinuities such as the cathode glass ring and the internal structure of the tube, and even the cathode-grid capacity in the absence of electrons, can be inserted into this network.

The same can be done with the circuit between the anode-grid space and the reference plane BB'. Thus we can describe the circuit of fig. 17 by three fourpoles in cascade (fig. 18).

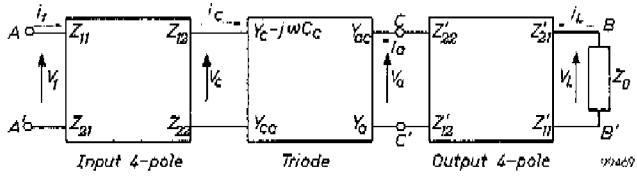

Fig. 18. Equivalent circuit of the triode amplifier in fig. 17.

Let the three fourpoles, referred to as the input fourpole, triode fourpole and output fourpole, be given by:

$$\left.\begin{aligned} v_1 &= i_1 Z_{11} - i_c Z_{12}, \\ v_c &= i_1 Z_{21} - i_c Z_{22}, \end{aligned}\right\} \tag{89}$$

$$\left.\begin{aligned} i_c &= (Y_c - j\omega C_c)\, v_c + Y_{ac} v_a, \\ i_a &= Y_{ca} v_c + Y_a v_a, \end{aligned}\right\} \tag{90}$$

$$\left.\begin{aligned} v_a &= -i_a Z_{22}' + i_L Z_{21}', \\ v_L &= -i_a Z_{12}' + i_L Z_{11}'. \end{aligned}\right\} \tag{91}$$

Since the input and output fourpoles are passive and reciprocal: $Z_{12} = Z_{21}$ and $Z_{12}' = Z_{21}'$. For reasons which will become clear later in this section we assume the cathode-grid capacity to be part of the input fourpole. Therefore the triode fourpole equations depart somewhat from the corresponding ones defined in chapter 2. The consequences of this difference will be discussed later in this section and, as far as noise is concerned, in sec. 4.12.

First the measurement of the input fourpole impedances will be discussed. When the input fourpole is loaded with three known lumped (in our case capacitive) impedances, measurement of the relative input impedance will be shown to give sufficient information on the input fourpole to allow of any unknown load impedance to be related to the relative impedance measured in the input waveguide [52]).

This relative impedance is found from the voltage standing wave pattern measured with a standing-wave ratio meter in the input waveguide.

The three different capacitive loads can be obtained by varying the filament current of the triode since in an EC 57 the cathode grid distance is a function of the cathode temperature [5]). The capacity variations, caused by changing the

filament current, can be measured in a bridge circuit at low frequencies. This is possible because at low and at high frequencies the form of the electric field is congruent and because in both cases there is no magnetic field between the cathode and the grid.

The relative input impedance of the fourpole is measured in the following three cases:

a. At the nominal filament current I_f. The cathode-grid capacitance C_e is supposed to be a part of the input fourpole. When the grid voltage is made so strongly negative that no electrons can penetrate into the cathode-grid space, total-emission damping is avoided. The input fourpole is now loaded with an infinite impedance. In this case the relative input impedance, ζ_a as follows from measurements with the standing-wave ratio meter in the input waveguide, is given by:

$$\zeta_a = \frac{Z_{11}}{Z_0}, \tag{92}$$

where Z_0 is the characteristic impedance of the waveguide.

b. At a somewhat higher filament current, $I_f + \Delta I_f$. Now the increase of capacity introduced is C_1, and the impedance change (compared with case a) is $Z_b = 1/j\omega C_1$. So the input fourpole is loaded with Z_b and the measured relative input impedance in the reference plane AA' is:

$$\zeta_b = \frac{Z_{11}}{Z_0} - \frac{Z_{12}^2}{Z_0 (Z_{22} + Z_b)}. \tag{93a}$$

c. At a heater current $I_f - \Delta I_f$. The capacity change is C_2, which is of course negative. This gives an impedance change $Z_c = 1/j\omega C_2$ (compared again with case a). The relative input impedance is

$$\zeta_c = \frac{Z_{11}}{Z_0} - \frac{Z_{12}^2}{Z_0 (Z_{22} + Z_c)}. \tag{93b}$$

From eqs (92), (93a) and (93b) Z_{12}^2/Z_0 and Z_{22} are found to be equal to

$$\frac{Z_{12}^2}{Z_0} = \frac{Z_c \quad Z_b}{1 \quad 1} \qquad (94)$$
$$\zeta_a - \zeta_c \quad \zeta_a - \zeta_b$$

and

$$Z_{22} = \frac{Z_c (\zeta_a - \zeta_c) - Z_b (\zeta_a - \zeta_b)}{\zeta_c - \zeta_b}, \tag{95}$$

or:

$$Z_{22} = \frac{Z_{12}^2}{Z_0 (\zeta_a - \zeta_b)} - Z_b = \frac{Z_{12}^2}{Z_0 (\zeta_a - \zeta_c)} - Z_c. \tag{95a}$$

When ζ_a, ζ_b and ζ_c have been measured we can deduce (after having determined Z_b and Z_c) the constants Z_{11}/Z_0, Z_{12}^2/Z_0 and Z_{22} from eqs (92), (94) and (95a).

If now the load impedance is Z_e (which can, for example, be caused by electron flow in the triode) this impedance is found from:

$$Z_e = \frac{Z_{12}^2}{Z_0(\zeta_a - \zeta_{in})} - Z_{22}, \tag{96}$$

where ζ_{in} is the relative input impedance in the input waveguide measured in this case.

In eq. (96) the quantities Z_{12}^2/Z_0, ζ_a and Z_{22} are known and ζ_{in} can be measured, so the value of Z_e, the input impedance of the triode fourpole, can be calculated. From this equation it can also be deduced that the value of Z_0 is not material to the calculation since it disappears from the results. The reason for this is that the input fourpole constants are measured by comparing actual impedances (capacitances) with relative impedances measured with a standing-wave ratio meter in the input waveguide.

In order to measure the output fourpole we must construct a dummy with variable anode-grid distance. The measurement can be performed in the same manner as in the case of the input fourpole. From these measurements we obtain

$$Z_{22}' \quad ; \quad \frac{Z_{12}'^2}{Z_0} \quad \text{and} \quad \frac{Z_{11}'}{Z_0} \quad .$$

as this fourpole is measured in the reverse direction (cf. fig. 18).

4.3. Measurement of the triode-fourpole admittances

With a knowledge of the properties of the input and output fourpoles the measured properties of the total fourpole between the two reference planes AA′ and BB′ (fig. 17) can be related to the properties of the triode fourpole only.

The triode fourpole is mainly characterized by the values of Y_c, Y_{ac} and Y_{ca}. The admittance Y_a is less important since it is mainly a capacitance (see eq. (21)). This capacitance is compensated by the susceptance of the tuned anode cavity. The real part of Y_a is much smaller than the conductivity of the anode circuit in parallel with Y_a.

We first discuss the determination of Y_c, which is the input admittance of the triode fourpole with short-circuited anode. This short circuit is approximated by detuning the anode cavity. (In practice, where the input admittance is measured as a function of the anode tuning, and therefore as a function of the anode plunger position, the input admittance for a completely detuned anode ($b_L = \pm\infty$) can be found from the input admittance circle which is discussed in sec. 2.5). Therefore, when the relative input impedance of the input fourpole is measured for the case of a detuned anode cavity this input fourpole is loaded

with $Y_c - j\omega C_c$. The capacitance $j\omega C_c$ must be substracted since this capacitance is assumed to be a part of the input fourpole (see sec. 4.2). From eqs (96) and (18) we find:

$$\frac{1}{Y_c - j\omega C_c} = \frac{1}{S_1} = \frac{Z_{12}^2}{Z_0(\zeta_a - \zeta_{in})} - Z_{22}, \tag{96a}$$

where ζ_{in} is the measured input impedance and ζ_a is defined in eq. (92).

We now come to the determination of the transadmittance Y_{ca} which is nearly equal to S_2. This admittance can be found from a comparison of the voltages in the output and input reference planes. These voltages are proportional to the electric field strengths in the reference planes. During the measurements of S_2 the anode-cavity plunger (fig. 1) was removed from the amplifier so that the triode fourpole was loaded with a non-resonant circuit consisting of a 23Ω coaxial line forming a part of the amplifier block. This 23Ω coaxial line is terminated in a matched load. Normally the triode is loaded with 1 kΩ when the anode cavity is tuned [6]). Therefore the anode-grid circuit can be assumed to be nearly short circuited, and the input admittance of the triode fourpole is S_1. The voltage gain of the triode fourpole, loaded with the input admittance Y_L of the output fourpole (see fig. 18), is given by

$$\frac{v_a}{v_c} = -\frac{Y_{ca}}{Y_L + Y_a} = -\frac{Y_{ca}}{Y_L} = \frac{S_2}{Y_L}, \tag{97}$$

where Y_L is much larger than Y_a.

The voltage gain between the reference planes AA′ and BB′ is calculated with the help of eq. (97), and is given by (see fig. 18)

$$\frac{v_L}{v_1} = \frac{v_L}{v_a}\,\frac{v_a}{v_c}\,\frac{v_c}{v_1} = \frac{Z_{12}\,Z_{12}'\,S_2}{Z_0\left(\frac{Z_{11}'}{Z_0}+1\right)\left(\frac{Z_{11}}{Z_0}+\frac{Z_{11}Z_{22}-Z_{12}^2}{Z_0}S_1\right)}. \tag{98}$$

The input and output fourpole admittances are all known from the measuring methods discussed in the preceding sections. The value of S_1 is known from the measurement suggested by eq. (96a). So, once v_L/v_1 being measured, S_2 can be calculated.

Finally we refer to sec. 2.5 for the determination of Y_{ac}. In that section it is explained that from the measurement of the input admittance of the triode fourpole as a function of the anode tuning the admittance Y_{ca} can be calculated.

4.4. Experimental apparatus for the measurement of the triode-fourpole admittances

In order to find the properties of the passive input and output fourpoles and of the triode fourpole three kinds of measurements must be performed. They are

(1) The measurement of the input-capacity variation of a triode as a function of the filament current.

(2) The measurement of the input impedance of the input fourpole.

(3) The measurement of the quotient of the field strength sin the output and the input reference planes. This quotient is equal to the quotient v_L/v_1, which is given by eq. (98).

The first measurement can be performed by using a conventional bridge circuit at low frequencies (450 kc/s has been used). The capacity variation must be measured when the electron current in the triode is completely suppressed. Therefore the grid must be strongly biased negatively during this measurement.

The microwave circuit, used to determine the input admittance of the input fourpole, is shown in fig. 19.

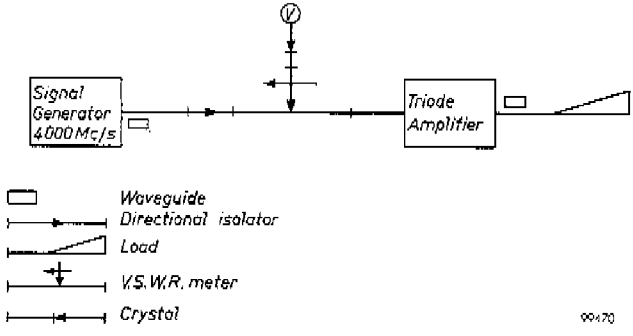

Fig. 19. Diagram of the apparatus used for the measurement of the input admittance.

The input admittance is measured as a function of the anode-cavity plunger position.

The measurement of the ratio of the field strengths in the input and output reference planes, which is equal to v_L/v_1 (fig. 18), is somewhat more complicated. The circuit is shown in fig. 20. The signal from a continuous-wave signal-generator is split up into two parts, I and II. Part I passes through a V.S.W.R. meter, the triode amplifier (from which the anode-cavity plunger is removed in accordance with the discussion of the preceding section), a calibrated variable attenuator, a calibrated variable phase shifter and a directional isolator to a second V.S.W.R. meter (SW). Part I of the signal is finally absorbed in the isolator 1. Part II of the signal is used as a reference signal which comes through isolator 1 directly to the second V.S.W.R. meter (SW). This reference signal is absorbed in the directional isolator 2.

If the amplitudes of the signals I and II are equal, a standing-wave pattern with an infinite standing-wave ratio is present in the V.S.W.R. meter between

the isolators 1 and 2. Therefore the place of a minimum can be determined accurately.

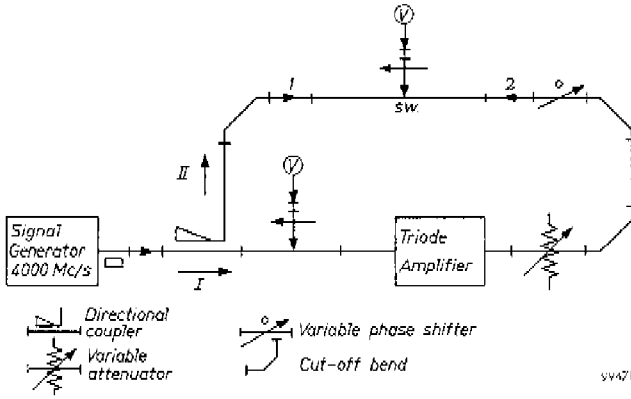

Fig. 20. Diagram of the apparatus used for the measurement of the transadmittance, S_{21}.

The ratio of the field strength is found from the following two measurements:

(1) The triode amplifier, between the reference planes AA′ and BB′ (fig. 18), is replaced by an unobstructed piece of wave-guide. By adjusting the attenuator the voltage standing-wave ratio is made infinite and the position of a minimum in the V.S.W.R. meter (SW, cf. fig. 20) is detected.

(2) The triode amplifier is now replaced. Then the standing-wave pattern in SW is made completely equal to that under 1 by adjusting the attenuator and the phase shifter. If the phase shift necessary is $\Delta\phi$, the required attenuation of the voltage amplitude necessary is a, and the phase shift of the empty piece of waveguide is ϕ_0 then the voltage gain of the amplifier is

$$\frac{v_L}{v_1} = a\, e^{j(\phi_0 + \Delta\phi)}. \tag{99}$$

4.5. Noise measurements at microwaves

We now arrive at the measurement of the four characteristic noise quantities of the amplifier, i.e. triode fourpole plus input and output fourpoles. Therefore a method to describe and to determine the noise behaviour of microwave fourpoles will be given in the following sections.

For microwaves the electromagnetic phenomena may be described in two ways. The first is a description based on the transmission of waves through, and their reflection in, a waveguide section with discontinuities or on their behaviour in a microwave amplifier. With such a description the noise properties of a microwave fourpole can be given by assuming two noise waves to be

present in the input waveguide, moving in opposite directions and being partly cross-correlated [58]).

The second way is that of describing the properties of microwave fourpoles with lumped circuit analogues. Just as is the case at low frequencies, here the noise properties are described by a noise-voltage and a noise-current source [51]). In our case we follow this latter way of description.

However the determination of the noise sources contains a difficulty analogous to that encountered in microwave admittance measurements and that is that only the relative value of admittances can be measured in waveguides, since the value of the characteristic admittance of a waveguide is unknown. We shall discuss this difficulty, using the example of a matched load at room temperature delivering noise power to a detector. The available power of the load is $kT\delta f$. Therefore, since the load and the detector are both matched to the wave guide this available power is detected. Let the load be described by a resistance and a series noise-voltage source. The resistance has the value Z_0 and the r.m.s. value of the noise voltage is $E = (4\,kTZ_0\delta f)^{1/2}$, where k is the Boltzmann constant and δf is the bandwidth. Since only the noise power $kT\delta f$ could be detected the value of E remains unknown. Only $EZ_0^{-1/2}$ is known. If the load were described by an admittance $1/Z_0$ and a noise-current source generating a current with a r.m.s. amplitude of $J = (4\,kTZ_0^{-1}\delta f)^{1/2}$ in parallel, only $JZ_0^{1/2}$ would be determined. From the next sections, however, it will appear that a knowledge of the relative noise sources $EZ_0^{-1/2}$ and $JZ_0^{1/2}$ is sufficient for a complete description of the noise properties of a microwave fourpole.

4.6. Measurement of the noise quantities

The method of measuring the characteristic noise quantities of a microwave fourpole, which will be used here, can be applied at all frequencies. It is, however, particularly advantageous at microwave frequencies, because it requires a minimum of measurements and calculations. The method will first be discussed for a fourpole at low frequencies where the difficulty in dealing with relative noise sources is not encountered.

Any noisy linear fourpole can be described by a noise-free fourpole preceded by a noise current source and a noise voltage source (cf. sec. 2.7 and ref [24])). Suppose we have such a noisy fourpole and a noise source, with internal impedance R_g, connected to its input terminals. Let it be further assumed that the input impedance of the fourpole is matched to the noise source (fig. 21). The noise ouput power is measured with a quadratic detector so that the output meter reading, n_4, is proportional to the noise power delivered to the input of the linear fourpole.

The noise generator can be described as a noise-free resistance R_g in series with a voltage source. The r.m.s. value E_g of the noise e.m.f. (see fig. 21) is

equal to E_k, where

$$E_k = \sqrt{4kTR_g\,\delta f},$$

if R_g is at room temperature T (° Kelvin), and is equal to E_s, where

$$E_s = \sqrt{4kT_sR_g\,\delta f},$$

if R_g has the temperature T_s. These two values correspond to the case in which the noise generator is switched off and when it is switched on.

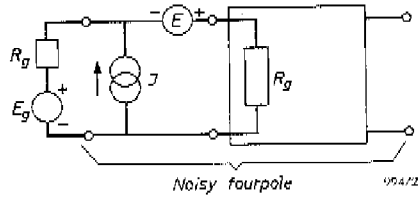

Fig. 21. Noisy fourpole with input impedance R_g and with a noise generator with internal impedance Z_g connected to its input terminals. When the generator is matched $Z_g = R_g$.

In order to determine the noise quantities of the noisy fourpole the output power must be measured under the following conditions:

(1) the noise generator switched off,
(2) the noise generator switched on,
(3) the input of the fourpole short-circuited,
(4) the input of the fourpole open,
(5) a reactance jR_g connected across the input of the fourpole.

Table II, on the left-hand side, gives the power delivered to the input of the noise-free fourpole under each condition in terms of the output-meter reading n_i, which is, as previously mentioned, proportional to the input power. The right-hand side of this table will be discussed in sec. 4.7.

After rearranging the data in Table II it will be seen that

$$\frac{EE^*}{E_kE_k^*} = \frac{n_3}{4(n_2-n_1)}\,\frac{T_s-T_k}{T_k}, \tag{100}$$

$$\frac{JJ^*\,R_g^2}{E_kE_k^*} = \frac{n_4}{4(n_2-n_1)}\,\frac{T_s-T_k}{T_k}, \tag{101}$$

$$R_g\,\frac{\overline{EJ^*}+\overline{E^*J}}{E_kE_k^*} = \frac{4n_1-(n_3+n_4)}{4(n_2-n_1)}\,\frac{T_s-T_k}{T_k}-1, \tag{102}$$

$$jR_g\,\frac{EJ^*-E^*J}{E_kE_k^*} = \frac{2n_5-(n_3+n_4)}{4(n_2-n_1)}\,\frac{T_s-T_k}{T_k} \tag{103}$$

TABLE II

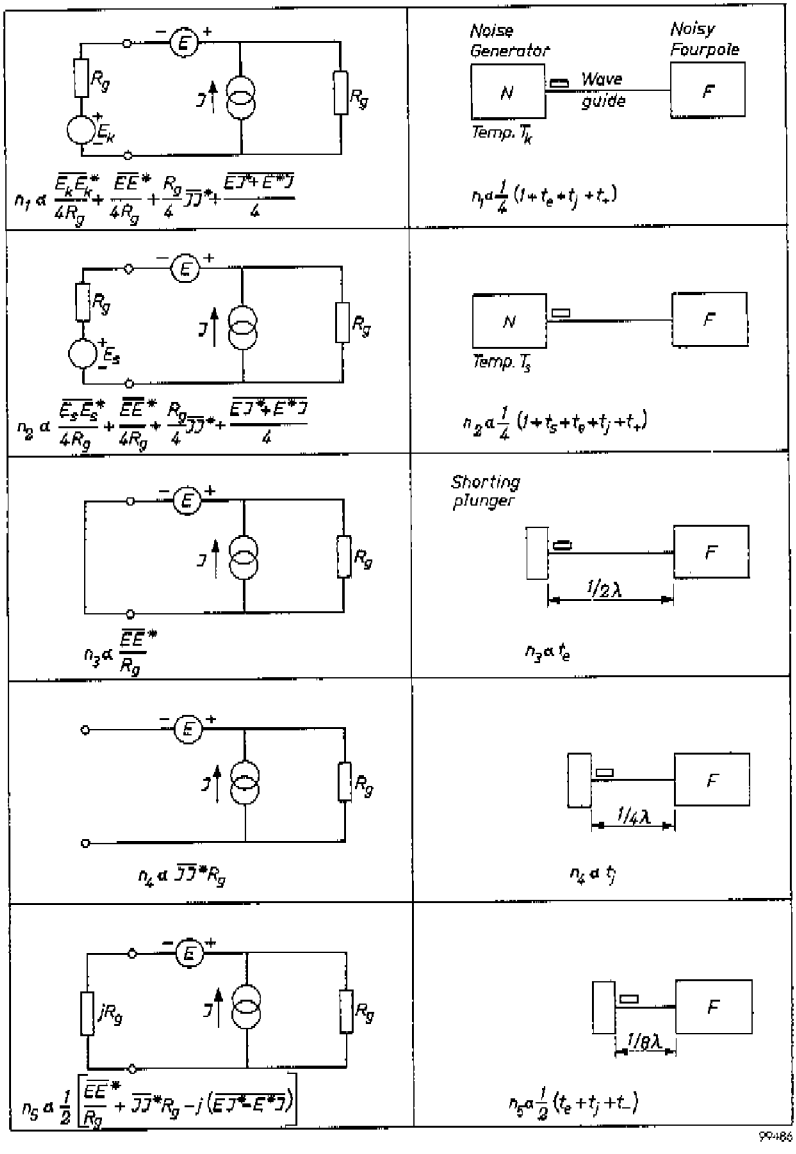

$n_1 \alpha \frac{\overline{E_k E_k^*}}{4R_g} + \frac{\overline{EE^*}}{4R_g} + \frac{R_g}{4}\overline{JJ^*} + \frac{\overline{EJ^* + E^*J}}{4}$

$n_1 \alpha \frac{1}{4}(1 + t_e + t_j + t_+)$

$n_2 \alpha \frac{\overline{E_s E_s^*}}{4R_g} + \frac{\overline{EE^*}}{4R_g} + \frac{R_g}{4}\overline{JJ^*} + \frac{\overline{EJ^* + E^*J}}{4}$

$n_2 \alpha \frac{1}{4}(1 + t_s + t_e + t_j + t_+)$

$n_3 \alpha \frac{\overline{EE^*}}{R_g}$

$n_3 \alpha t_e$

$n_4 \alpha \overline{JJ^*} R_g$

$n_4 \alpha t_j$

$n_5 \alpha \frac{1}{2}\left[\frac{\overline{EE^*}}{R_g} + \overline{JJ^*} R_g - j\left(\overline{EJ^* - E^*J}\right)\right]$

$n_5 \alpha \frac{1}{2}(t_e + t_j + t_-)$

99-486

With these equations the four noise quantities R_{eq}, G_r, ζ and κ, defined by eq. (32) can be determined from the readings of the n's, when E_k and T_s are known.

4.7. Application to microwaves

The results of the preceding section can be readily adapted to microwave fourpoles [51]). The noise source, mostly containing a gas-discharge tube [54]), has been so constructed that the internal impedance equals Z_0, the characteristic impedance of the waveguide used. When also the input of the noisy fourpole under investigation is adjusted to Z_0 (V.S.W.R. = 1), Z_0 takes the place of R_g in all formulas of the preceding sections.

The three conditions of open circuit, short circuit and the reactance jZ_0 can be readily created with a short-circuit plunger of sufficiently loss-free construction in the input waveguide of the fourpole. The impedance in the input reference plane of the input fourpole caused by this plunger is given by

$$Z = j\,Z_0 \tan \frac{2\pi x}{\lambda},$$

where λ is the wavelength and x is the distance between the plunger and the input plane. Now, when $x = 0$, $^1/_4\lambda$ and $^1/_8\lambda$ or $^3/_8\lambda$, Z is 0, ∞ and $\pm jZ_0$, respectively. With these impedances the conditions (3), (4) and (5) of sec. 4.6 are brought about.

To simplify the formulas of the preceding section we define the four characteristic noise quantities in a somewhat different way:

$$\begin{aligned}
\overline{EE^*} &= 4\,kTt_e\,Z_0\,\delta f,\\
\overline{JJ^*} &= 4\,kTt_j\,Z_0^{-1}\,\delta f,\\
\overline{EJ^*} + \overline{E^*J} &= 4\,kTt_+\,\delta f,\\
\overline{EJ^*} - \overline{E^*J} &= j4\,kTt_-\,\delta f.
\end{aligned}$$

The values t_e, t_j, t_+ and t_- will be called "relative noise temperatures"; they are essentially related to $EZ_0^{-1/2}$ and $JZ_0^{1/2}$. After substitution in eqs (100) to (103) we find

$$t_e = \frac{n_3}{4(n_2-n_1)}\,t_s, \tag{100a}$$

$$t_j = \frac{n_4}{4(n_2-n_1)}\,t_s, \tag{101a}$$

$$t_+ = \frac{4\,n_1-(n_3+n_4)}{4\,(n_2-n_1)}\,t_s - 1, \tag{102a}$$

$$t_- = \frac{2n_5 - (n_3 + n_4)}{4(n_2 - n_1)} t_s, \tag{103a}$$

where $t_s = \dfrac{T_s - T_k}{T_k}$.

This substitution has been performed in the right-hand side of table II. With the aid of the relative temperatures thus obtained we can calculate the noise figure to be (cf. eqs (32) and (33)):

$$F - 1 = \frac{t_e + (a^2 + b^2)t_j + at_+ + bt_-}{a}, \tag{104}$$

where the internal impedance of the generator is taken to be $Z_g = Z_0(a + jb)$.

Just as in the low-frequency case the relative impedance $(a+jb)_{opt}$, for which F attains a minimum, is given by:

$$a_{opt} = \sqrt{\frac{t_e}{t_j} - \frac{t_-^2}{4t_j^2}}, \tag{105}$$

$$b_{opt} = -\frac{t_-}{2t_j}. \tag{106}$$

Substituting these values in eq. (104) yields:

$$F_{min} - 1 = t_+ + \sqrt{4t_e t_j - t_-^2}. \tag{107}$$

As was already mentioned at the end of sec. 4.5 a knowledge of the relative temperatures, which are essentially derived from $EZ^{-1/2}_0$ and $JZ_0^{1/2}$, is sufficient to give a complete description of the noise properties of a microwave fourpole. Also only the relative value of the optimum generator impedance is known.

4.8. Noise measuring circuit

In this section the circuit used for measuring the relative noise temperatures of the microwave triode amplifier, consisting of the input fourpole, the triode fourpole and the output fourpole, will be described.

The circuit has been sketched in fig. 22. The noise generator is a gas discharge tube. Its noise temperature is about 25 000 °K, so the relative temperature t_s is 85 [55]). This noise generator is used to obtain the values of n_1 and n_2.

In order to obtain the values of n_3, n_4 and n_5 (table II) this noise generator is replaced by a short-circuit plunger. During the measurements both the noise generator and the triode amplifier were matched to the waveguide.

The noise signal from the triode amplifier is mixed with a local oscillator signal differing by 45 Mc/s. The bandwidth of the input circuit of the triode amplifier ($\approx$100 Mc/s) is much larger than the overall bandwidth of the circuit.

The latter is determined by the intermediate-frequency amplifier, which has a bandwidth of 7 Mc/s around an average frequency of 45 Mc/s.

In order to suppress the image-noise power a bandpass filter, having 40 Mc/s bandwidth, is inserted in the circuit between the triode-amplifier and the mixer.

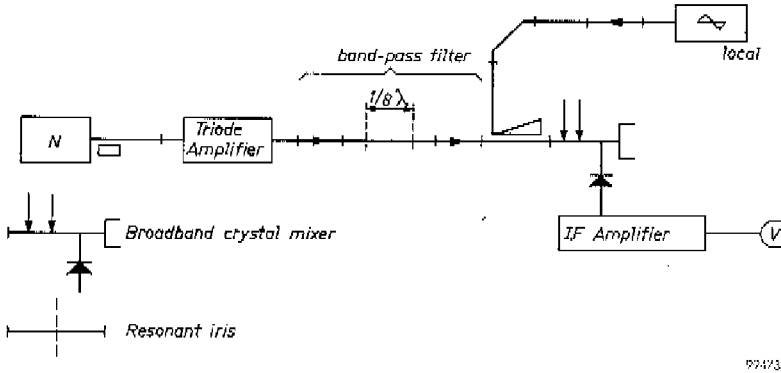

Fig. 22. Diagram of the noise measuring apparatus.

The local oscillator has been constructed using an EC 57. The stability is sufficient for the purpose of noise measurements.

4.9. Transformation of the measured noise quantities across the input fourpole

The four noise quantities t_e, t_j, t_+ and t_- describing the noise properties of the complete amplifier between both reference planes AA′ and BB′ can be obtained using the methods discussed in the preceding sections. The next problem is to transform them across the passive input fourpole in order to get the characteristic noise quantities of the triode fourpole itself. In this section the equations transforming t_e, t_j, t_+ and t_- into the triode fourpole noise-quanties R_{eq}, G_r, ζ and κ will be derived.

In order to do this the input fourpole, preceded by the noise sources E and J, must be transformed into an input fourpole followed by the noise sources E' and J'. The relation between the latter noise sources E' and J' and the first two E and J can be found from the requirement that the circuit of fig. 23 is

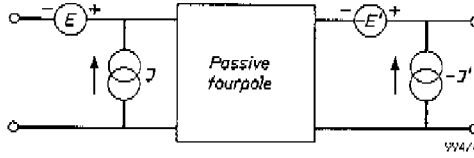

Fig. 23. If this circuit is noise free E' and J' are the values of the noise sources after transformation across the input fourpole.

noise-free. This yields

$$J' = \frac{Z_{11}J - E}{Z_{12}}, \tag{108}$$

$$E' = \frac{-DJ + Z_{22}E}{Z_{12}}, \tag{109}$$

where $D = Z_{11}Z_{22} - Z_{12}^2$, the determinant of the input-fourpole matrix, eq. (89).

Using these equations, the relative noise temperatures measured for the complete amplifier can be expressed in the four characteristic noise quantities of the triode fourpole alone. We first repeat the definitions:

$$\left.\begin{aligned} \overline{E'E'^*} &= 4kTR_{eq}\,\delta f \quad ; \overline{EE^*} = 4kTt_e Z_0\,\delta f \\ \overline{J'J'^*} &= 4kTG_r\,\delta f \quad ; \overline{JJ^*} = 4kTt_j Z_0^{-1}\,\delta f \\ \overline{E'J'^*} &= 2kT(\zeta + j\kappa)\,\delta f; \ \overline{EJ^*} = 2kT(t_+ + jt_-)\,\delta f \end{aligned}\right\} \tag{110}$$

Using eqs (108), (109) and (110) the transformation of the noise quantities is given by

$$R_{eq} = \frac{1}{|Z_{12}|^2}\left\{|D|^2\frac{t_j}{Z_0} + |Z_{22}|^2 t_e Z_0 - \mathrm{Re}\,(DZ_{22}^*)t_+ - \mathrm{Im}\,(DZ_{22}^*)t_-\right\}, \tag{111}$$

$$G_r = \frac{1}{|Z_{12}|^2}\left\{|Z_{11}|\,t_j + Z_0\,t_e - \mathrm{Re}\,(Z_{11})\,t_+ - \mathrm{Im}\,(Z_{11})\,t_-\right\}, \tag{112}$$

$$\zeta = \frac{1}{|Z_{12}|^2}\left\{-2\,\mathrm{Re}\,(DZ_{11}^*)\frac{t_j}{Z_0} - 2\,\mathrm{Re}\,(Z_{22})\,t_e Z_0 + \right.$$
$$\left. + \mathrm{Re}\,(D + Z_{11}Z_{22}^*)\,t_+ + \mathrm{Im}\,(D + Z_{11}Z_{22}^*)\,t_-\right\}, \tag{113}$$

$$\kappa = \frac{1}{|Z_{12}|^2}\left\{-2\,\mathrm{Im}\,(DZ_{11}^*)\frac{t_j}{Z_0} - 2\,\mathrm{Im}\,(Z_{22})\,t_e Z_0 - \right.$$
$$\left. - \mathrm{Re}\,(D - Z_{11}Z_{22}^*)\,t_- + \mathrm{Im}\,(D - Z_{11}Z_{22}^*)\,t_+\right\}. \tag{114}$$

If the measured constants characterizing the input fourpole Z_{11}/Z_0, Z_{12}^2/Z_0 and Z_{22} are substituted in these equations, the characteristic impedance of the waveguide Z_0 disappears from the equations.

4.10. Some general properties of the transformation

Z_{11}, Z_{12} and Z_{22} are imaginary when the input fourpole is loss-free. In this case eq. (113) reduces to:

$$\zeta = t_+. \tag{115}$$

Since then also the noise figure of the total fourpole between the reference planes AA' and BB' (fig. 17) is invariant for the transformation of the noise sources across the input fourpole, we have from eqs (107) and (34):

$$F_{\min} = 1 - t_+ + \sqrt{4\, t_e t_j - t_-^2} = \zeta + \sqrt{4\, R_{eq}\, G_r} - \kappa^2.$$

Therefore also [47]):

$$4\, t_e t_j - t_-^2 = 4\, R_{eq}\, G_r - \kappa^2. \tag{116}$$

Unfortunately in a microwave triode amplifier the input fourpole cannot be considered as loss-free. In order to calculate the effect of the input fourpole on the noise figure of the total amplifier we use the well-known equation for the overall noise figure of two noisy fourpoles in cascade [56])

$$F - 1 = F_i + \frac{F_t - 1}{g_e}, \tag{117}$$

where F is the overall noise figure, F_i is the noise figure of the input fourpole, F_t is the noise figure of the triode fourpole and g_e is the exchangeable gain of the input fourpole. g_e is defined as the quotient of the available output power and the available input power of a fourpole *).

The available input power delivered by a generator with internal impedance Z_0 to the input fourpole is:

$$P_{in} = \frac{|v_0|^2}{4Z_0}, \tag{118}$$

where v_0 is the effective value of the e.m.f. The available output power of the input fourpole is found from an application of Thevenin's theorem to the input fourpole having the generator with impedance Z_0 at its input side. This yields

$$P_{out} = \left| \frac{Z_{12} v_0}{Z_{11} + Z_0} \right|^2 \frac{1}{4\mathrm{Re}(Z_{out})}, \tag{119}$$

where Z_{out} is the output impedance of the input fourpole. Therefore, the exchangeable gain is:

$$g_e = \frac{P_{out}}{P_{in}} = \frac{|Z_{12}|^2}{Z_0} \left\{ \left| \frac{Z_{11}}{Z_0} + 1 \right|^2 \mathrm{Re}(Z_{out}) \right\}^{-1}, \tag{120}$$

with

$$Z_{out} = Z_{22} - \frac{Z_{12}^2}{Z_{11} + Z_0}. \tag{121}$$

The noise figure of the input fourpole follows directly from its definition.

*) We can use here the term "available power" since no negative resistances occur in the input fourpole[22]); the term "available gain" is omitted since it suggests the maximum gain.

The total available noise power at the output is $kT\delta f$. The total available noise power at the output if the noise generator were the only noise producing element is $kT\delta f g_e$. Thus F_t is given by

$$F_t = \frac{1}{g_e}. \tag{122}$$

From eqs (117), (120) and (122) the effect of the input fourpole losses on the overall noise figure of a triode amplifier can be determined.

Of course the input fourpole is designed so that losses are kept very low. Therefore it is possible to make the approximation that $F_t - 1 \ll F_t - 1$. To give a numerical example $F_t - 1$ is about 0·1 and $F_t - 1$ is about 50 for a triode amplifier. Therefore we can write for eq. (117):

$$F - 1 = \frac{F_t - 1}{g_e}. \tag{123}$$

In general we find $0{\cdot}85 < g_e < 0{\cdot}95$. From eq. (123) we can find the influence of the input fourpole on the triode-amplifier noise figure.

Equation (123) also provides a check on the numerical calculations concerning the transformation. When the input fourpole is matched to the waveguide (as is the case during the measurements) we find for the overall noise figure of the triode amplifier (see eq. (104) with $b = 0$ and $a = 1$)

$$F = 1 + t_+ + t_e + t_j. \tag{124}$$

This overall noise figure is also given by eq. (123). The noise figure of the triode fourpole, which has the impedance Z_{out} (cf. eq. (121)) connected to the input terminals, is given by (see eq. (33)):

$$F_t - 1 = \frac{R_{eq} + G_r|Z_{out}|^2 + \zeta \mathrm{Re}\,(Z_{out}) + \kappa \mathrm{Im}\,(Z_{out})}{\mathrm{Re}(Z_{out})}. \tag{125}$$

Substituting eqs (120), (124) and (125) into eq. (123) we find:

$$t_e + t_j + t_+ = \frac{R_{eq} + G_r|Z_{out}|^2 + \zeta \mathrm{Re}(Z_{out}) + \kappa \mathrm{Im}(Z_{out})}{\dfrac{|Z_{12}|^2}{Z_0}\left|\dfrac{Z_{11}}{Z_0} + 1\right|^{-2}}, \tag{126}$$

which equation must be satisfied for each transformation of noise quantities across a passive reciprocal fourpole.

Finally, there is a combination of noise quantities which remains always constant during the transformation of noise sources across passive reciproce fourpoles irrespective whether these fourpoles have losses or not. If the noise generated in the passive input fourpole is assumed to be generated in the noise sources of the total triode amplifier we have [47]):

$$4t_e t_j - t_+^2 - t_-^2 = 4R_{eq}\, G_r - \zeta^2 - \kappa^2. \tag{127}$$

In conclusion it can be said that eqs (126) and (127) are correct for transformations of the noise sources across the passive input fourpole. However, since the losses in the input fourpole are not very important (about 10% of the input energy is lost), the equations (115) and (116) can be used as approximations and are convenient for confirming the numerical calculations.

4.11. Noise sources of the input fourpole

In eq. (123) the noise figure of the input fourpole could be neglected. It is, however, possible that one of the measured noise quantities is very small. In this case it is difficult to determine whether this quantity results from the input fourpole noise or from the triode noise. Therefore the noise sources of the input fourpole will be calculated.

The output noise voltage of the input fourpole and the noise generator, with internal impedance Z_g at room temperature, connected to its input is given by

$$\overline{|v_0|^2} = 4kT\,\mathrm{Re}\,(Z'_{\mathrm{out}})\,\delta f, \tag{128}$$

where the whole circuit is assumed to be at room temperature and where Z'_{out} is defined in eq. (121), when Z_0 is replaced by Z_g.

If we now describe the noise properties of the input fourpole by a noise voltage source E_i and a noise current source J_i (fig. 24), we find for the output noise voltage:

$$\overline{|v_0|^2} = \left|\frac{Z_{12}}{Z_{11}+Z_g}\right|^2 \overline{|E_g + E_i + J_i Z_g|^2}, \tag{129}$$

where E_g is the noise e.m.f. and Z_g the internal impedance of the generator.

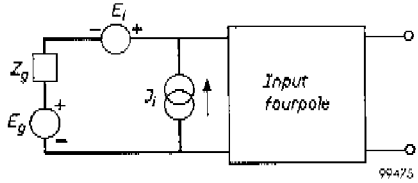

Fig. 24. On the calculation of the input-fourpole noise sources.

Since the eqs (128) and (129) must be identical for every value of Z_g we have:

$$\begin{aligned} &t_{ei}Z_0 = |Z_{12}|^{-2}\,\mathrm{Re}(DZ_{11}^*),\quad t_{ji}Z_0^{-1} = |Z_{12}|^{-2}\,\mathrm{Re}(Z_{22}),\\ &t_{+i} + jt_{-i} = |Z_{12}|^{-2}\,\mathrm{Re}(D + Z_{11}Z_{22}^*) - 1, \end{aligned} \tag{130}$$

where t_{ei} , t_{ji} , t_{+i} and t_{-i} are the relative noise temperatures of the input fourpole.

4.12. Input capacity

In chapters 2 and 3 the input capacity C_c in the absence of electrons was assumed to be a part of the triode fourpole. However, throughout the discussions on the methods of measurement this input capacity was assumed to be part of the input fourpole. For the discussion of the results of the measurements it is more convenient to consider the capacity C_c as a part of the triode fourpole.

Therefore the noise sources measured must be transformed across the capacity C_c. For this transformation of course ζ is invariant (see eq. (115)). Also R_{eq} appears to be invariant. The values of G_r and κ for the triode fourpole, complete with the capacity C_c at its input, are related to G_{rm}, κ_m and R_{eq}, the measured values,by:

$$\begin{aligned} G_r &= G_{rm} - \omega C_c \kappa_m + \omega^2 C_c^2 R_{eq}, \\ \kappa &= \kappa_m - 2\omega C_c R_{eq}. \end{aligned} \tag{131}$$

These transformed values of the measured noise quantities can be used for further theoretical discussion in connection with the theory of the two preceding chapters.

5. MEASUREMENTS AND CONCLUSIONS

5.1. Introduction

The methods of measurement described in the preceding chapter have been applied to microwave triodes in order to determine the triode-fourpole admittances (secs 2.4 and 4.3): Y_c, Y_{ca}, Y_{ac} and Y_a and the four characteristic noise quantities (secs 2.8 and 4.9): R_{eq}, G_r, ζ and κ.

The results of the admittance measurements will be compared with the results of the single-velocity transit-time theory. The electronic admittances of the EC 57, viz., S_1 ($\approx Y_c - j\omega C_c$) and S_2 ($\approx -Y_{ca}$), have been measured as a function of the current density. Their magnitudes and phases are compared with the theoretical results of sec. 3.3. S_1 has also been measured for the EC 59, a 10-Watt triode for the 4000 Mc/s band [7]).

The passive feedback, expressed mainly by Y_{ac} (sec. 2.4), is obtained from the measurement of the input admittance as a function of the anode circuit detuning and from a direct measurement of the power transfer through a "cold" triode as is suggested by Diemer [15]). These methods have been applied to both the EC 57 and the EC 59.

The noise measurements have been performed on the EC 57 only. A direct comparison between the theory and the experimental results is in this case impossible since the effect of the space charge on the noise propagation between the cathode and the potential minimum is unknown. Therefore the results of the noise measurements will be used in order to obtain the values of K, L, p and

ϕ characterizing the random fluctuations at the cathode surface of the simplified model given in sec. 3.5.

However, in chapter 3 several effects which probably cause additional noise in a microwave triode have not yet been discussed. These effects are the "total-emission" noise and the spread of the transit times of the individual electrons. Also the internal feedback (sec. 1.3(*b*)) can have an effect on the noise properties of a triode. The discussion of these effects has been delayed up to now in order to estimate their relative importance on the basis of the experiments. Therefore before determining the values of K, L, p and ϕ these effects will be discussed.

After having found the values of K, L, p and ϕ for a triode the theory of sec 3.10 can be used to determine Haus' noise parameters S and Π of an electron beam [46]), originating from the same cathode under identical circumstances. Then it is also possible to estimate the minimum noise figure of an electron beam amplifier equipped with an identical cathode. In this manner the noise in microwave triodes can be compared with the more extensively studied noise in electron beam amplifiers.

A final question to be answered is whether the noise performance of a microwave triode can be improved by inserting an additional passive feedback in the triode amplifier. Experimentally this problem is very involved since it is impracticable to bring about a desired amount of feedback in a complicated microwave circuit such as that of a triode amplifier. However, using a theory which has recently been developed by Haus and Adler [23]) this question can be answered from a knowledge of the triode fourpole equations and the equivalent noise quantities.

5.2. Measurement of the input admittance

The purpose of this section is to give an example of the measurement of the input admittance of an EC 57. In later sections only the results of the measurements will be given.

As has been discussed in secs 4.2 and 4.3 the input admittance of the triode fourpole can be calculated from the relative input impedance, ζ_{in}, of the input fourpole, provided that the input fourpole impedances are known. The latter impedances are determined from the measured values of the relative input impedance of the input fourpole when this fourpole is loaded with three known capacities.

A typical set of impedance measurements, plotted in a Smith diagram is given in fig. 25. The large circle refers to the measurement of the input impedance as a function of the heater current I_f. Using the symbols of sec. 4.2 where ζ_a is the measured input impedance at the nominal heater current, ζ_b that at a somewhat higher heater current and ζ_c at a somewhat lower heater current and C_1 and C_2 the corresponding cathode-grid capacity variations respectively, we find from fig. 25:

$\zeta_a = j\,0{\cdot}345$; $\zeta_b = j\,0{\cdot}850$ and $\zeta_c = -j\,0{\cdot}460$.

$C_1 = 0{\cdot}35$ pF, $C_2 = -0{\cdot}52$ pF; $Z_b = -j\,118\ \Omega$ and $Z_c = j\,78\ \Omega$. *)

Substitution of these numbers into eqs (94) and (95) gives:

$$\frac{Z_{11}}{Z_0} = j\,0{\cdot}345; \quad \frac{Z_{12}^2}{Z_0} = -60{\cdot}7\ \Omega \text{ and } Z_{22} = -j\,2{\cdot}6\ \Omega.$$

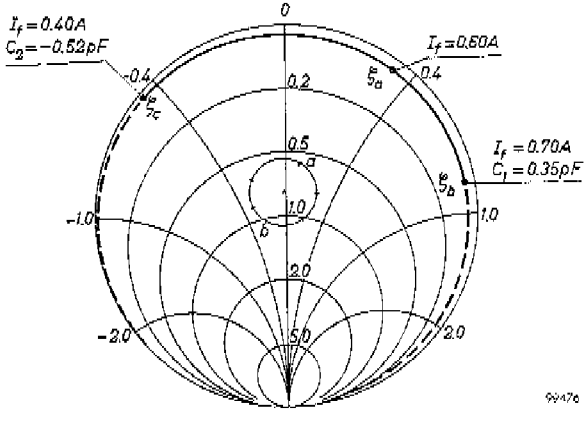

Fig. 25. Relative input impedance measured in the input reference plane AA′ (cf. fig. 17). The large circle refers to the measurement of the input impedance as a function of the heater current, I_f. The nominal value of $I_f = 0{\cdot}60$ A. The small circle gives the input impedance as a function of the anode circuit tuning. The measured tube is an EC 57 (no 53) with an anode current of 30 mA.

The losses in the input fourpole have been neglected in this example (V.S.W.R > 30).

The relative input impedance of the input fourpole as a function of the detuning of the anode circuit is given by the small circle in fig. 25. The transformation of these relative impedances into the input admittances of the triode fourpole is carried out with the aid of eq. (96a). The points a and b, b referring to the special case of a completely detuned anode cavity, are given by:

$$\zeta_{in\cdot a} = 0{\cdot}58 + j\,0{\cdot}09 \text{ and } \zeta_{in\cdot b} = 1{\cdot}04 - j\,0{\cdot}18.$$

Substitution of these values, together with the input fourpole impedances, in eq. (96) gives:

$$Y_{in\cdot a} = (9{\cdot}3 - j\,5{\cdot}7)\ \text{mA/V} \text{ and } Y_{in\cdot b} = (16{\cdot}7 - j\,9{\cdot}2)\text{mA/V}.$$

*) The last decimal of all quantities given is uncertain.

The result of the transformation of the complete input impedance circle of fig. 25 into the input admittance circle of the triode fourpole is given in fig. 26.

In an analogous manner the input admittance of the triode fourpole can be measured as a function of the anode current (see sec. 4.3).

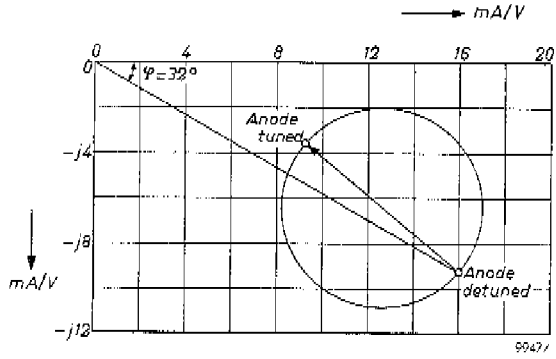

Fig. 26. Input admittance of the triode fourpole as a function of the anode circuit detuning. This admittance circle has been deduced from the measurements given in fig. 25.

5.3. Electronic admittances S_1 and S_2

In this section the results of the measurements of the electronic admittances S_1 ($\approx Y_e - j\omega C_e$) and of S_2 ($\approx Y_{ea}$) as a function of the current density will be discussed (S_1 and S_2 are defined in sec. 2.2 and Y_e and Y_{ea} in sec. 2.4).

(a) S_1 as a function of the anode current density in an EC 57

The results of the measurement of S_1 for the case of two tubes of type EC 57 have already been reported [57]). Therefore they are only summarized here. For tube no 46, referred to as tube II in the reference quoted, the results are given in figs 27 and 28 in a manner differing slightly from that used in the reference. In fig. 27 the real part of the measured value of S_1, divided by the real part of S_1, calculated from the single-velocity transit-time theory (sec. 3.3 and table I), has been plotted. In fig. 28 the imaginary part of S_1' ($= S_1 + j\omega C_e$) divided by $j\omega C_e$ has been plotted. From the single-velocity transit-time theory it can be deduced that $\mathrm{Im}\,(S_1 + j\omega C_e) = \frac{4}{5}\omega C_e$ provided that the transit-time angle β_1 is smaller than about $1{\cdot}2\,\pi$ [10]).

From the measurements the following conclusions can be drawn:

(I) At small current-densities ($< 0{\cdot}3$ A/cm^2), $\mathrm{Re}(S_1)$ is much larger than the theoretical value. This difference is due to the fact that the electrons returning in front of the potential minimum cross a considerable part of the cathode-grid space and can therefore absorb an appreciable amount of energy from the high-frequency electric field ("total-emission damping"; compare secs 1.3(*a*)

and 3.1). If the anode current density is 0·15 A/cm², the distance between the cathode and the potential minimum is about 15 μ, which is rather large in comparison with the cathode-grid distance d_{cg} of about 40 μ.

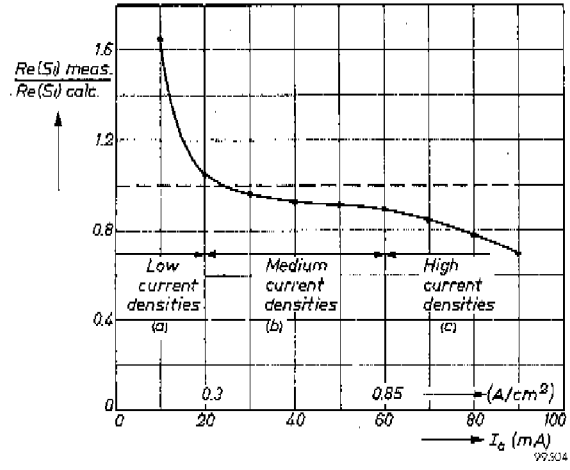

Fig. 27. Re(S_1) measured in an EC 57 divided by the value of Re(S_1) calculated from the single-velocity transit-time theory, as a function of the anode current I_a (tube no 46; heater current 0·62 A; cathode diameter is 3 mm).

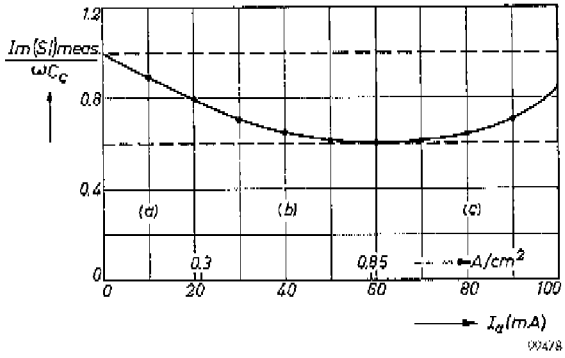

Fig. 28. Im(S_1') divided by $j\omega C_c$ as a function of the current density for the same tube as in fig. 27.

The results obtained are in agreement with Robertsons' measurements [12]). The measurements were also performed at about 4000 Mc/s. However, the triode which he used had a cathode-grid distance of 15 μ. At a current density of 0·15 A/cm² the value of Re(S_1) appeared to be twice as large as g_m, due to the fact that the potential minimum was close to the grid.

(2) At medium current densities $\mathrm{Re}(S_1)$ agrees within 10% and $\mathrm{Im}(S_1')$, within 20% with the theoretical values. The theoretical values of S_1' have been calculated on the basis of the tube geometry only (sec. 3.3 and table I). The dimensions of tube no. 46 with $I_f = 0{\cdot}62$ A are: $d_{cg} = 35\ \mu$, $d_{ag} = 240\ \mu$, $s = 50\ \mu$ and $2c = 7{\cdot}5\ \mu$ (see fig. 29). The anode voltage of all tubes during the measurements was 180 V.

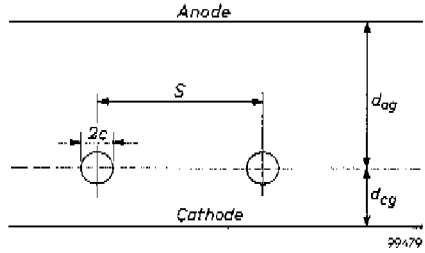

Fig. 29. Geometry of a triode.

(3) If the current density is higher than 0·85 A/cm² ($I_a \geq 60$ mA) the value of S_1 differs again from the theoretical value. The reason for this descrepancy is that the transconductance g_m does not increase linearly with $I_a^{1/3}$ as is found from Childs' law, eq. (43). Small parts of the cathode can become saturated long before the cathode as a whole is saturated (the mean saturation current density is about 3·5 A/cm²). Therefore the surface contributing to the increase of the anode current and so to g_m decreases. This explanation is supported by the fact that the measured phase angle of S_1 exhibits no shift with the calculated angle at high current densities. Therefore we may assume that the single-velocity transit-time theory provides a good approximation for the small-signal behaviour of a microwave triode at high current densities as well.

(*b*) S_1, *measured for an EC 59*

In order to check this assumption at very high current densities the admittance S_1 of a power triode, type EC 59 [7], has been measured. Due to the water-cooled anode the current density of this triode can be increased to more than 2 A/cm².

The dimensions of this triode are:
cathode area $\sigma = 0{\cdot}16$ cm²; $d_{cg} = 60\ \mu$, $d_{ag} = 300\ \mu$, $2c = 30\ \mu$ and $s = 130\ \mu$ (cf. fig. 29). It can be seen from these numbers that the EC 59 is a triode with "Inselbildung" (diode effect) since the grid pitch, s, is more than twice as large as d_{cg}. This makes the calculation of the high-frequency properties rather complicated, since the transit time of an electron depends on the place where it is emitted. Furthermore the calculation of g_m is impossible due to the partial saturation of the cathode at high current densities.

We therefore omitted the calculation of g_m and measured it at low frequencies in a simple bridge circuit. It is then possible to plot the measured values of S_1

divided by g_m in the admittance plane. This quotient is equal to (see eq. (49))

$$\frac{S_1}{g_m} = \frac{1}{\Phi_6(\beta_1)} - \frac{j\omega C_c}{g_m} = \frac{1}{\Phi_6(\beta_1)} - \frac{\beta_1}{2}, \tag{132}$$

where β_1 is the transit-time angle in the cathode-grid space. The function $\Phi_6^{-1}(\beta_1) - \frac{1}{2}\beta_1$ has been plotted in the figs 30 and 14. Since due to Inselbildung the transit time of an electron depends on the place on the cathode surface where this electron is emitted, we calculated the average value of the transit-time angle, $\langle\beta_1\rangle$. The averaging process is based essentially on the assumption that all electrons travel in a direction perpendicular to the cathode. At low anode currents this assumption is supported by the fact that most electrons are emitted just between and not below the grid wires. At high anode currents it is supported by the fact that the equivalent grid-potential variations as a function of the position are much smaller than at low currents where the grid potential is far below the cathode potential. The calculation of $\langle\beta_1\rangle$ is given in detail in appendix 2. The results are given, together with the measured values of g_m in table III for the case of an EC 59 (tube 49 AF no 303).

TABLE III

Measured values of g_m and calculated values of $\langle\beta_1\rangle$ as a function of the anode current density.

Anode Current (mA)	350	300	250	200	150	100	50	20	10
Current density (averaged) (A/cm²)	2·23	1·90	1·57	1·28	0·96	0·64	0·35	0·14	0·064
g_m (mA/V)	28·9	28·6	26·8	23·6	19·2	15·3	16·3	6·0	3·8
$\langle\beta_1\rangle$(rad)	2·24	2·36	2·55	2·65	2·80	3·0	3·5	4·0	4·7

The values of S_1/g_m, measured for a triode of the type EC 59 (49 AF no 303*)) as a function of the anode current-density can also be plotted as a function of the average transit-time angle using table III. These values should agree with the calculated values of $\Phi_6^{-1}(\beta_1) - \frac{1}{2}\beta_1$ for the same transit-time angle. In fig. 30 it can be seen that the agreement is very good for values of $\langle\beta_1\rangle \leqslant 4$ rad i.e., for average anode current densities $> 0{\cdot}14$ A/cm².

It can therefore be concluded that the single-velocity transit-time theory can be applied to the cathode-grid space of a microwave triode provided that the cathode potential-minimum distance is small in comparison with the cathode-grid distance. Similar results have been obtained for the tube 49 AK no 2*). The agreement between theory and experiments is within 10% for both tubes.

*) The 49 AF and 49 AK are prototypes of the EC 59 having identical dimensions of the active space but slightly different construction.

(c) Transadmittance S_2 of an EC 57

The measurement of the input fourpole can be performed using the tube under test itself, since the cathode-grid distance can be varied with the heater current. The output fourpole, however, is measured using three dummies having different anode-grid distances. It is very difficult to make the external dimensions of the three dummies identical with those of the tube under test. Therefore the measurement of S_2 is less accurate than the measurement of S_1 since in the former case both the input fourpole and the output fourpole must be known.

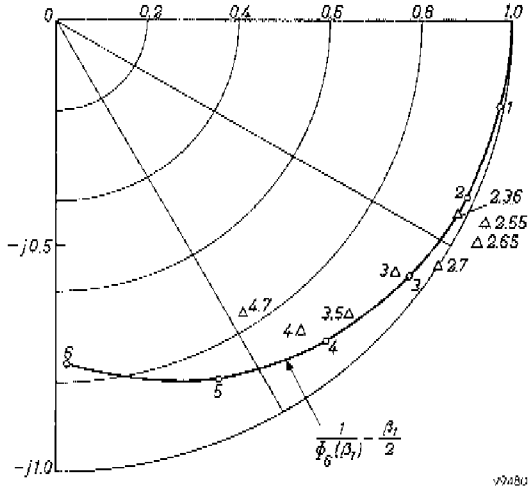

Fig. 30. Plot of S_1/g_m of a triode in the complex admittance plane with the transit-time angle as parameter (solid line). The points (△) are the values of S_1/g_m, measured for an EC 59. For each point the average transit-time angle calculated according to appendix 2 has been given.

On the other hand the single-velocity transit-time theory can be applied to the electron flow in the anode-grid space of a triode without any restriction. Therefore it may be assumed that the measured values of S_2 agree with the calculated ones for the same current densities as those for which S_1 agrees with its theoretical value.

Results of the measurement of S_2 for two tubes [57]) show that the phase of S_2 agrees within 12° with the theoretical value (which is about 135°) for medium current densities (between 0·3 and 0·85 A/cm). At low current densities there is of course a discrepancy due to the large cathode potential-minimum distance. At high current densities we have the effect of partial saturation of the cathode which decreases g_m and thus also $|S_1|$ and $|S_2|$, in a way not predicted by theory. This decrease is, at high current densities, still further enhanced by the grid current, which decreases the anode current according to:

$$\frac{\delta I_a}{\delta V_g} = \frac{\delta I_c}{\delta V_g} - \frac{\delta I_g}{\delta V_g}, \tag{133}$$

where I_a, I_c and I_g are the dc anode, cathode and grid currents, respectively. An increase of I_g decreases $|S_2|$ since I_c is determined by the cathode only ($|S_1|$ is not influenced by the grid current).

Figure 31 gives the value of S_2, measured for one of these tubes (no 46) with a heater current of 0·62 A, as a function of the current density.

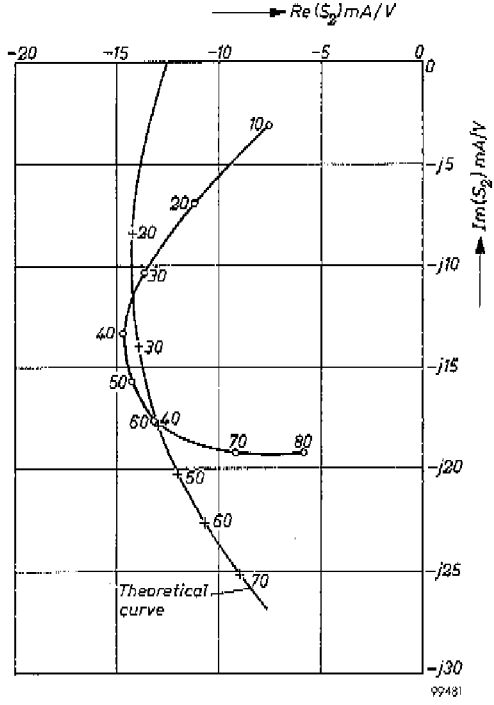

Fig. 31. Plot of S_2 as a function of the current density for tube no. 46 with $I_f = 0{\cdot}62$ A. The numbers along the curves give the anode current in mA.

(d) Conclusion

The single-velocity transit-time theory appears to give a good description of the high-frequency small-signal performance of microwave triodes for those cases in which the distance between the cathode and the potential minimum is small compared with the cathode-grid distance; this means: when Childs' law is a good approximation for the static characteristic of these triodes, i.e. when the current density is sufficiently high, (cf. secs 3.1 and 3.2).

5.4. Passive feedback

We now come to the determination of the feedback admittance Y_{ac}, which is given by (see eq. (19))

$$Y_{ac} = -\frac{S_1 + j\omega C_c}{\mu}\left(1 - \frac{\omega^2}{\omega_0^2} + j\omega r \mu C_a\right). \tag{134}$$

C_c and C_a, the cathode-grid capacity and the anode-grid capacity can be determined from the geometry of the triode. S_1 can be calculated from the transit time theory (preferably using the measured value of g_m) and the amplification factor, μ, is known from the static characteristic of a triode. Therefore the only unknown quantities in eq. (134) are ω_0 and r; ω_0 is the frequency at which the inductive feedback compensates the capacitive feedback and r is the resistance of the grid wires.

As has already been discussed in sec. 2.5 the value of Y_{ac} can be calculated from the circle in the admittance plane giving the input admittance of a triode fourpole as a function of the anode tuning. In fig. 26 such an admittance circle has been given for tube no 53 of type EC 57 at a heater current of 600 mA. This measurement will be used to determine the values of ω_0 and r of tube no 53.

(a) Determination of the feedback properties from the input admittance

The diameter of the circle connecting the points for which the anode is tuned and completely detuned, respectively, is given by (see eqs (23) and (19)):

$$2P = -\frac{Y_{ac}Y_{ca}}{\mathrm{Re}(Y_a) + g_L + g_0} = -\frac{S_1' S_2}{\mu}\,\frac{\left(1 - \dfrac{\omega^2}{\omega_0^2} + j\omega r \mu C_a\right)}{\mathrm{Re}(Y_a) + g_L + g_0}, \tag{135}$$

where g_L and g_0 are the load conductance and the cavity conductance transformed to the active space of the triode.

The values of $2P$ and S_1 can be found in fig. 26 to be equal to: $2P = (-6{\cdot}5 + j\,5{\cdot}9)$mA/V, and $S_1 = (16{\cdot}7 - j\,9{\cdot}2)$mA/V. The value of S_2 is in an EC 57, at an anode current of 30 mA and an anode voltage of 180 V, equal to $(-0{\cdot}55 - j\,0{\cdot}69)\,g_m$. The static characteristic of the same tube under identical conditions is given in fig. 32, showing that $g_m = 22$ mA/V and $\mu = 40$. The capacitance ωC_c, which cannot be measured since the capacitances of the disks of the triode are unknown, can be expressed in terms of g_m and β_1. This yields

$$j\omega C_c = g_m \frac{\beta_1}{2}, \tag{136}$$

which can be proved using Childs' law. Since $\beta_1 = 3{\cdot}6$ rad, when $I_a = 30$ mA, $\omega C_c = 37$ mA/V. Furthermore $C_a = (d_{cg}/d_{ag})C_c = 1/6\ C_c$ so that $\omega C_a = 6.2$

mA/V. Finally the value of $g_L + g_0$ amounts to 0·83 mA/V in an amplifier with 100 Mc/s bandwidth [6]).

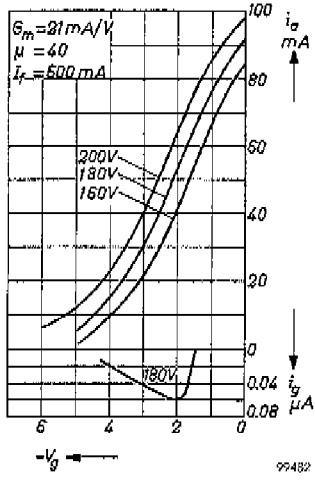

Fig. 32. Static characteristic of an EC 57 (no 53; I_f = 600 mA).

Substitution of the numbers given in the preceding paragraph in eq. (135) yields:

$$f_0 = \frac{\omega_0}{2\pi} \approx 5300 \text{ Mc/s and } r = 0{\cdot}8\ \Omega$$

when $\mathrm{Re}(Y_a)$ is neglected. Substitution of these results in eq. (21) shows that $\mathrm{Re}(Y_a) = -0{\cdot}016$ mA/V, so that within the measuring accuracy $\mathrm{Re}(Y_a)$ can indeed be neglected.

The value of M, the inductance in series with the grid, follows from eq. (12): $M = 1{\cdot}5 \cdot 10^{-10}$ H.

(b) Discussion of the results

In a similar manner the values of ω_0 and r are obtained for three more tubes. In the first place for tube EC 57, no 46 (referred to in figs 27, 28, 31). The result is $M = 1{\cdot}5 \cdot 10^{-10}$ H, $\omega_0 \approx 4900$ Mc/s and $r = 0{\cdot}9\ \Omega$. Remembering the approximations used in the deduction of the equations for the triode fourpole we conclude that the compensation frequency of an EC 57 lies at about 5000 Mc/s and that the damping of the feedback circuit in the grid lead is described by a series resistance of about 0·8 Ω.

In the second place the values of ω_0 and r have been obtained for the two power tubes for which the electronic admittances have been described in sec.

5.3(*b*). For both tubes (49 AF no 303 and 49 AK no 3) we found a compensation frequency of about 4400 Mc/s, so $M = 10^{-10}$ H, and a resistance $r = 0{\cdot}25\ \Omega$.

As has been said in sec. 2.5 it is possible to obtain the value of ω_0 from direct measurement of the power transfer through a "cold" triode (grid biased negatively so that S_1 and S_2 are zero). These measurements [6]) resulted in a compensation frequency (for which the power transfer is at a minimum) of 5200 Mc/s for the case of an EC 57. The compensation frequency of the EC 59, also obtained from direct power transfer measurements through a "cold" triode is is 4200 Mc/s [8]). These frequencies are in good agreement with the values obtained from the input-admittance measurements.

However, the values of r obtained from input admittance measurements and those obtained from direct power transfer measurements do not agree. For an EC 57 the value of r (see eq. (25)) obtained from direct measurements is 0·01 Ω and for an EC 59 this value is 0·1 Ω. Probably the feedback circuit is damped by the presence of electrons in a manner which is not accounted for in the approximate equations of the triode fourpole, so that r obtained from input admittance measurements is much larger than that obtained from power transfer measurements. In further discussions we prefer the value obtained from admittance

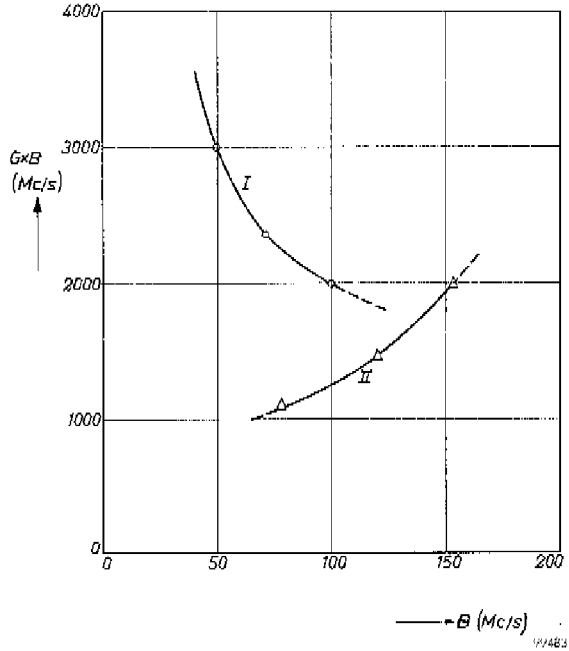

Fig. 33. Gain-band product as a function of the bandwidth. I for an EC 57 in the 4000 Mc/s band; II for a 6000 Mc/s-triode in the 6000 Mc/s band.

measurements since here the tube is measured under the same conditions as when it is normally used. After all the magnitude of r has no important effect on the properties of a microwave triode.

The value of f_0 has an important effect on the gain-band product (eq. (26)) of a microwave triode. As has been said in sec. 2.6 the gain-band product depends on the bandwidth in such a way that it increases with decreasing bandwidth if the compensation frequency is larger than the work frequency.

For an EC 57 this is indeed the case: $f_0 = 5200$ Mc/s and the work frequency is 4000 Mc/s. Results of the measurement of the gain-band product of an EC 57 as a function of the bandwidth are plotted in fig. 33 which does indeed show this dependence [6]).

Similar measurements with the 6000 Mc/s triode [9]) showed the inverse effect (fig. 33). From these measurements it may be concluded that the compensation frequency (which has not been measured directly for this tube) lies below the work frequency. This is undesirable since in this case $\mathrm{Re}(P) > 0$ (see eqs (23) and (135) and sec. 2.6) which means that the passive feedback decreases the gainband product in this tube.

(c) *Equivalent circuit*

From the measurements in the preceding sections it can be concluded that the small-signal behaviour of a microwave triode can be described by the equivalent circuit suggested in chapter 2 (fig. 6). The electronic admittances S_1 and S_2 occurring in this circuit can be deduced from the single-velocity transit-time theory as discussed in chapter 3, provided that the current density is so high that the distance between the potential minimum and the cathode is much smaller than the cathode-grid distance d_{cg}. Other admittances occurring in the equivalent circuit such as of the capacities C_c and C_a and also the amplification factor μ can be calculated from the tube geometry or from the static characteristic, using the fact that according to the single velocity transit-time theory

$$g_m \frac{\beta_1}{2} \approx j\omega C_c \text{ and } C_a \approx \frac{d_{cg}}{d_{ag}} C_c.$$

The calculation of the feedback properties from the tube geometry is very involved and has not yet been performed. However, in two different manners the compensation frequency and so the inductance M can be measured independently, giving results which agree reasonably well. The resistance r, as is obtained from the input admittance measurements, completes the equivalent circuit of a microwave triode given in fig. 6.

Finally we would make some remarks concerning the accuracy. The complete equations necessary for the description of the triode fourpole and for the deter-

mination of the input and output fourpoles are too involved to give a reliable calculation of the error in the results. In the next section, however, we shall see that the exchangeable gain g_e of the input fourpole is $0{\cdot}9 \pm 0{\cdot}05$, measured for several tubes. This shows that the spread in a quantity obtained directly from the input fourpole impedances is 5% of the average value. When we add the independent possible error of maximally about 5% of the capacity measurement we arrive at an uncertainty of about 10% in the input fourpole impedances. Therefore we estimate the possible error in the measurement of S_1 to be about 10%. The possible error in S_2 is maximally 20%, since for the measurement of S_2 two passive fourpoles had to be measured.

5.5. Available gain and noise of the input fourpole

We now come to the discussion of the measurements of the four characteristic noise quantities of the triode fourpole R_{eq}, G_r, ζ and κ (see sec. 2.8). In order to obtain these quantities we first have to measure the four relative noise temperatures t_e, t_f, t_+ and t of the total microwave triode amplifier which can be imagined to consist of the input fourpole, the triode fourpole and the output fourpole. These quantities must be transformed across the passive input fourpole, which necessitates a knowledge of the input-fourpole impedances (sec. 4.9). Furthermore the exchangeable gain and the noise sources of the input fourpole are of importance for this transformation (sec. 4.10).

In order to discuss the measurements in somewhat more detail we shall give the measured values of the output noise powers $n_1 \ldots . n_5$ (sec. 4.7), the input fourpole constants and all quantities which are of interest in the transformation of the noise sources across the input fourpole, calculated from the results of the measurements for the special case of one tube. This tube is the EC 57, no 119, with an anode current $I_a = 60$ mA and with an increased heater current $I_f = 700$ mA (the reason for the high I_f will be discussed in sec. 5.8).

In this section we restrict ourselves to the determination of the input-fourpole constants, the exchangeable gain and the noise sources of the input fourpole of tube 119.

During the noise measurements the input fourpole was matched to the waveguide. This is not essential for these measurements but by doing so the equations (sec. 4.6) relating the output noise powers with the relative noise temperatures become relatively simple. Furthermore, in the next section a check on the measurements, which is only possible for the case of a matched input fourpole, will be discussed. In order to match the input fourpole to the waveguide variable tuning stubs had to be used in the input waveguide. These stubs may increase the losses in the input fourpole. (For the admittance measurements the input matching was not necessary. Therefore no stubs were used in this case so that the input-fourpole losses could be neglected).

For the tube EC 57 no 119 with an anode current of 60 mA*) we found for the input fourpole impedances:

$$\frac{Z_{11}}{Z_0} = 0{\cdot}10 + j\,0{\cdot}525; \frac{Z_{12}^2}{Z_0} = -66{\cdot}2 + j\,5{\cdot}9\ \Omega;$$

$$Z_{22} = 1{\cdot}8 + j\,15{\cdot}3\ \Omega.$$

From eq. (120) we find for the exchangeable gain:
$g_e = 0{\cdot}92$. From all input fourpole measurements we observed that the value of $g_e = 0{\cdot}90 \pm 0{\cdot}05$. Together with the 5% possible error in the capacity measurement this means that the maximum possible error in g_e and probably also in the other quantities calculated from the input fourpole impedances is about 10% (cf. sec. 5.4).

Finally we use eq. (130) in order to calculate the relative noise temperatures of the input fourpoles:

$$t_{ei} \approx 0{\cdot}06;\ t_{ji} \approx 0{\cdot}03;\ t_{+i} \approx 0{\cdot}001;\ t_{-i} \approx -0{\cdot}06,$$

which quantities lie well within the measuring accuracy of the relative noise temperatures of a working amplifier. Therefore they will be neglected.

5.6. Measurement of the relative noise temperatures

According to the discussion of the measuring methods in sec. 4.7 the relative noise temperatures t_e, t_j, t_+ and t_- of the complete amplifier are calculated from the output power measured in the five different cases mentioned in sec. 4.6 and table II.

The intrinsic noise power of the measuring equipment (which is small in comparison with the noise power from the EC 57) has been substracted in each measurement from the output noise power n.

Before taking the measurements referred to above, the output noise power of the amplifier was measured as a function of the position of the shorting plunger in the input waveguide. Theoretically it can be proved [51]) that this function is sinusoidal if the input fourpole is matched to the waveguide. The effect of a mismatch has been shown in fig. 4 of the paper quoted.

The output noise power readings obtained for the EC 57 no 119 at an anode current of 60 mA are:

$$n_1 = 22{\cdot}3;\ n_2 = 64{\cdot}9;\ n_3 = 24{\cdot}2;\ n_4 = 24{\cdot}7;\ n_5 = 18{\cdot}7.$$

From eqs (100a) to (103a) we find for the relative noise temperatures:

$$t_e = 12;\ t_j = 12;\ t_+ = 19 \text{ and } t_- = -6.$$

*) The anode current I_a, which determines the input admittance of the triode fourpole, must be mentioned since the input fourpole matches the waveguide to the triode fourpole. So for different I_a we find different input fourpoles.

It is very difficult to estimate the maximum possible errors in this measurement. The accuracy depends on all components of the circuit of fig. 22. However, the fluctuations of the output meter and the error in the output meter reading appear to account for the most important errors. The fluctuations of the meter are at the most about 1·5% of the output meter reading. The non-systematic error of the reading of the output meter is about 1%. Of course this is only true when the circuit is switched on for a long time and when all voltages used and the air-cooling of the EC 57 are stabilized. A maximal error of 2·5% in the output noise power readings n_i causes, as is found from eqs (100a) to (103a), the maximum error in the relative noise temperatures t to be

$$t_e : 6\%;\ t_j : 6\%;\ t_{|} : 12\% \text{ and } t_{-} : 25\%.$$

5.7. Transformation of the noise quantities

Using eqs (111) to (114) the noise quantities R_{eq}, G_r, ζ and κ can be calculated from the relative noise temperatures t_e, t_j, t_+ and t_-, given in the preceding section, and the input fourpole impedances given in sec. 5.5

The result is:

$$R_{eq} = 580\ \Omega;\ G_r = 0{\cdot}25\ \text{A/V};\ \zeta = 17;\ \kappa = 9$$

The output impedance of the input fourpole is (eq.(121))

$$Z_{out} = (49 - j\ 12)\ \Omega$$

Using the results of sec. 4.10 we can check the numerical calculations necessary for the transformation:

(1) As is found in eq. (115) $t_{|} = \zeta$ for a loss-free input fourpole. In our case there are only small power losses so that t_+ and ζ are somewhere about the same (19 and 17, respectively).

(2) Equation (126) will now be used in order to check the result of the transformation. The total noise figure calculated from the relative temperatures (using the fact that the input fourpole is matched to the waveguide) is given by:

$$F - 1 = t_e + t_j + t_{|} = 43$$

(cf. eq. (124)). The excess noise figure of the triode fourpole, $F_t - 1$, divided by the available gain of the input fourpole is given by the right hand side of eq. (126). Substituting the values obtained for tube no 119 we find:

$$(F_t - 1)/g_e = 44.$$

The small difference is due to the rounding off of the numbers in the calculation.

(3) Finally we check the calculations using eq. (127):

$$4t_e t_j - t_{|}^2 - t_{-}^2 = 190 \text{ and } 4R_{eq}\,G_r - \zeta^2 - \kappa^2 = 190.$$

Of course these equations can also be used in order to omit the substitution of one of the transformation equations, which is most laborious, for example that of κ, eq. (114).

An estimation of the errors in the characteristic noise quantities of the triode fourpole is based on the following considerations. In the first place, since $t_+ \approx \zeta$ the error in the latter quantity will be of the same order as that in t_+. As for the other quantities, the error of 10% in the input fourpole impedances must probably be added to the error in the relative noise temperatures. The value of κ is mainly determined by t_e and t_j and only to a small extent by t_-. Therefore we arrive at the following estimation of the possible errors in the characteristic noise quantities

$$R_{eq} : 15\%,\ G_r : 15\%,\ \zeta : 12\% \text{ and } \kappa : 20\%.$$

As has been said earlier the input capacity C_c of the triode has been assumed to be a part of the input fourpole (cf. secs 4.2 and 4.12). However, all theoretical calculations of chapter 3 have been performed for the case that this capacity is part of the triode fourpole. Therefore the measured values of the characteristic noise quantities have to be corrected for this capacity according to sec. 4.12, giving:

$$R_{eq} = 580\ \Omega;\ G_r = 0{\cdot}63\ \text{A/V};\ \zeta = 17;\ \kappa = -31.$$

5.8. Survey of the measured noise quantities

Up to now we have discussed the noise measurement for one tube (no 119). In this section we shall give the results of the measurements for several tubes. These results are listed in table IV.

From the values obtained for the noise figure we observe that the minimum value of F is obtained when $I_a \approx 25$ mA, as has also been found at low frequencies. At lower currents, F increases since the temperature limited region, where the space-charge suppression at the potential minimum is insufficient, is approached.

The same effect which decreases g_m to a value below its theoretical value, i.e. the partial saturation of the cathode, is also responsible for the increase of F at high anode currents. If a small part of the cathode surface is saturated and if the dimensions of this part are of the same order of magnitude or larger than the distance between the cathode and the potential minimum the space-charge suppression mechanism [41]) is not working *). In this case the low-frequency value of R_{eq} and apparently (see table IV) also its high-frequency value increase.

*) W. Dahlke proposed to use this effect as a measure for the quality of productional cathodes, cf. Proc. Inst. Radio Engrs, *46*, 1639-1645, 1958.

For low frequencies this effect is demonstrated in fig. 34 where the measured values of $g_m R_{eq}$, which product is theoretically given by eq. (68), have been plotted as a function of the anode current. A minimum value is indeed found at the normal cathode temperature of 1400 °K for about 25 mA. When the cathode temperature is decreased the minimum shifts to lower currents. This is explained by the fact that at a low cathode temperature more parts of the surface will be saturated at a certain anode current than at a high cathode temperature.

At high frequencies this effect is demonstrated by the measurements of tube 243 at 30 mA. In order to avoid difficulties with this partial-saturation effect the cathode temperatures of tubes 119 and 120 have been raised so far that the low frequency value of $g_m R_{eq}$ was close to the calculated value of 3·9, cf. the tables IV and IX.

TABLE IV.

Characteristic noise quantities and noise figures of triodes at 4000 Mc/s. Tubes 119 and 120 are measured at increased cathode temperature.

tube	I_f (mA)	I_a (mA)	R_{eq} Ω	G_r*) A/V	ζ	κ*)	Z_{out}(cf.eq. 121) Ω	F
16	650	10	2100	0·15	26	19	94 — j 61	65
	,,	20	1500	0·19	21	23	67 — j 72	56
	,,	30	1870	0·19	25	23	74 — j 80	58
	,,	40	1730	0·25	28	21	70 — j 45	72
243	650	10	2140	0·11	23	14	115 — j 54	60
	,,	30	1250	0·18	19	17	83 — j 52	50
	620	30	6060	0·22	27	49	144 — j 78	106
	650	50	1610	0·26	28	21	77 — j 42	71
46	650	20	1400	0·09	17	2	117 — j 46	44
	,,	25	1270	0·10	17	5	80 — j 35	44
119	700	60	580	0·25	17	9	49 — j 13	43
120	680	30	740	0·13	15	7	75 — j 27	40

The value of ζ is very high at microwave frequencies. However, as will be shown later, this large correlation between the noise-voltage and the noise-current source cannot be used to improve the noise performance of a triode, as is often suggested.

*) The values of G_r and κ apply to the case of a triode fourpole without the "cold" input capacity, C_c.

In table IV we observe that the tubes 16 and 243 have similar noise quantities. Tubes 119 and 120, which had an increased cathode temperature and therefore a good cathode emission have also similar characteristic noise quantities. Apparently tube 46 has a good cathode emission at the nominal heater current as can be concluded from its low noise figure. Therefore the noise quantities of this tube resemble those of tube 119 and 120.

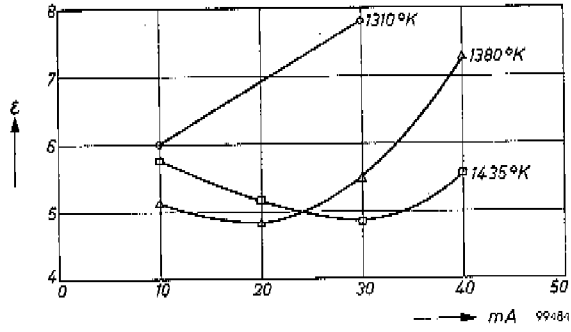

Fig. 34. Plot of $g_m R_{eq}$ as a function of the current density with the cathode temperature as parameter. The measurements were performed at a frequency of 6 Mc/s. For the tube considered the value of $g_m R_{eq}$ is higher than its theoretical value of 3·9.

5.9. Total-emission noise

Before calculating the values of the four quantities K, L, p and ϕ which characterize the fluctuations in the electron stream in the vicinity of the cathode (sec. 3.5), we must first discuss the effect of some sources of noise which has not yet been estimated in chapter 3. These sources of noise are (1), the fluctuations in the stream of electrons returning to the cathode ("total emission noise"), (2), the transit time spread of the individual electrons and (3), the internal feedback. In this section we shall show that the effect of total-emission noise on the noise sources of a microwave triode is negligible at current densities normally used.

The noise current caused by the returning electrons will be for the major part uncorrelated with the noise currents due to the electron stream crossing the potential minimum. The returning electrons contribute mainly to i_1, the short circuit noise current in the cathode-grid circuit, while the crossing electrons contribute to both i_1 and i_2. Therefore the part of i_1, which is uncorrelated with i_2 might be due to the returning electrons. If these electrons provide the major contribution to the uncorrelated part of i_1, this part should decrease for increasing anode current since then the contribution of the returning electrons decreases. At increasing currents the potential minimum approaches the cathode, so the length over which the interaction between the returning elec-

trons and the high-frequency electric field occurs decreases. This lowers both the total-emission conductance (sec. 5.3) and the total-emission noise.

The uncorrelated part of i_1 can be easily found from the measured values of R_{eq}, G_r, ζ and κ. Since the voltage source E and the current source J are given by (cf. eq.(28))

$$J = -i_2 \frac{S_1}{S_2} + i_1 \qquad \text{and } E = -\frac{i_2}{S_2},$$

the part of J which is uncorrelated to E is equal to the part of i_1 which is uncorrelated with i_2.

We assume the current source to be split up in J_u and J_c, being the part uncorrelated and the part correlated with E, respectively:

$$J = J_c + J_u = Y E + J_u, \tag{137}$$

where Y is called the correlation admittance.

The value of Y is found by multiplying eq.(137) with E^* and averaging this product over a sufficiently long time:

$$2E^*J - 2EE^*Y = (EJ^* + E^*J) - (EJ^* - E^*J) = 4kT(\zeta - j\kappa)\delta f, \tag{138}$$

where the definitions of sec. 2.8 are used. Therefore

$$Y = \frac{\overline{E^*J}}{E^*E} = \frac{\zeta - j\kappa}{2R_{eq}}.$$

The mean square amplitude of J_u follows from:

$$J_uJ_u^* = JJ^* - EE^*|Y|^2, \quad \text{or} \quad G_{ru} = G_r - \frac{\zeta^2 + \kappa^2}{4R_{eq}}. \tag{139}$$

In table V the values of G_{ru} have been calculated from the measurements in table IV.

We observe in table V that the uncorrelated part of J increases with increasing current density and that this trend is noticed with every tube. This is contrary to what would be expected in the case that the returning electrons contribute the major part to J_u, since in that case J_u (or G_{ru}) should decrease with increasing current density. It is thus concluded that we may neglect the total emission noise for sufficiently high current density, as was already assumed in chapter 3.

A further argument is given by the measurement with lowered heater current (tube 243, table V). The saturation current in this case is lower since the cathode temperature is lower (this can be seen from the high value of R_{eq}). So the number of returning electrons must be smaller but even in this case G_{ru} is much higher than in the case with higher cathode temperature.

TABLE V

Values of G_{ru} for the different measurements given in table IV*)

tube \ I_a (mA)	10	20	25	30	40	50	60
16	0·023	0·035	—	0·032	0·075	—	—
13	—	0·022	—	—	—	—	—
243 (I_f = 650 mA)	0·019	—	—	0·046	—	0·072	—
243 (I_f = 620 mA)	—	—	—	0·087	—	—	—
120	—	—	—	0·038	—	—	—
119	—	—	—	—	—	—	0·138
46	—	0·038	0·038	—	—	—	—

From the admittance measurements [57]) (see fig. 27), it follows that the difference between the measured value of the input conductance, $\mathrm{Re}(S_1)$ and its theoretical value is about 3 mA/V for 10 mA anode current. If we assume this difference to be the total-emission conductance, which is caused by the returning electrons, this conductance must give total-emission noise. It can be assumed that the returning electrons remain in thermal equilibrium with the cathode; so the total-emission conductance must be assumed to have cathode temperature (about 5 times room temperature). Since the noise conductance G_{ru} is assumed to be at room temperature this means that the part of G_{ru} due to the total emission noise is 5 times as high as the total-emission conductance, i.e. 0·015 A/V. We see that this value compares well with the measured value of G_{ru} for 10 mA.

Thus it may be concluded that the total-emission noise becomes a leading noise source at low current densities when the distance between the cathode and the potential minimum is of the same order of magnitude as the cathode-grid distance d_{cg}.

At higher current density the total-emission conductance decreases rapidly and therefore the total-emission noise also decreases.

5.10. Transit times and noise

Electrons emitted from various points of the cathode will follow different paths between the cathode and the anode. The different transit times of the various electron groups and their different paths will influence the current pulses induced in the cathode and anode circuits and can cause uncorrelated noise.

*) The numbers occurring in this table are not calculated from the numbers in table IV but from the corresponding numbers before they were rounded off. This is the case with all calculations in this chapter.

In order to find out experimentally whether this is an important effect at 4000 Mc/s the characteristic noise quantities of a triode of type EC 57 equipped with a grid wound with 30 μ wires, were measured. The pitch of the grid was chosen so that the amplification factor was about the same as in a normal tube with 7·5 μ wires. This pitch is 90 μ and the cathode-grid distance is 40 μ. Therefore a large diode effect ("Inselbildung") can be expected in this triode, which means a large spread of the transit times of the individual electrons.

TABLE VI

Characteristic noise quantities of a triode with "Inselbildung".

tube	$R_{eq}(\Omega)$	G_r(A/V)	ζ	κ	F	G_{ru}(A/V)	I_a(mA)
186	2900	0·11	28	5	72	0·037	30

In table VI we observe a high value of R_{eq}. This is due to the fact that the transconductance of this tube is very low (about 9·5 mA/V). The noise-current source G_r is of the same order of magnitude as that of several of the normal tubes (tube 46 and 120). When the uncorrelated part is now calculated, the result is that G_{ru} has about the same value as that of the other tubes with the same anode current, namely 0·037 A/V. This shows that it is very unlikely that transit-time spread influences the noise properties of triodes at microwaves.

Another argument is obtained in the following way. Suppose, for simplicity, that the velocity fluctuations were the only noise source at the cathode and divide the triode in a large number (n) of parallel triodes. For each triode the equivalent grid voltage is given in appendix 2, eq.(A-7), as a function of the position. Then for each triode the short-circuit noise currents i_{1n} and i_{2n} are calculated, assuming that the electron paths remain perpendicular to the cathode surface ("one-dimensional treatment"). The correlation C between the total currents becomes

$$C = \frac{\Sigma_n\, i_{1n}\ \Sigma_m\, i_{2m}^*}{(\Sigma_n\, i_{1n} i_{1n}^*\ \Sigma i_{2n} i_{2n}^*)^{1/2}} = \frac{\Sigma_n\, i_{1n}\, i_{2n}^*}{(\Sigma_n\, i_{1n} i_{1n}^*\ \Sigma i_{2n} i_{2n}^*)^{1/2}}. \qquad (140)$$

Since the noise in the different triode parts is not cross-correlated the two sums in the numerator of eq.(140) can be replaced by one. When this calculation is performed for an EC 59 (the power triode with large diode effect, see sec. 5.3(b) we find $|C|^2 = 0{\cdot}92$*). This value is calculated for the case that the cathode is just non-emitting below the grid wires and that between the wires the equivalent grid-voltage is maximally 12·2 V. When the same calculation is performed for an EC 57 with a grid having a somewhat increased pitch (60 μ instead of 50 μ) we arrive at a value of $|C|^2 = 0{\cdot}95$ for $I_a = 30$ mA at 4000 MHz.

*) The calculation suggested here is based on the theory of the equivalent grid voltage given in appendix 2.

In this calculation the transit-time effect is exaggerated since the electron paths have less spread in time as has been suggested. The electrons emitted below the grid wires are forced to pass the grid plane at a place with higher equivalent grid voltage than that assumed in the one-dimensional model.

We now calculate the cross-correlation between the measured short-circuit noise currents i_1 and i_2. Using eq. (28) we find

$$|C|^2 = \frac{\overline{i_1 i_2^*}\ \ \overline{i_1^* i_2}}{\overline{i_1 i_1^*}\ \ \overline{i_2 i_2^*}} = \frac{\overline{(ES_1 - J)E^* S_2^*}\ \ \overline{(ES_1 - J)^* ES_2}}{\overline{(ES_1 - J)(ES_1 - J)^*}\ \ \overline{ES_2 E^* S_2^*}}. \qquad (141)$$

Using the definition of the noise quantities, eq. (32), and eqs (138) and (139), eq. (141) transforms to

$$|C|^2 = \left\{1 + \frac{G_{ru}}{R_{eq}} |S_1 - Y|^{-2}\right\}^{-1}, \qquad (142)$$

where Y is defined in eq.(137).

Unfortunately the values of $\{\mathrm{Re}(S_1) - \mathrm{Re}(Y)\}$ and of $\{\mathrm{Im}(S_1) - \mathrm{Im}(Y)\}$ are small compared with the values of their separate terms so that this calculation cannot be very accurate. In every case, however, $|C|^2$ was much less than 0·95, the value calculated from eq.(140), see table VII.

TABLE VII

Correlation, $|C|^2$ (in %), between the noise currents i_1 and i_2

I_a(mA) / tube no.	10	20	30	40
16	39 %	53 %	84 %	63 %

Hence the correlation differs much from its maximum value 1. From the above discussion it may be concluded that only a small part of the deviation of $|C|^2$ from its maximum value can be explained by the spread in the transit times of the electrons.

One might suggest that there is still another effect resulting from the different electron paths, i.e. that an electron already induces a current in the anode before it has passed the grid. This must, however, be a small effect in an EC 57 since the anode-grid distance is about 5 times the grid pitch.

5.11. The effect of feedback

The effect of feedback on the noise quantities can be calculated from the equations of sec. 2.8, where the values of E and J of a triode fourpole

including feedback are calculated from the values of E' and J' of an idealised tube without feedback ($\mu = \infty$).

The value of the ideal-triode fourpole-admittances occurring in these equations are given in sec. 2.2, eq. (4). If we substitute normally occurring values for these admittances as have been measured (cf. table VIII and ref. [37]), the influence of the feedback on the noise sources can be calculated.

TABLE VIII

Electronic admittances, capacitances and characteristic noise quantities of tube no 46.

tube 46	S_1 (mA/V)	S_2 (mA/V)	$j\omega C_c$ (mA/V)	$j\omega C_a$ (mA/V)	R_{eq} (Ω)	G_r (A/V)	ζ	κ
$I_a = 25$ mA	14 - j 9	- 13 - j 9	j 28	j 4·7	1270	0·10	17	5

The value of Z_t, the feedback impedance in series with the grid, can be calculated from eq. (11):

$$Z_t = r + \frac{1}{j\omega\mu C_a}\left(1 - \frac{\omega^2}{\omega_0^2}\right).$$

Since the compensation frequency is about 5200 Mc/s, $\mu = 40$ and $r = 0{\cdot}8$, cf.sec. 5.4 (*a*), we find $Z_t \approx (0{\cdot}8 - j\,2{\cdot}3)\ \Omega$. A simple calculation shows that $Z_t D' \ll Y'_{ca}$, so (cf. sec. 2.8)

$$J' \approx J$$

$$E' \approx E - J\,Z_t\,\frac{Y_a' - Y_{ca}'}{Y_{ca}'} = E + J(0{\cdot}1 - j\,2{\cdot}1).$$

Substitution of the values of the characteristic noise quantities (table VIII) shows that feedback has practically little influence on the noise quantities.

The next question is whether the noise figure of a triode amplifier can be reduced by some artificial feedback. Indeed it appears to be possible to reduce this noise figure by a capacitive feedback. However, the gain of the amplifier also decreases in this case. Therefore, if we assume this amplifier to be the first stage of a cascade amplifier, a reduced gain means that the contribution of the second stage to the overall noise figure is increased. This can lead to an increase of the overall noise figure of the cascade amplifier in spite of the reduced noise figure of the first stage.

Haus and Adler [23]) have shown that the noise measure M_e, defined by

$$M_e = \frac{F - 1}{1 - \frac{1}{g_e}}$$

(g_e = exchangeable gain), is a better criterion for the noise performance of a noisy fourpole. Application of their theory to the microwave triode shows that the minimum value of the noise measure cannot be decreased by some artificial feedback.

5.12. Estimation of the values of K, L, p and ϕ

In the three preceding sections we have learned that the effect of "total emission noise", of the spread in the transit times of the individual electrons and of the internal feedback on the noise properties of a triode is negligible at microwave frequencies and at sufficiently high current densities ($> 0{\cdot}2$ A/cm^2).

Hence there remain two important sources of noise, viz., random emission of electrons by the cathode and reflection of electrons at the anode surface.

In order to find the relative importance of the two sources of noise we shall consider the characteristic noise quantities measured in three tubes. These quantities are given in table IX for the case that the "cold" input capacitance, ωC_c, of the triode is part of the triode fourpole. Besides, the values of the transconductance, g_m, and of the equivalent noise resistance at low frequencies, $R_{eq}(o)$, are given in this table.

TABLE IX

Characteristic noise quantities of the triode fourpole (including the capacity C_c) of three tubes together with g_m and the low frequency value of $R_{eq}(o)$

tube no	R_{eq} (Ω)	G_r (A/V)	ζ	κ	$R_{eq}(o)$ (Ω)	g_m (mA/V)	$g_m R_{eq}(o)$
120	740	0·89	15	—48	200	20·8	4·16
119	580	0·63	17	—31	170	24·8	4·24
243	1250	0·56	19	—47	450	16·3	7·3

As can be seen from the tables IV and IX the heater currents of the tubes 119 and 120 were chosen in such a way that the low frequency value of the product of $R_{eq}g_m$ is almost equal to its theoretical value, 3·9. This has been done in order to avoid difficulties with partial saturation of the cathode. The low frequency value of $R_{eq}g_m$ of tube 243 is about twice its theoretical value. It is in this case doubtful whether the condition of full space charge, underlying all calculations of chapter 3, is fulfilled. However, it will be shown that the final conclusions concerning the values of K, L, p and ϕ are still about the same.

For the three tubes referred to in table IX first the effect of the reflection of electrons at the anode on the triode noise is calculated. The parts of the characteristic noise quantities, which are due to the reflections are calculated with the aid of the theory given in sec. 3.10. In this section these parts, called R_{nr},

G_{rr}, ζ_r and κ_r, are given by eqs (85) to (88). The reflection coefficient, r, is assumed to be equal to 0·03, which is a realistic value for an anode covered with BaO [20]).

As is discussed in sec. 3.10 the quantities R_{nr}, G_{rr}, ζ_r and κ_r can be simply subtracted from the measured characteristic noise quantities (table IX) since the reflection noise is uncorrelated with the cathode noise. The remaining parts of the characteristic noise quantities, called R_{nc}, G_{rc}, ζ_c and κ_c, must be due to the random emission from the cathode. In the theory of chapter 3 these quantities are related to K, L, p and ϕ which characterize the effect of the space charge and the velocity spread of the electrons on the initial fluctuations at the cathode surface of an actual triode. This effect is not accounted for by the single-velocity transit-time theory which is used in the simplified model of sec. 3.5 and is therefore taken into account by introducing K, L, p and ϕ.

The results of the calculations suggested above are given in table X.

TABLE X

Characteristic noise quantities due to reflections and to random cathode emission and the values of K, L, p and ϕ obtained from these quantities *).

tube no:	120	119	243
β_1(rad)	3·6	2·8	3·6
$\beta_2 = \frac{1}{2}\beta_1$(rad)	1·2	1·2	1·2
R_{nr} (Ω)	110	190	180
G_{rr} (A/V)	0·08	0·12	0·06
ζ_r	3	5	4
κ_r	—5	—7	—6
R_{nc} (Ω)	630	390	1070
G_{rc} (A/V)	0·81	0·51	0·50
ζ_c	12	12	15
κ_c	—43	—24	—41
K	1·4	1·4	1·2
L	2	2	1·5
p	0·7	0·7	0·7
ϕ (rad)	—3·1	—3·1	—3·1

It should be remembered that the results in table X can only be a first order approximation since the exact values of β_1, β_r, r and of the measured noise

*) In spite of the large difference in characteristic noise quantities the values of K, L, p and ϕ for the tubes 120 and 119 are similar. This is due to the different values of β_1, g_m and R_{eq} (o).

quantities (possible error 10 — 20%) are unknown. However, several important facts concerning K, L, p and ϕ can be found in table X.

1. The value of L obtained from the triode noise measurements is of the order of 2. Theories of Bloom, Siegman and Watkins [44]) led to a similar result. The value 2 is also in accordance with Tien's calculation [42]). It may be assumed that the value of L will not be much larger than 2. At low frequencies the shot noise is almost completely suppressed (so L is very small). This means that an original convection-current fluctuation is compensated for by extra currents originating in the potential minimum. At high frequencies these compensating currents are probably in phase with the original disturbance and must be counted up, which means that L is about 2.

2. If L is as a maximum somewhere about 2, it must be assumed that $K > 1$ in order to explain the high value of R_{eq} at microwaves (the coefficient of K^2 in eq. (69) is about 10 times as high as the coefficient of L^2 when $\beta \approx \pi$). This result is not in accordance with Tien's calculation [42]), which gave $K = 1$. The disagreement is probably due to the fact that in an actual triode the noise propagation between the cathode and the potential minimum is essentially three-dimensional (cf. sec. 3.4), while Tien assumed a one-dimensional electron flow.

3. The phase angle ϕ is somewhere about $-\pi$. This means that the correlated parts of the velocity fluctuations and the convection-current fluctuations are out of phase. This is what must be expected, since at increasing velocity of the negative electrons the positive current to the anode decreases.

5.13. Comparison with noise measurements on electron beams

As has been suggested in sec. 3.10 the results of the preceding section can be compared with the results of the measurements of Haus' beam-noise parameters S and Π [46]).

Measurements of electron-beam noise have been performed recently at the M.I.T. [58]) [59]) [60]). In these measurements the value of S is obtained from the noise standing-wave ratio ρ_n in the beam. The value of Π/S has been obtained in three different ways. The first way is the calculation of Π/S from the minimum noise figure obtained with an amplifier including an electron beam for which S is known, cf. eq.(74) [58]) [59]). The second way is the calculation of Π/S from the change in the noise standing-wave ratio ρ_n when the beam passes a power-absorbing structure [58]). The third way is the calculation of Π/S from the quotient of the amplitudes of the two noise space-charge waves on the beam [60]).

The relation between K, L, p and ϕ and Haus' noise parameters S and Π is given by eqs (75) and (76). In table XI we compare the values of S and Π, obtained from beam noise measurements with those obtained from our triode measurements. We also compare them with minimum noise-figure measurements in travelling-wave tubes equipped with L-cathodes [61]).

TABLE XI

Comparison of the beam noise fluctuations obtained from electron-beam measurements with those obtained from triode measurements *).

	S and Π, obtained from electron-beam measurements					S and Π obtained from triode measurements
	ref. 58 L-cathodes	ref. 58 Oxide cathodes	ref. 59	ref. 60	ref. 61 L-cathodes	
$S \cdot 10^{21}$	3—10	10	6—10	9	—	8—9
Π/S	0·33	0·3—0·7	0·3—0·6	0·3	—	0·7
F	4—12	5·7—12	5·9—10·5	11	6	5

From the comparison in table XI *we may conclude that the agreement between the different measurements is quite satisfactory, especially if one considers the approximations concerning the multi-velocity region in the vicinity of the potential minimum.* We should, however, remember that also the physical circumstances in the multi-velocity regions of triodes and of electron-beam amplifiers are somewhat different. In the first place the focussing magnetic field, necessary in electron-beam amplifiers, is not present in triodes. Secondly, the geometry of the multi-velocity region close to the cathode is different, which may result in a different excitation of higher-order space-charge wave modes. This may be the cause of the relatively large value of Π/S in microwaves triodes. *The value of* F_{min} ($\approx$ 5) *obtained from the triode measurements* (cf. eq. (74)) *compares very well with the corresponding value measured for traveling-wave tubes equipped with L-cathodes.*

5.14. Physical picture of the triode noise properties

The measurements on type EC 57 triodes at 4000 Mc/s yielded the following physical picture of the origin of the noise in microwave triodes.

The most important source of noise in a microwave triode is the random emission from the cathode. This random emission results in fluctuations of the instantaneous values of the average convection current and of the average velocity. The noise currents arising from these fluctuations can be calculated by means of the single-velocity transit-time theory of Llewellyn and Peterson.

However, this single-velocity transit-time theory does not account for the effects caused by the space charge of the electrons rejected in front of the potential minimum and those caused by the multi-velocity character of the electron

*) For reasons of partial saturation the values of K, L, p and ϕ for tube no. 243 have not been considered.

flow near the cathode. Furthermore, effects arising from the inhomogeneity of the electrostatic field in the cathode-grid space ("transit time spread") and those resulting from internal feedback are not described by this theory either.

Finally, the noise caused by reflected electrons must be considered separately. However, this can be done by applying the single-velocity transit-time theory to the motion of the reflected electrons.

On the basis of our measurements we may conclude that the effects caused by the transit-time spread and the feedback are negligible (cf. sec. 5.10 and 5.11, respectively).

Total emission noise has also a negligible effect at sufficiently high current densities. At low current densities ($< 0{\cdot}15$ A/cm^2), however, the total-emission noise becomes an important noise source, as might be expected (cf. sec. 5.9).

The noise caused by the reflected electrons has been calculated to be of moderate importance (see sec. 5.10).

The effects caused by the space charge on the original fluctuations at the cathode surface (given by the shot noise equation, eq. (50), and by the Rack velocity fluctuation, eq. (51)), and those caused by the multi-velocity character of the electron stream have been taken into account in the simplified model of sec. 3.5 by the factors K and L and the correlation constant $p\,e^{j\phi}$ *). The magnitudes of K, L, p and ϕ have been obtained from the measurement of the characteristic noise quantities of microwave triodes, which are related to them by eqs (69) to (72), and are given in table X for three cases.

The values of K, L, p and ϕ obtained from the triode-noise measurements can be compared with corresponding quantities obtained from electron-beam noise measurements. The correspondence is very satisfactory, especially in consideration of the assumptions made during the setting up of the theory.

However, the difference between the noise figure of microwave triodes and the minimum noise figure of electron-beam amplifiers is very large, in spite of the fact that they result from similar fluctuations at the cathode surface. This large difference is explained by two facts. In the first place in electron-beam amplifiers the point where the beam enters the region in which it interacts with the electromagnetic circuit can be chosen in such a way that the noise power induced in the output circuit is at a minimum. This is impossible in microwave triodes. Secondly, in an electron-beam amplifier the beam transducer between the electron gun and the interaction region must have no power exchange with its surroundings, since the amplitude of the slow space-charge noise-wave, which is amplified in the interaction region, would increase. In a microwave triode the electrons already induce noise power in the input circuit directly after leaving the cathode.

*) Apparently the noise-sources E and J originate from the convection-current fluctuations as well as from the velocity fluctuation. This explains partly the low correlation of the induced grid noise with the anode noise current at intermediate frequencies.

Appendix 1

Properties of transit-time functions

Some of the properties of transit-time functions, which have been used, will be given in this appendix.
They are:

$$\mathrm{Re}\,\{\beta e^{\beta}\,\Phi_6(\beta)\;\Theta(\beta)\} \equiv 0 \qquad (\mathrm{A}-1)$$

$$\mathrm{Re}\,\{\;e^{\beta}\,\Phi_6(\beta)\;\Xi(\beta)\} \equiv 0 \qquad (\mathrm{A}-2)$$

$$\arg\;\Theta(\beta) = \arg\frac{\Xi(\beta)}{\beta} \qquad (\mathrm{A}-3)$$

$$\Phi_2\left(\frac{\beta}{2}\right) - e^{\frac{\beta}{2}}\Phi_3\left(\frac{\beta}{2}\right) = \frac{2}{3}\beta\,\Phi_4(\beta) \qquad (\mathrm{A}-4)$$

The first two are very important since it is due to these porperties that ζ is proportional to p, (see eq. (71)). Putting β equal to $j\alpha$ and substituting the transit time functions we find after some calculation;

$$\beta e^{\beta}\Phi_6(\beta)\;\Theta(\beta) = j\,\frac{4}{\alpha^3}\left\{2\cos\alpha - 2 - \alpha^2 + \frac{\alpha^4}{6}\right\} \qquad (\mathrm{A}-5)$$

and

$$\beta e^{\beta}\Phi_6(\beta)\,\frac{\Xi(\beta)}{\beta} = j\,\frac{12}{\alpha^5}\{4\cos\alpha - 2\sin\alpha\}, \qquad (\mathrm{A}-6)$$

which proves the first two identities.

The third property can be found partly from the first two which prove that Θ and Ξ/β have the same or opposite directions. From figs (15) and (16) it can be seen that their directions are equal.

The last property is found simply by writing out the left-hand terms of eq. (A — 4).

Appendix 2

Calculation of the average transit times of the electrons in a triode with "Inselbildung"

The electron transit-time in a triode with "Inselbildung" is a function of the distance y (cf. fig. 35). In order to calculate the average transit time of the electrons, we first consider the equivalent-grid voltage and the current density which are, of course, also functions of y. If we now assume that the direction of the electron flow is always perpendicular to the cathode surface we can calculate from the equivalent grid voltage the value of the transit-time angle as a function of y. When this function is known the average value of y is easily calculated.

The equivalent grid voltage V_e is given by:

$$V_e(y) = \frac{V_g + D_{ag}\left(1 - \delta\cos\frac{2\pi y}{s}\right) V_a}{1 + D_{ag}\left(1 - \delta\cos\frac{2\pi y}{s}\right)\left(1 + \frac{4}{3}\frac{d_{ag}}{d_{cg}}\right)}, \qquad (A - 7)$$

where D_{ag} is the penetration factor of the anode field through the grid plane [62]) and V_a and V_g are the anode voltage and the applied grid voltage respectively. The value of δ is given by

$$\delta = 2\left(1 - \frac{2\pi^2 c^2}{s^2}\right)\left(1 + \frac{1}{D_{cg}} + \frac{d_1 - \frac{\pi c^2}{s}}{d_2 - \frac{\pi c^2}{s}}\right) e^{-\frac{2\pi d}{s}}, \qquad (A - 8)$$

where D_{cg} is the penetration factor of the cathode field through the grid plane*).

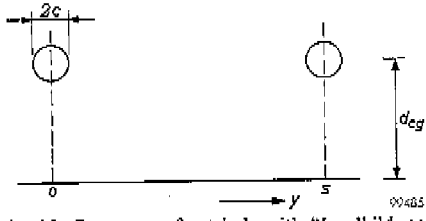

Fig. 35. Geometry of a triode with "Inselbildung".

Eq. (A — 7) is simplified by putting:

$$V_e' = \frac{V_g + D_{ag} V_a}{1 + D_{ag}\left(1 + \frac{4}{3}\frac{d_{ag}}{d_{cg}}\right)}; \quad a = \frac{\delta D_{ag} V_a}{V_g + D_{ag} V_a}$$

and

$$b = \frac{\delta D_{ag}\left(1 + \frac{4}{3}\frac{d_{ag}}{d_{cg}}\right)}{1 + D_{ag}\left(1 + \frac{4}{3}\frac{d_{ag}}{d_{cg}}\right)}.$$

Using this, eq. (A — 7) reduces to:

$$V_e(y) = V_e' \frac{1 - a\cos\frac{2\pi y}{s}}{1 - b\cos\frac{2\pi y}{s}} \approx V_e'\left\{1 - (a-b)\cos\frac{2\pi y}{s} - ab\cos^2\frac{2\pi y}{s}\right\}, \qquad (A - 9)$$

since $b \ll 1$ in an EC 59.

*) eq. (A — 7) is equal to eq. (65) if D_{ag} is replaced by $D_{ag}(1 - \delta\cos 2\pi y/s)$, cf. [63]) eq. (29).

From eq. (A — 9) we know the dependence of $V_e(y)$ on y. Using eqs (43) and (46), the dependence of the current density $J(y)$ on y and of the transit-time angle $\beta_1(y)$ on y are also known. The value of $\langle\beta_1\rangle$ averaged over all electrons is given by:

$$\langle\beta_1\rangle = \frac{\int_0^s J(y)\beta_1(y)\mathrm{d}y}{\int_0^s J(y)\mathrm{d}y} = j\,\frac{744\,.\,10^{-6} f_0 \int_0^s V_e(y)\,\mathrm{d}y}{d\int_0^s J(y)\mathrm{d}y} \qquad \text{(A — 10)}$$

where eq. (43) is used to eliminate the current density from eq. (46) (in this equation the current density is given by I_a/σ), so that the current density does not occur in the numerator. The denominator is found simply from the static characteristic.

Substituting eq. (A — 9) into eq. (A — 10) and performing the integration we find

$$\langle\beta_1\rangle = \frac{7{\cdot}44\,.\,10^{-4} f_0 V_e'}{d\int_0^s J(y)\mathrm{d}y}\left[\left(1 - \frac{ab}{2}\right)y - (a-b)\,\frac{s}{2\pi}\sin\frac{2\pi y}{s} - \frac{sab}{2\pi}\sin\frac{4\pi y}{s}\right]_0^s. \qquad \text{(A — 11)}$$

As for the limits of integration we should make the following remark: When $V_e(y)$ becomes negative in the vicinity of the grid wires we assume $J(y)$ to be zero for these values of y.

The values of $\langle\beta_1\rangle$ of table III have been obtained from eq. (A — 11). However when the current density is high (> 1 A/cm^2 in an EC 59) the effect of the "Inselbildung" on the transit-time spread appears to be negligible and eq. (46) can be used to obtain the value of $\langle\beta_1\rangle$.

SAMENVATTING

Hoewel reeds in 1946 triodes werden ontwikkeld voor het versterken van signalen met een frequentie van 4000 MHz, is het onderzoek naar de eigenschappen van deze triodes veel minder intensief geweest dan dat naar de eigenschappen van de eerst later tot ontwikkeling gekomen lopendegolfbuizen.

De succesvolle toepassing van deze triodes maakte echter een dieper inzicht gewenst en interessant. Het onderzoek dat in verband hiermee is ingesteld naar de eigenschappen van microgolftriodes vormt het onderwerp van dit proefschrift. Eerst wordt hierin een theoretische beschrijving van de eigenschappen van microgolftriodes gegeven en worden vervolgens de meetmethoden behandeld waarmee deze eigenschappen experimenteel bestudeerd kunnen worden. Tenslotte worden de theorie en de uit metingen aan enige triodes verkregen resultaten gecombineerd, ten einde inzicht te verkrijgen in de fysische oorzaken van het gedrag van triodes bij kleine signalen en van hun ruiseigenschappen.

Het opbouwen van de theoretische beschrijving is gesplitst in twee etappes. Eerst wordt een vervangingsschema van een microgolftriode opgesteld (hoofdstuk 2). Dit vervangingsschema verschilt daarin van dat van een ideale triode — waaronder we hier een triode zonder koppeling tussen uitgangs- en ingangscircuit verstaan —, dat in de roosterleiding een serieschakeling van een weerstand, een zelfinductie en een capaciteit is opgenomen. De ruiseigenschappen van de triode worden in dit vervangingsschema vertolkt door een ruisstroombron en een ruisspanningsbron aan de ingangsklemmen.

De tweede etappe is het berekenen van de elementen van dit vervangingsschema, voor zover deze elementen het gevolg zijn van de modulatie van de beweging der elektronen van katode naar anode (hoofdstuk 3). De berekening van deze elementen is gebaseerd op de looptijdtheorie volgens Llewellyn en Peterson. Aangezien in deze theorie wordt aangenomen dat alle elektronen, die zich op eenzelfde afstand van de katode bevinden, dezelfde snelheid hebben — wat zeker niet het geval is tussen de katode en het potentiaalminimum —, moesten vooral bij het berekenen van de ruisfluctuaties speciale veronderstellingen gemaakt worden.

Deze veronderstellingen houden in dat de eigenschappen van triodes inderdaad op grond van de looptijdtheorie van Llewellyn en Peterson beschreven kunnen worden. De invloed van de ruimtelading bij het potentiaalminimum op de oorspronkelijke ruisfluctuaties in de elektronenbundel wordt nu in hoofdstuk 3 in rekening gebracht door de beide oorspronkelijke fluctuaties — de snelheidsfluctuatie en de convectiestroomfluctuatie — met respectievelijk een factor K en L te vermenigvuldigen en ze onderling gecorreleerd te veronderstellen, waarbij de correlatieconstante $pe^{j\Phi}$ is.

De invloed van de reflecties van elektronen aan de anode kan eveneens met behulp van de bovengenoemde looptijdtheorie geschat worden.

De meetmethoden, die in hoofdstuk 4 beschreven worden, zijn tamelijk gecompliceerd doordat de afstand tussen het meetobject en de plaats waar gemeten wordt bij de beschouwde frequentie van dezelfde orde van grootte is als de golflengte. De gemeten waarden van de admittanties en de ruisbronnen moeten derhalve getransformeerd worden over de passieve circuits die gelegen zijn tussen de plaatsen waar gemeten wordt en de actieve ruimte van de triode. De desbetreffende transformatie-formules worden eveneens in hoofdstuk 4 afgeleid.

Uit de vergelijking van de resultaten van de in hoofdstuk 5 beschreven experimenten met de in hoofdstuk 2 en 3 opgestelde theorie volgt dat wat betreft het gedrag bij kleine signalen inderdaad de genoemde looptijdtheorie mag worden toegepast, mits de stroomdichtheid groot genoeg is. De terugkoppeleigenschappen van triodes worden door de seriekring in de roosterleiding bevredigend gekarakteriseerd.

De ruisstromen die door de vóór het potentiaalminimum omkerende elektronen geïnduceerd worden, zijn bij grote stroomdichtheden verwaarloosbaar. Dit geldt eveneens voor de invloed van de looptijdspreiding der individuele elektronen en voor de invloed van de inwendige passieve terugkoppeling op de ruiseigenschappen. Voorts blijkt de reflectie van elektronen aan de anode een tamelijk belangrijke ruisoorzaak te zijn.

De fluctuaties in de door de katode geëmitteerde elektronenstroom zijn echter de belangrijkste ruisoorzaken in microgolftriodes. De gemeten waarden van de karakteristieke ruisgrootheden zijn gebruikt om de eerder genoemde waarden van K, L, p en ϕ te bepalen.

Wanneer men voor de ruis in elektronenbundelversterkers veronderstellingen maakt die analoog zijn aan de in de triodetheorie gebruikte, dan kan men de resultaten van ruismetingen in elektronenbundels vergelijken met die in triodes. Het blijkt dat voor beide typen versterkers de ruisfluctuaties bij het potentiaalminimum bevredigend overeenstemmen, maar dat ten gevolge van de verschillende wisselwerking van de bundels met de elektromagnetische circuits het ruisgetal van triodes aanzienlijk verschilt van dat van bundelversterkers.

Het in dit proefschrift beschreven onderzoek is verricht in het Natuurkundig Laboratorium der N.V. Philips' Gloeilampenfabrieken. Voor de mij geboden vrijheid bij het onderzoek en voor de mogelijkheid de resultaten van dit onderzoek op deze wijze te publiceren, betuig ik mijn oprechte dank. Van de vele collega's, die op enigerlei wijze een bijdrage tot dit onderzoek geleverd hebben, wil ik vooral Dr. H. Groendijk dank zeggen voor de verhelderende discussies en de bereidheid het manuscript kritisch te lezen. Voorts dank ik Ir. P. A. H. Hart en Ir. C. W. Elenga voor hun medewerking bij bepaalde delen van dit onderzoek.

Tenslotte wil ik de N.V. Eindhovensche Drukkerij betrekken in dit dankwoord, voor de snelle en voortreffelijke wijze waarop dit proefschrift typografisch is verzorgd.

REFERENCES

[1]) L. De Forest, U.S. Patents Nos 841387 (1908) and 879532 (1908).
[2]) J. A. Morton, Bell Labs Record **27**, 166-170, 1949.
[3]) H. Groendijk, Proc. Instn elect. Engrs B **105**, 577-582, 1958.
[4]) J. A. Morton and R. M. Ryder, Bell System tech. J. **29**, 496-530, 1950.
[5]) G. Diemer, K. Rodenhuis and J. G. van Wijngaarden, Philips tech. Rev. **18**, 317-324 1956/57.
[6]) J. P. M. Gieles, Philips tech. Rev. **19**, 145-156, 1957/58.
[7]) V. V. Schwab and J. G. van Wijngaarden, Philips tech. Rev. **20**, 225-233, 1958/59.
[8]) J. P. M. Gieles and G. Andrieux, Philips tech. Rev. **21**, 1959/60.
[9]) M. T. Vlaardingerbroek, Philips tech. Rev. **21**, 1959/60.
[10]) F. B. Llewellyn and L. C. Peterson, Proc. Inst. Radio Engrs **32**, 144-166, 1944.
F. B. Llewellyn, Electron inertia effects, Cambridge Univ. Press, 1943.
[11]) A. van der Ziel, Noise, Prentice Hall, New York, 1954.
[12]) S. D. Robertson, Bell Syst. tech. J. **28**, 619-655, 1949.
[13]) H. J. Lemmens, M. J. Jansen and R. Loosjes, Philips tech. Rev. **11**, 341-350, 1950.
[14]) G. Diemer and K. S. Knol, Philips Res. Repts **4**, 321-333, 1949.
[15]) G. Diemer, Philips Res. Repts **5**, 423-434, 1950.
[16]) H. A. Haus and F. N. H. Robinson, Proc. Inst. Radio Engrs **43**, 981-991, 1955.
[17]) M. R. Currie and D. C. Forster, Proc. Inst. Radio Engrs **46**, 570-579, 1958; J. appl. Phys. **30**, 94-103, 1959.
[18]) W. R. Beam, Proc. Instn elect. Engrs B **105**, 790-795, 1958.
[19]) A. J. Rack, Bell Syst. tech. J. **17**, 592-619, 1938.
[20]) T. E. Talpey and A. B. MacNee, Proc. Inst. Radio Engrs **43**, 449-454, 1955.
[21]) J. H. van der Boorn, private communication.
[22]) A. van der Ziel and A. Versnel, Philips Res. Repts **3**, 13-23, 1948.
[23]) H. A. Haus and R. B. Adler, Proc. Inst. Radio Engrs **46**, 1517-1533, 1958.
H. A. Haus and R. B. Adler, Circuit Theory of Linear Noisy Networks, John Wiley & Sons, New York, 1959.
[24]) A. G. Th. Becking, H. Groendijk and K. S. Knol, Philips Res. Repts **10**, 349-357, 1955.
[25]) A. van der Ziel, Philips Res. Repts **1**, 381-399, 1946.
[26]) B. D. H. Tellegen, Physica **5**, 301-315, 1925.
[27]) G. de Vries, private communication.
[28]) W. A. Harries, I.R.E. Convention Record, **3**, 10-15, 1955.
[29]) A. van der Ziel and K. S. Knol, Philips Res. Repts **4**, 168-178, 1949.
[30]) J. G. v. Wijngaarden, Onde électr. **36**, 888-892, 1957.
[31]) H. C. Montgomery, Proc. Inst. Radio Engrs **40**, 1461-1471, 1952.
[32]) A. G. Th. Becking, H. Groendijk and K. S. Knol, Nachrichtentechn. Fachber. **2**, 37-40, 1955.
[33]) C. N. Smith, Nature **157**, 841, 1946.
A. van der Ziel and A. Versnel, Philips Res. Repts **3**, 13-23, 1948.
[34]) I. Langmuir, Phys. Rev. **21**, 419-435, 1923.
[35]) C. D. Child, Phys. Rev. **32**, 492-511, 1911.
[36]) W. E. Benham, Phil. Mag. **5**, 641-662, 1928.
W. E. Benham, Proc. Inst. Radio Engrs **26**, 1093-1170, 1938.
[37]) J. Müller, Hochfrequenztechn. Elektroakust. **41**, 156-167, 1933.
[38]) C. J. Bakker and G. de Vries, Physica **2**, 683-697, 1935.
W. R. Ferris, Proc. Inst. Radio Engrs **24**, 82-107, 1936.
D. O. North, Proc. Inst. Radio Engrs **24**, 108-136, 1936.
[39]) W. E. Benham and I. A. Harries, The ultra high frequency performance of receiving valves, Mac Donald, London, 1957.
[40]) W. Schottky, Ann. der Physik. **57**, 541-567, 1918.
[41]) W. Schottky, Wiss. Veröffentl. Siemens-Werke **16**, 1-19, 1937.
E. Spenke, Wiss. Veröffentl. Siemens-Werke **16**, 19-41, 1937.
[42]) P. K. Tien and J. Moshman, J. appl. Phys. **27**, 1067-1078, 1956.

[43]) J. R. Whinnery, Trans. Inst. Radio Engrs ED-**1**, 221-237, 1954.
[44]) D. A. Watkins, J. appl. Phys. **26**, 622-624, 1955.
A. E. Siegman and D. A. Watkins, Trans. Inst. Radio Engrs ED-**4**, 82-86, 1957.
S. Bloom and A. E. Siegman, Trans. Inst. Radio Engrs ED-**4**, 295-299, 1957.
[45]) A. E. Siegman, J. appl. Phys. **28**, 1132-1138, 1957.
A. E. Siegman, D. A. Watkins and Hsung-Cheng Hsieh, J. appl. Phys. **28**, 1138-1148, 1957.
[46]) H. A. Haus, J. appl. Phys. **26**, 560-571, 1955.
[47]) M. T. Vlaardingerbroek, Philips Res. Repts **14**, 327-336, 1959.
[48]) H. Groendijk and P. A. H. Hart, Measurement of the noise of an EC 57 at 100 Mc/s, unpublished.
[49]) C. J. Bakker, Physica **8**, 23-43, 1941.
[50]) J. H. L. Jonker, Philips Res. Repts **12**, 249-258, 1957.
[51]) M. T. Vlaardingerbroek, K. S. Knol and P. A. H. Hart, Philips Res. Repts **12**, 324-332, 1957.
[52]) F. W. Gundlach und H. Lohnsdorfer, Fernmeldetechn. Z. **6**, 305-309, 1955.
[53]) H. Bauer und H. Rothe, Arch. elektr. Übertr. **10**, 241-252, 1956.
[54]) G. C. Southworth, J. Franklin Inst. **239**, 285-297, 1945.
W. W. Mumford, Bell Syst. tech. J. **28**, 608-618, 1949.
[55]) K. S. Knol, Philips Res. Repts **6**, 288-302, 1951 and **12**, 123-126, 1957.
[56]) H. F. Friis, Proc. Inst. Radio Engrs **32**, 419-422, 1944.
[57]) M. T. Vlaardingerbroek, Proc. Instn elect. Engrs **B 105**, 563-566, 1958.
[58]) A. Bers, S. M. thesis Dept. of Elect. Engng, M.I.T. Cambridge, Mass. 1955.
[59]) T. J. Connor, S. M. thesis Dept. of Elect. Engng, M.I.T. Cambridge, Mass. 1956.
[60]) S. Saito, Trans. Inst. Radio Engrs ED-**5**, 264-275, 1958.
[61]) A. Versnel, Tijdschr. Ned. Radio Gen. **24**, 101-111, 1959.
[62]) P. H. J. A. Kleynen, Philips Res. Repts **6**, 15-33, 1951.
[63]) W. Dahlke, Telefunken Z. **24**, 213-222, 1951.

STELLINGEN

I

De berekening van de elektrische doorslagspanning van zuiver neon bij hoge frequenties, zoals die door Harries en Von Engel is uitgevoerd, leidt niet tot de experimentele waarde. De genoemde berekening is echter in ongewijzigde vorm van toepassing op bepaalde neon-argon-mengsels.

W. L. Harries and A. van Engel, Proc. Royal Soc. A **222**. 490-508, 1954

II

De wiskundige formulering, die wordt gebruikt bij het beschrijven van het ruisgedrag van lineaire netwerk vierpolen, kan eveneens worden toegepast op de ruiseigenschappen van elektronenbundelversterkers, en op microgolfvierpolen; men kan daardoor ook analoge meetmethoden aangeven.

A. G. Th. Becking, H. Groendijk and K. S. Knol, Philips Res. Repts **10**, 349-357, 1955

III

Het is niet mogelijk om, zoals is gesuggereerd, met de gevoeligste ruismeetmethoden die momenteel voor het microgolfgebied beschikbaar zijn met enige nauwkeurigheid de constante van Planck te bepalen.

L. D. Storm, Wescon Conv. Rec. **1**, 188-194, 1957.
A. van der Ziel, Noise, Prentice Hall, New York, 1954, blz 14.

IV

Men geeft in communicatiesystemen werkend in het microgolfgebied vaak de voorkeur aan het gebruik van lopendegolfbuizen boven het gebruik van triodes. De motivering hiervoor is weinig overtuigend.

V

De ruis-e.m.k. van een passieve tweepool is ondubbelzinnig bepaald door de grootte van de resistantie van deze tweepool; voor tweepolen met een negatieve resistantie geldt een dergelijk verband in het algemeen niet.

VI

De domeinstruktuur in polykristallijne ferro-elektrica wordt niet uitsluitend bepaald door de elektrische energie, maar ook door de mechanische spanningen.

J. de Boer, Chem. Weekbl. **54**, 137-141, 1958.

VII

Bij het integrerend meten van stromen met behulp van een versterker met stroomtegenkoppeling via een condensator wordt de integratietijd beperkt door de tijdconstante van het terugkoppelelement. Indien men bij het integrerend meten van spanningen gebruik maakt van een spanningstegenkoppeling via een *wederzijdse* inductie, is een dergelijke beperking niet aanwezig.

VIII

Het onderdrukken van de reflectie van elektronen aan de anode van een triode heeft geen belangrijke verbetering van het ruisgetal ten gevolge.

T. E. Talpey and A. B. Mac Nee, Proc. Inst. Radio Engels 43, 449-454, 1955. Paragraaf 3.11 van dit proefschrift.

IX

Het omrekenen van de gemeten relatieve ingangsadmittantie van een triodeversterker voor centimetergolven in de ingangsadmittantie van de equivalente vierpool van een triode kan worden vermeden door een eenvoudige constructie toe te passen.

Paragraaf 4.3 van dit proefschrift.

X

Ondanks het feit dat ingangsadmittantie en ruistemperaturen van een triodeversterker slechts kunnen worden gemeten met betrekking tot de niet-ondubbelzinnig gedefinieerde karakteristieke impedantie van de golfpijp, kan men er de admittanties en de karakteristieke ruisgrootheden van de triodevierpool ondubbelzinnig uit bepalen.

Hoofdstuk 4 van dit proefschrift.

XI

Bij de studie van de natuurkunde is het belangrijk ook aandacht te wijden aan de niet-rationele elementen, die de ontwikkeling van de natuurkunde hebben beïnvloed.

XII

Het verdient aanbeveling sommige interne bedrijfsopleidingen, zoals die bij verschillende industrieën gegeven worden, af te sluiten met examens, die ook buiten deze industrieën erkend kunnen worden.

M. T. Vlaardingerbroek

15 December 1959.